POLITECNICO DI TORINO

III Facoltà di Ingegneria dell'Informazione

Corso di Laurea in Ingegneria Meccatronica

Tesi di Laurea Specialistica

Adaptive current reference generator for active power filters

Relatore:

Chiar.mo Prof. Marcello Chiaberge

Candidato:

Fabrizio Nicolino

Luglio 2013

AALTO UNIVERSITY

Department of Electrical Engineering

Final Project

Adaptive current reference generator for active power filters

Supervisor:

Prof. Seppo Ovaska

Candidate:

Fabrizio Nicolino

July 2013

AALTO UNIVERSITY
SCHOOL OF ELECTRICAL ENGINEERING

ABSTRACT OF THE
FINAL PROJECT

Author: Fabrizio Nicolino

Title: Adaptive Current Reference Generator for Active Power Filters

Date: 16.07.2013 Language: English Number of pages: 10+78

Department of Electrical Engineering

Professorship: Industrial Electronics Code: S-81

Supervisor: Prof. Seppo Ovaska

The electricity distribution networks are increasingly characterized by the presence of non-linear power electronic devices and power plant equipment capable to create problems of harmonic pollution. However, to have the best performance of attenuation of the harmonics introduced by various non-linear loads it is common to use an Active Power Filter (APF).

In this thesis is presented the analysis of one of these filters and the development of possible improvements. I realized a Matlab code that could reproduce the operation of the filter and tested its efficiency.

Subsequently the goal was to learn and explain why the original algorithm, in addition to filtering the harmonics present in the input signal, introduced new harmonics.

The second goal was to analyze a possible simplification of the filtering algorithm, reducing the number of algebraic multiplications, so that it can be implemented effectively on Field Programmable Gate Arrays (FPGAs).

Keywords: Power Electronics, Harmonics, Filtering, Active Power Filter, Adaptive Filter

Preface

The thesis was carried out in the Department of Electrical Engineering, Aalto University School of Electrical Engineering.

I would like to acknowledge the direct and indirect contribution and involvement of different people in this work.

First of all, I would like to thank my supervisor Professor Seppo Ovaska for interest and support for my thesis. Your constructive feedback gave purpose and motivation to complete the thesis.

I am incredibly thankful to my Italian supervisor, Professor Marcello Chiaberge who has always helped me during my Erasmus period, providing useful advice whenever I needed.

Many thanks to the Student Affairs Secretary Niina Huovinen for clarity and simplicity demonstrated in the solutions to all my problems faced during my year of studies here at Aalto University.

I would also like to thank all the people which I met here in these beautiful eleven months, because it is also thanks to them and the fun times spent together, that I have been able to accomplish this goal.

Espoo, Finland, 16.07.2013 Fabrizio Nicolino

Contents

List of figures

List of tables

...a mè päre e a mè märe,

agli amici di una vita,

to all the people I have met during this amazing year

...kiitos paljon!

1. Introduction

The electricity distribution networks are increasingly characterized by the presence of non-linear power electronic devices and power plant equipment capable to create problems of harmonic pollution and consequent loss of power, harmful malfunctioning or even risk of equipment damage. In an industrial power network the waveform of the current and voltage is therefore quite different from a pure sine wave. For many applications, the harmonic distortion is the most important problem of power quality and this is linked primarily to the fact that many devices are designed only with reference to the fundamental frequency, leaving aside the problem of non-ideality of the waveform.

Considering the emerging energy problems that affect the world nowadays, we should pay more attention to all those fields where we can find a solution to the smallest problem of energy efficiency. From more than 20 years now, various studies have been made and several solutions have been proposed trying to solve in the best way this problem of harmonic distortion. Obviously the best approach would be to develop and use device topologies that do not produce excessive harmonics. However the proposed solutions are based mainly on the use of filters, passive or active, that have the purpose to attenuate the harmonics introduced by various non-linear loads from the electrical current of the network [2].

The filters that give the best performance for attenuating current harmonics in supply networks at the low to medium voltage distribution level, are called Active Power Filters (APF).

The aim of this study was precisely the analysis of one of these filters and the development of possible improvements.

First of all, I started studying the filtering algorithm and its operation. Starting from the basic equations of the algorithm, I realized a Matlab code that could reproduce the operation and using ideal input signals I tested the actual accuracy of the results. This initial part was proven very useful to understand the logical operation of the filter and test its efficiency studying the output waveform and comparing it with that in the input.

Once ascertained the actual correct operation of the algorithm, the next step was to learn why the original algorithm, in addition to filtering the harmonics present in the input signal, introduced new harmonics, although very small and mostly negligible, into the output signal. At this point the goal was to simulate this new harmonics generation and tabulate the birth of new harmonics according to the harmonics present in the input signal. The idea of studying this new harmonics generation was dictated

by the fact that creating the two adaptive coefficients on which the filter is based, we noted a periodic oscillation of the coefficients. Therefore, on the one hand the filter carries out the operation of filtering of the harmonics present in the input signal, but on the other hand there is a negative effect of new harmonics generation. The objective was then to find out how and where these new harmonics were born.

The second goal of my research was to analyze a possible simplification of the filtering algorithm, reducing the number of algebraic multiplications, so that it can be implemented effectively on Field Programmable Gate Arrays (FPGAs).

The structure of this thesis is therefore linked to the objectives that were set for the thesis. In the opening chapters I explain the problem of the harmonic distortion, the main sources of harmonics and the undesirable effects caused by harmonic distortion.

Starting from chapter 5 is presented the algorithm used for harmonics filtering, its operation and, with the help of simulations and graphics, the verification of its usefulness. In the last part of the thesis I will explain the results of the tests on two possible improvements that could be introduced in the algorithm and studying the results obtained, I will verify their applicability.

The work done is useful to spread knowledge about more details and limits about the filtering algorithm analyzed. The focus on some negative aspects encountered and the reasons found, have allowed to point out what are some of the disadvantages of this type of filters. In addition, the research of possible improvements for the filter and the verification tests performed open a new area of development for engineers and scientists interested and active in research in this field.

2. The harmonic distortion

When the waveform of the alternating voltage or current differs from the pure sine, the fundamental frequency is typically corrupted by harmonic distortion. A non-sinusoidal waveform may be thought as consisting of a fundamental sine wave (50 Hz in the case of European electricity network) on which are overlapped other multiple-frequency sinusoids. The cause of harmonic distortion is the non-linear devices present in the power system, in which the current is not proportional to the applied voltage [1].

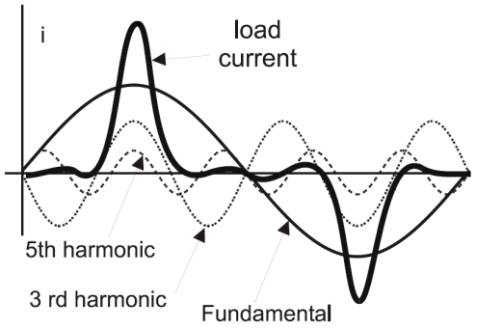

Figure 1 - Line current distortion [3]

Figure 1 shows a line current i_s absorbed by a power electronic system that changes it significantly from the sinusoidal shape. This distorted current induces some distortion also in the voltage of the power source.

To simplify the analysis, we can assume that the voltage supply is perfectly sinusoidal and has a fundamental frequency ($\omega_1 = \omega$ and $f_1 = f$), and for this we have:

$$v_s(t) = \sqrt{2}\, V_s sin(\omega_1 t) \qquad (2.1)$$

The input current in steady state is the sum of its Fourier series components (harmonics) and it can be written as:

$$i_s(t) = i_{s1}(t) + \sum_{h\neq 1} i_{sh}(t) \qquad (2.2)$$

where i_{s1} is the fundamental component (with the network frequency f_1) and i_{sh} is the component with the frequency of the h^{th} harmonic, f_h.

These current components are sinusoidal and they can be evaluated as:

$$i_s(t) = \sqrt{2}\, I_{s1} sin(\omega_1 t - \varphi_1) + \sum_{h\neq 1} \sqrt{2}\, I_{sh} sin(\omega_h t - \varphi_h) \qquad (2.3)$$

where φ_1 is the phase angle between the input voltage, assumed sinusoidal, and i_{s1}.

The rms value of the line current can be calculated by applying its definition, as shown in the following equation (where $T_1 = 1/f_1 = 2\pi/\omega_1$):

$$I_s = \sqrt{\frac{1}{T}\int_0^{T_1} i_s(t)^2 dt} \qquad (2.4)$$

Substituting in the equation (2.4) the value i_s of the equation (2.3) and taking into account that the integrals of all mixed products (i.e. the product of two terms with different frequencies) are individually equal to zero, we have:

$$I_s = \sqrt{{I_{s1}}^2 + \sum_{h\neq 1} {I_{sh}}^2} \qquad (2.5)$$

The amount of distortion in the waveforms of the voltage and current is quantified with an index called Total Harmonic Distortion THD.

From the equation (2.2) the distortion component of the current is:

$$i_{dis}(t) = i_s(t) - i_{s1}(t) = \sum_{h\neq 1} i_{sh}(t) \qquad (2.6)$$

In terms of rms value, this current is:

$$I_{dis} = \sqrt{{I_s}^2 - {I_{s1}}^2} = \sqrt{\sum_{h\neq 1} {I_{sh}}^2} \qquad (2.7)$$

The THD can be obtained considering the distortion component of the current and it is the ratio between the rms value of the harmonics and the rms value of the fundamental:

$$\%THD_i = 100\frac{I_{dis}}{I_{s1}} = 100\frac{\sqrt{{I_s}^2 - {I_{s1}}^2}}{I_{s1}} = 100\sqrt{\sum_{h\neq 1}\left(\frac{I_{sh}}{I_{s1}}\right)^2} \qquad (2.8)$$

$$\%THD_v = 100\frac{V_{dis}}{V_{s1}} = 100\frac{\sqrt{{V_s}^2 - {V_{s1}}^2}}{V_{s1}} = 100\sqrt{\sum_{h\neq 1}\left(\frac{V_{sh}}{V_{s1}}\right)^2} \qquad (2.9)$$

where the subscript *i* indicates the THD for the current while the subscript *v* indicates the THD for the voltage.

The voltage harmonic distortion is mainly caused by high levels of current harmonic distortion and the level depends strongly from the impedance of the generator. For big generator impedance we have a high level of voltage harmonic distortion.

Since this harmonic distortion is typically caused by non-linear loads, we usually speak about distorting loads that “inject harmonic currents”.

2.1. Sources of harmonic distortion

Any non-linear load that includes switching generates harmonics on the distribution network and the waveform associated with a load can be analyzed and decomposed to provide the spectrum of harmonics. The following examples are only some cases of apparatus and systems that generate harmonics [4]:

- Compressors, freezers and microwave ovens
- Elevators and escalators
- Equipment for heating, ventilation and air conditioning (HVAC)
- Fluorescent lamps and energy saving lamps
- Low voltage lighting with electronic transformers
- Motors, fans and pumps
- Personal computers, monitors, printers and copiers
- Rectifiers, power converters and control units with thyristors
- Uninterruptible Power Supply (UPS)
- Variable speed drives and switching power supplies

In general, electronic power converter loads represent the most important class of nonlinear loads in the power system and have a capacity for producing harmonic currents [1]. The category of personal computers, monitors, printers and copiers represents a very big portion of devices that generate harmonics, considering their increased utilization in every workplace. The principal cause of the production of harmonic currents and voltages is the employment of switched-mode power supplies which are responsible of the injection of harmonics into the network (especially the third harmonic).

In a certain way, the category of lighting with fluorescent lamps and energy saving lamps is linked to that outlined above. In fact, also in this case switched-mode power supplies are used to increase the fluorescent tube efficiency and permit more sophisticated control, such as dimming. Moreover, it is very important to consider the harmonic generation from the lighting because it typically accounts a high percent of a commercial building load and, for this reason, it is one of those main categories to which it is important to find a solution.

2.2. The effects of harmonic distortion

The current and voltage harmonics can cause different kinds of problems in electrical/electronic systems. The problems may be more or less serious and dangerous; certain types of effects are visible immediately, while others occur after a certain period of time. The negative effects of the presence of harmonics in the network can range from the increase by a certain percentage of the error of measuring instruments, like voltmeters, amperometers or oscilloscopes [5], to more serious problems linked to operations of circuit breakers, like Residual Current Devices (RDCs) used to disconnect the power supply if it detects that the sum between the currents that flow in the phase and neutral conductors is not within a certain limit. The presence of harmonics can distort that sum and cause malfunctions in the safety system of a building.

Other negative effects to consider are the generation of noise and vibration in electromechanical devices caused by pulsating mechanical torques linked to electrodynamic forces generated because of the presence of harmonic currents [5].

The harmonic distortion can also cause effects of overheating and therefore power losses. The impedance of the capacitors, for example, decreases as the frequency increases, and so the harmonic currents at higher frequencies flow through the capacitor connected to the circuit generating high voltages on the dielectric of the capacitors and this can lead to excessive stresses and premature failure.

More overheating problems are related to rotating machines, in which the losses are caused by the considerable difference in speed between the harmonics that create the rotating fields and the speed of the rotor [6], and to transformers in which the losses are caused by the skin effect (because of it the resistance of a conductor increases with the frequency). In general, the skin effect causes overheating of all power cables and equipment [7].

Returning to consider immediate negative effects, the presence of harmonics can cause interferences on communication and control circuits. The currents may produce unwanted magnetic and electric fields to disturb the performance of the communication system concerned [7].

Finally, we can still consider the overloading of the neutral wire in three-phase systems: it is the common return conductor for the currents present on the individual phases (Figure 2). If the loads of the three phases are approximately equivalent, the current in the neutral conductor is equal to zero since the three phase currents are equal in amplitude but out of phase with each other. Due to the presence of harmonics on the phase currents, these may have different amplitude values and the zeroing of the

neutral current does not occur. If the neutral conductor is undersized, as often happens in the oldest buildings, it might be subjected to dangerous overheating [8].

We may further deepen the negative effects due to the presence of harmonic distortion whereas more specifically the loss of electric power, the increase of the apparent power and the oversizing of the power sources, the effects of harmonic resonance and the sequences of negative rotation in the motors [9], but I think that the problems presented so far are sufficient to understand how important it is to try to eliminate as much as possible the harmonic distortion from the network.

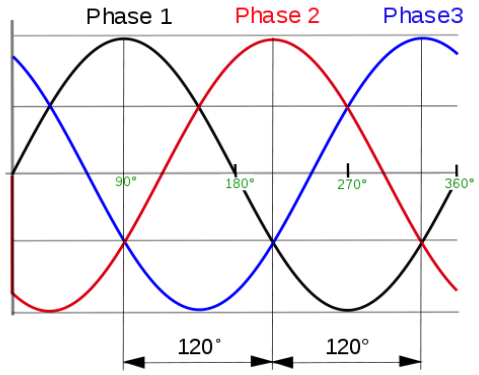

Figure 2 - Currents in a three-phase system

3. Filtering of harmonic distortion

There are several solutions to try to limit and attenuate the problem of harmonic pollution. If the adverse effects are tolerable, the solution is often to proceed in a simple oversizing of the cables and to accept the presence of harmonics. If instead it is desired to clean the current from the harmonics, the most common technique is filtering.

The filtering operation can be carried out using two different categories of filters:

- Passive filters
- Active filters

I will describe the main features of each category in the following subsections.

3.1. Passive filters

Generally the most common method used to limit the presence of harmonic voltages in the network is to use a passive filtering system.

A passive filter must be able to [10]:

- Reduce the harmonic content of currents and voltages within the limits set by the regulations
- Produce reactive power useful to rephase the load

They mainly consist of inductors and capacitors suitably connected to the purpose of [10]:

- Create a high impedance in series with the load to ensure that current harmonics are as low as possible. Of course this type of filter, given the nature of the connection with the load, must be dimensioned to withstand the maximum line voltage and the maximum load current. It is not appropriate in case we have many distorting loads because it seeks to prevent the harmonic currents to flow in pathways at low impedance towards the network and then causes a distortion of the voltage.
- Create a low impedance path that connect to the ground the harmonic components unwanted. These filters are placed in parallel with the load and must be sized for harmonic currents which will arise. For this reason, generally, the parallel filters are less expensive than those in series and, in addition, these filters allow to provide reactive power at the fundamental frequency, useful for power factor

correction (while the series filters absorb reactive power at the fundamental frequency).

3.2. Active filters

Active filters constitute a more sophisticated solution then passive filters and are relatively new devices used for the problem of harmonics. Being constituted by more complex components, they are also more expensive but present the advantage that they can be used in all circumstance in which the passive filters cannot operate successfully [1].

The scheme in the Figure 3 shows the single-phase diagram relating to the operation of a shunt active filter. The current absorbed by a non-linear load consists of a fundamental component and a distortion component. The current in the load is measured and filtered so as to provide a signal proportional to the component of distortion. Then, with a reference to an ideal case, the harmonics present in the network current are deleted.

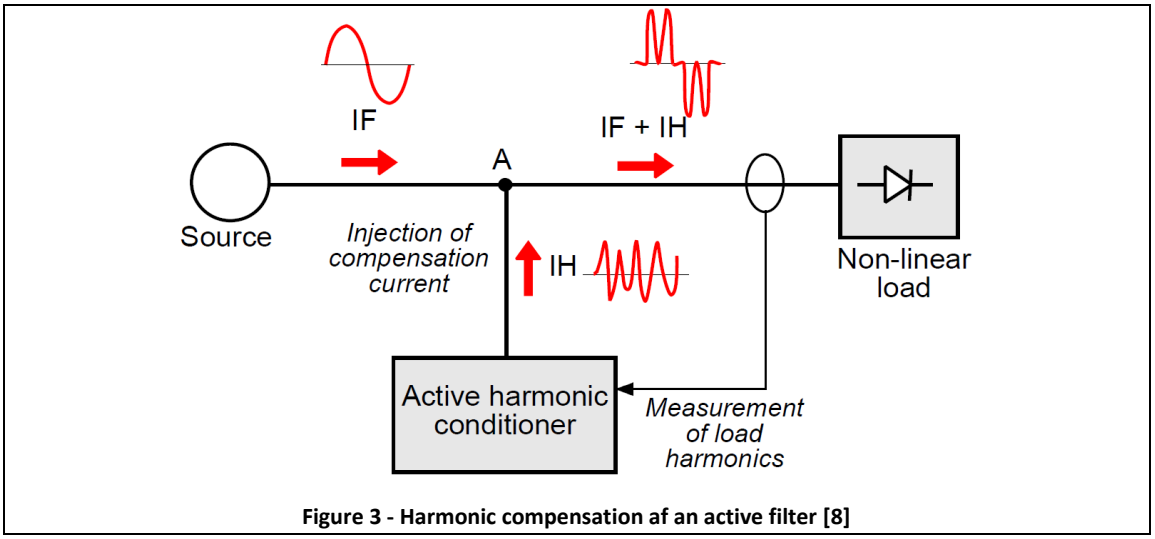

Figure 3 - Harmonic compensation af an active filter [8]

4. Current reference generator

The publication of different techniques of harmonic extraction has begun since the early 1980s, when it was understood that with the rapid power electronics development, the high levels of harmonics led to distribution systems problems [11].

Noting that the active filters were those with the best performance, researchers began to conduct studies on them. There are two types of active filters: shunt and series active filters. The shunt filters are the most used and base their operation on the injection of a current in phase opposition but with the same amplitude of the harmonic components, so to delete them. This type of filters are based on harmonic current extraction techniques, and they can be divided mainly into two categories:

- Frequency-domain methods
- Time-domain methods

In the following subsections I will present some details of the main techniques which belong to these two categories.

4.1. Frequency-domain methods

When we think about the frequency domain, the first instrument that comes to mind and that is almost always used to conduct studies in this field is the Fourier transform. Some of the proposed techniques base their operation just on it, in its forms of Discrete Fourier Transform (DFT) and Fast Fourier Transform (FFT). The basic operation of an APF requires extracting harmonics to be eliminated from the current waveform of the load and, therefore, these kind of techniques are a powerful tool for harmonic analyses in active power filters as well. The disadvantages are that algorithms which use these transforms are steady state concepts and have a slow response because of the time delay caused by the structure and computational complexity [11].

Another kind of technique is based on the use of the Kalman filter. It is a recursive optimal estimator that requires a state variable model for the parameters to be estimated and a measurement equation that relates the discrete measurement to the state variable (parameters) [11]. If on one hand this type of technique has the advantage to provide a convenient measure of estimation accuracy, on the other hand it has the disadvantage of computational complexity.

The wavelet bases method studies the active and reactive power on the time-frequency domain. Using the complex wavelet transform, voltage and current are transformed to the time-frequency domain with scaling and translation parameters to set the frequency range and localize the frequency respectively [11]. The disadvantage of this kind of technique is the complexity associated with using frequency decomposition before analysis.

4.2. Time-domain methods

This category is the one on which more studies have been conducted. The proposed techniques are based on different and various theories. The advantages of time-domain methods are that their design is straightforward and fewer computational steps are required; hence smaller processor memory is required. Their common disadvantages are time delay, phase delay and attenuation distortion.

The instantaneous reactive power theory is based on the instantaneous value concept of the active and reactive power and their compensation [11]. The main advantage of this method is the ability to generate sinusoidal reference for each phase in case of current imbalance in a three-phase system. The drawback is that we have to know certain network parameters to calculate the values of the powers.

The cross vector theory defines an instantaneous real power and three instantaneous imaginary powers and it has some similarities with the previous theory: the current is divided into active and reactive parts and the compensating currents are calculated considering the instantaneous real power and the three instantaneous imaginary powers [11]. Also in this technique there is the disadvantage of knowing values of network parameters to calculate the powers.

The rotating theory takes advantage of both instantaneous reactive power theory and cross vector theory: three power components are defined as linearity independent on a reference frame and the three current components are controlled independently to compensate the three instantaneous power components [11].

Another technique based on the geometrical concept of reference frame is the one that transforms the load currents from an *a-b-c* stationary reference frame to a *d-q* synchronously rotating reference frame. The current can be decomposed in the two active and reactive power components with the fundamental and the harmonic part [11]. The major advantages of this proposed technique are the simplicity of the algorithm, the frequency independence, the accuracy of the extraction and a fast transient response.

There are numerous other techniques which could be explained in this subsection like, for example, the adaptive interference canceling technique, the capacitor voltage control, the correlation function technique and the sinusoidal tracking model, but everything that has been described so far serve primarily to give an idea of how large and diverse is the range of solutions which can be used to solve the problem of harmonic distortion.

The last technique proposed is based on filtering of the load currents, extracting the fundamental current component. Unfortunately this straightforward technique suffers from the phase and magnitude errors introduced by the fixed active filter. However, it is important because, basing on that, the adaptive filter studied in this thesis has been realized. The motivations for the work developed about this kind of filter are the simplicity of the algorithm, no need to know network parameters to calculate active or reactive powers and the ability to adapt easily to the frequency variations. Being an adaptive digital filter, it is important to recall some concepts of this type of filters.

5. Adaptive filtering

In recent decades there has been widespread use of digital signal processing techniques in numerous applications. The resulting digital signal processing systems are attractive due to their reliability, accuracy, small physical size and flexibility [12].

The block "Active harmonic conditioner" in Figure 3 could be a digital signal processing system that performs the activity of filtering and this is one of the main points of this thesis.

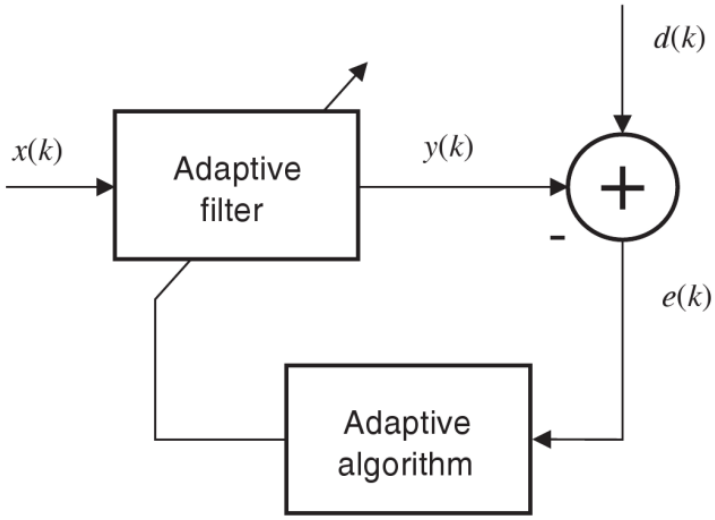

Figure 4 - General adaptive filter configuration [12]

Filtering is an operation that changes in some way the processed signal. A filter is then a device that takes care to bring to the output only the portion of the signal that we are interested. With reference to the digital field, a digital filter deals with signals processed in discrete time. To change the content of the signal taken into consideration, a digital filter makes use of some multiplicative parameters to weaken the signal samples that are not of interest. For time-invariant filters, the structure and the parameters of the filter are fixed and if the filter is linear, the output is a linear function of the input [12]. When it is impossible to satisfy the specifications by using a time-invariant filter, an adaptive filter is required. The main advantage of this kind of filter is that it self-adjusts its transfer function, going to modify its parameters, according to an optimization algorithm driven by an error signal. The modification of the parameters is done in on-line mode going to consider the error signal which is usually the estimate of the error between the output of the filter and a reference signal which represents the ideal output. In Figure 4, $x(k)$ represents the input of the filter, $y(k)$ is the output and $d(k)$ is the reference signal used to determinate the error signal $e(k)$ that is required to update the parameters of the filter.

5.1. Multiplicative general parameter filtering

The multiplicative general parameter (MGP) filter is an adaptive filter with a simple structure and high efficiency. It allows having a good attenuation of harmonics without phase shifting the fundamental line frequency and it possesses only two time-varying parameters which allow a good adaptation around the nominal frequency requiring only $N + 2$ additions (where N is the filter length) and five multiplications [13].

The presence of only two adaptive parameters is due to the fact that we need no more than two degrees of freedom in adaptation that is the capability to track the amplitude and phase of the fundamental component only. Only one parameter would not be sufficient and with more than two parameters we would have an algorithm that reacts to multiple correlating signal components and adjust the filter to pass also some harmonics [14].

The fact of having a low number of operations to be performed and then a low computational cost is very important because one of the main characteristic of this type of filters is that having a good computational efficiency, they can be implemented on low cost electronic devices such as simple microcontrollers or field programmable gate arrays (FPGAs) [14].

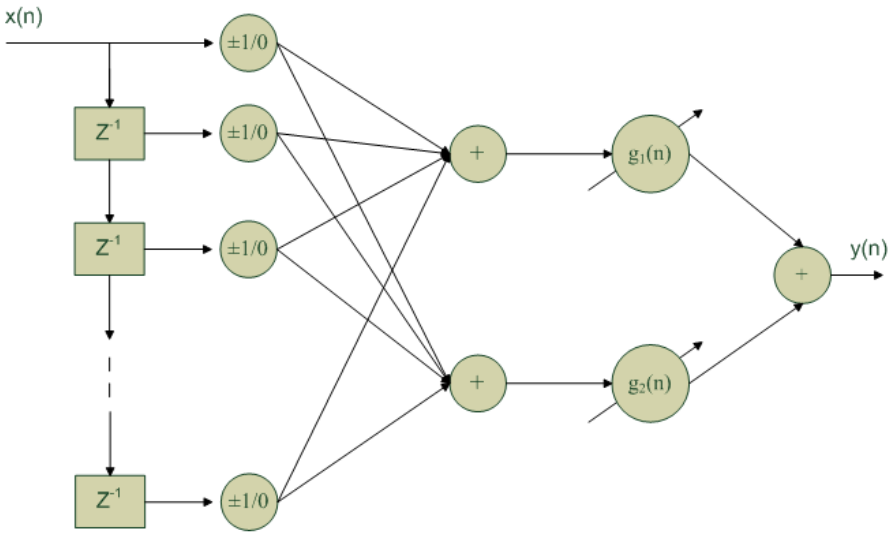

Figure 5 - MGP-FIR filter with two adaptive parameters

The MGP-FIR was introduced by Vainio and Ovaska in 2002 [15]. The filter output is computed as:

$$y(n)=g_1(n)\sum_{k=0}^{N-1}h_A(k)x(n-k)+g_2(n)\sum_{k=0}^{N-1}h_B(k)x(n-k) \qquad (5.1)$$

where $g_1(n)$ and $g_2(n)$ are the multiplicative general parameters and $h_A(k)$ and $h_B(k)$, with $k \in \{0, 1, 2,..., N\text{-}1\}$, are the fixed-basis filter coefficients which are determinated during an off-line optimizing stage better explained in the following subsections.

In a p-step-ahead prediction configuration, the multiplicative general parameters are updated according to the following equations:

$$g_1(n+1)=g_1(n)+\mu[x_F(n)-y(n-p)]\sum_{k=0}^{N-1} h_A(k)x(n-k) \quad (5.2)$$

$$g_2(n+1)=g_2(n)+\mu[x_F(n)-y(n-p)]\sum_{k=0}^{N-1} h_B(k)x(n-k) \quad (5.3)$$

where x_F is the ideal output and μ(<1) is the adaptation gain factor and it affects the parameters convergence during input transients, as well as the residual oscillations in steady state. Both of the multiplicative general parameters adapt to try to minimize the error between the output ant the reference signal [14].

5.2. Optimization of MGP-FIRs

It is easy to understand that one of the first things that we have to do to optimize the MGP-FIR algorithm is trying to find the best coefficients for the fixed part of the filter.

Returning to observe the equations (5.2) and (5.3), the terms $h_A(k)$ and $h_B(k)$ represent these coefficients and here they may only have discrete values of +1, 0 and -1.

We can search these coefficients using different types of algorithm considering that we are evaluating a discrete, constrained and non-linear optimization problem. Already more than thirty years ago, researchers came up with the ideas to solve this kind of problems by trying to imitate the model of natural and biological evolution, which was formulated for the first time by Charles Darwin [16]. Basing on concepts such as genes as transfer units of heredity, genetic algorithm and self-adaptation, evolutionary algorithms were born [16].

In typical evolutionary programming algorithms (EPA), the coefficients of the filter are real-valued and they are perturbed by real-valued random variables [15].

As already said before, considering coefficients with values only equal to +1, 0 or -1, the search for the best pairs of these coefficients is a discrete, constrained and highly non-linear optimization problem, but the solution is necessary in order to

optimize the computationally efficient of MGP-FIR filter. For this reason we need to use an advanced search method to address the filter optimization problem.

5.3. Evolutionary programming

With the development of computers more efficient and faster, evolutionary systems have become increasingly popular among researchers and engineers and the use of evolutionary algorithms, which are the core of evolutionary systems, proved to be an excellent method to solve complex optimization problems [16].

In the year 2004, Professor Ovaska introduced an optimization procedure for MGP-FIRs based on evolutionary programming, which is a nature-inspired search method. The algorithm starts from an initial random population of N_p candidate solutions, in which every candidate is a pair of two N-length vectors (h_A, h_B). As already mentioned above, the elements of the two vectors may only have values +1, 0 or -1 [13]. In addiction there are two important rules to follow: when some element of the vector h_A has value ±1, then the element in the same position of the vector h_B is equal to 0, and vice versa, and the number of nonzero coefficients between the two vectors has always to be equal to N [14].

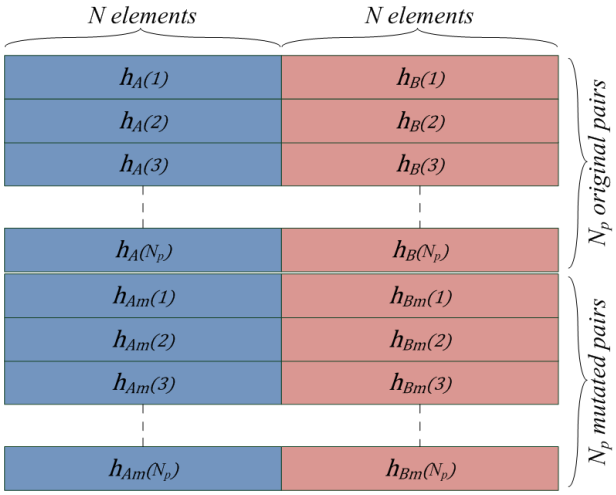

Figure 6 - Enhanced population

The second step is to perform single element mutations, so an element of the first vector is chosen randomly and altered in the following way: it is mutated from ±1 → 0 or from 0 → ±1 with equal probabilities and the corresponding element in the second vector has to be mutated according with the rules previously cited. At the end of this step, the mutated vector pairs are included to the original population and therefore the size of the enhanced population becomes $N_p + N_p = 2N_p$ [14]. The third step is the evaluation of the fitness of all candidate solutions in the enhanced population

represented in the Figure 6. The description of the calculation of the fitness function will be resumed in the following sections. Once we have the $2N_p$ values of fitness, we have to sort the population in the order of decreasing fitness scores and discard the N_p poorest solutions. In the end we have to go again to the second step and repeat this loop until when the termination condition (reaching a certain number of loops or of a certain value of fitness) is achieved [14].

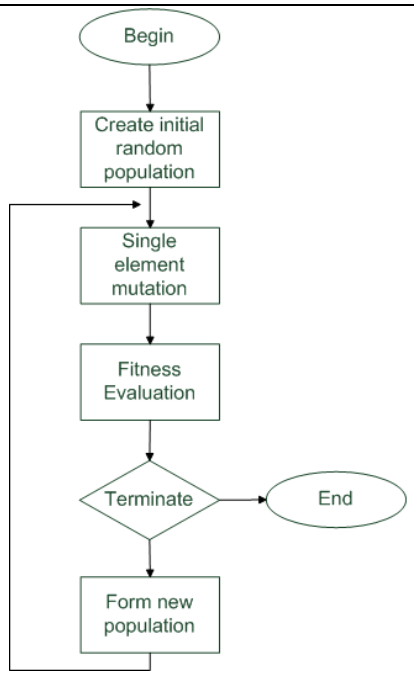

Figure 7 - Evolutionary programmin algorithm

With current computing platforms, like 2.27-GHz Intel® Core™, RAM 4 GB and running m-files on Matlab® 7 the algorithm is often able to provide competitive or nearly optimal solutions in a practical computing time, definable no more than 10-20 min.

5.4. Fitness function

The fitness function, mentioned in the previous section, is an index of our requirements on the candidate solution. It is calculated for all pairs that compose the scanned population in order to find the best solution during the sorting step of the algorithm. The following equation shows how to calculate the fitness function:

$$F = \frac{a}{ITAE \cdot max\{NG_{49\,Hz}, NG_{50\,Hz}, NG_{51\,Hz}\}} \qquad (5.4)$$

a = 1000 is a convenient scaling factor. The goal of this function is the simultaneous minimization of the two terms in the denominator.

The term *ITAE* is the integral of time absolute error based on the error term $e(n)$ that is the difference between the pure fundamental component $x_F(n)$ and the filter output that is predicted here two-step-ahead because it has to compensate the delays due to the computational and A/D conversion stages:

$$e(n) = x_F(n) - y(n-2) \quad (5.5)$$

We have to consider that usually in the European power systems the line frequency varies around the nominal value (50 Hz ± 2%) [13]. This ±1 Hz frequency tolerance is the reason why we need and adaptive filter in our delay-constrained application. The input signal is a fundamental sinusoid corrupted with odd-order harmonics and the filter is required to pass the pure sinusoid with two-step-ahead prediction and no amplitude attenuation. To optimize the filter for the nominal frequency variation, we use a test signal composed by three individual sequences of 300 samples: 49, 50 and 51 Hz corrupted by 3rd-13th order odd harmonics with an amplitude of 15% of the fundamental sinusoid and described by the following equation:

$$x(n) = sin(2\pi f_F T_S n) + \sum_{m\in\{3,5,7,9,11,13\}} 0.15 \cdot sin(2\pi m f_F T_S n) \quad (5.6)$$

where f_F = 49/50/51 Hz is the fundamental frequency and T_S = 0.6 ms is the sampling period. During this test stage, almost 98 percent of those 10-20 minutes needed for a single run of the code as discussed above, are spent in the fitness simulator code (see the Fitness evaluation part in Appendix A). Only 2 percent of that time is spent in the actual optimization algorithm.

We can calculate the value of ITAE with the following equation:

$$ITAE = \sum_{n=1}^{300} n|e(n)| + \sum_{n=301}^{600} (n-300)|e(n)| + \sum_{n=601}^{900} (n-600)|e(n)| \quad (5.7)$$

The second main term that we need to know is the maximum value of the white noise gain (*NG*) that we can calculate for every subsequence (49/50/51 Hz). We must take into account the maximum value so that we can consider the worst situation and then the result with lower efficiency that our filter can give us. For every subsequence, we can calculate the noise gain in the following way:

$$NG(n) = \sum_{k=0}^{N-1} [g_1(n_L)h_A(k)]^2 + \sum_{k=0}^{N-1} [g_2(n_L)h_B(k)]^2 \quad (5.8)$$

where n_L corresponds to the last sample index of the evaluative simulation, which takes a major proportion of time during the optimization process.

Summarizing, the role of the fitness function is to be a qualitative index, during the optimization process of the filter, of the solutions candidate to be the filtering part and therefore fundamental part of the filtering algorithm. Once we have found the best solution, it becomes the completing part of the filter and its efficiency is tested taking some qualitative conclusions on the results obtained from the filtering operation.

The full Matlab code of the algorithm is consultable in the Appendix A.

6. Sinusoids corrupted by harmonics

As I began to explain at the end of the previous chapter, the first step to deal with the study of this filter is the part of the optimization with evolutionary programming algorithm. The fitness function components, $ITAE$ and NG_{max}, are computed for each frequency and their values are used in equation (5.4) for fitness evaluation.

Once we found the optimum solution, after we have performed exhaustive optimization runs, we can use this solution into the filter and, providing the test signal corrupted by the odd harmonics at the input of the filter, verify if the results from the analysis of the output are more or less acceptable compared with those expected. But, how we can define "global optimum" the solution that we found? We cannot know it, but obviously, being our algorithm based on random perturbation used to find the coefficients of h_A and h_B, every time that we have a new run of the code we may obtain a new solution with a different value of the fitness score. In any case we can be satisfied considering runs with a sufficient number of generations and, in this way, we can obtain a competitive solution that we can consider good enough for our problem.

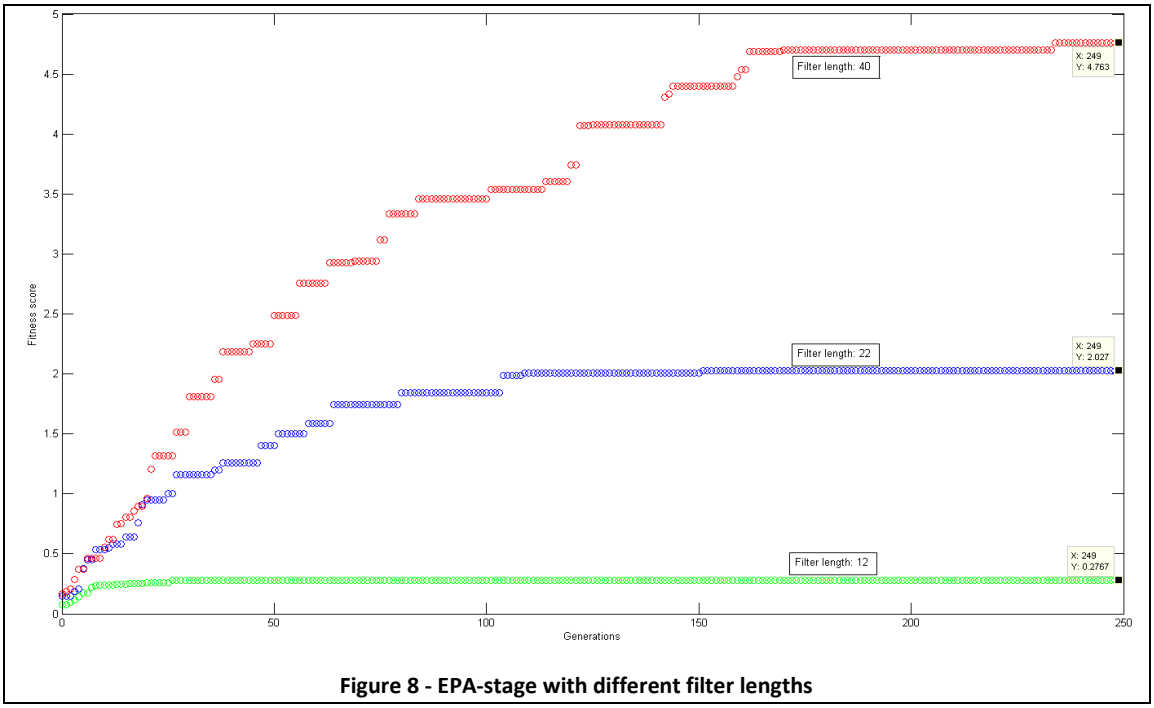

Figure 8 - EPA-stage with different filter lengths

6.1. MGP-FIR filter optimization

The number of candidate solutions N_p and the γ-constant are the only modifiable parameters during the process of optimization. According to the experiences presented in [14], it is practical to choose N_p near to N when designing an N-length filter.

Next the appropriate γ-constant has to be chosen considering that the longer filter we are designing, the smaller γ we should use during the optimization stage [13].

Once that we establish the value of γ, taking into account the results shown in the reference [13], it can be seen that the fitness value is consistently increasing with the length of the filter. This is normal, because longer filters have more degrees of freedom for both controlling the convergence rate and minimizing the noise gain [17]. Figure 8 shows the process of convergence to the optimal solutions of the subfilters coefficients h_A and h_B with different filter lengths. At those values of fitness score correspond different solutions composed by the optimized coefficients of h_A and h_B shown in the table below.

Table 1 - EPA-Optimized coefficients with different filter lengths

γ	N	h_A	h_B
0.004	12	-1-1-1000000111	0001111-1-1000
0.004	22	-1-1-100-100101 11111100010	0001-10-1-10-10 000000-1-1101
0.0005	40	-1-1-1-1-10-100101111 110100000-10-1-1-1-1 -1-1-1-1000001	00000-10-11010000 00-10-1-1-1-1-10-10000 0000111110

In a similar way, the trend of the fitness score has a different behavior if we modify the number of N_p candidate solutions. In this case, the fitness function will need more computational loops to reach the optimal solution and, therefore, a high value if the number of candidate solution is smaller. In Figure 9 there is a comparison between the trends of the fitness function of three EPA stages with N_p = 40, 10 and 4. Every time that we run the code we start from a new initial population and, as we can see considering the first 50 generations, different initial populations may lead to different optimization behavior which we can define to be random. After about 100 generations, the bigger is the number of the candidate solutions considered, the faster (in terms of the number of generations) is the reaching of the highest fitness score.

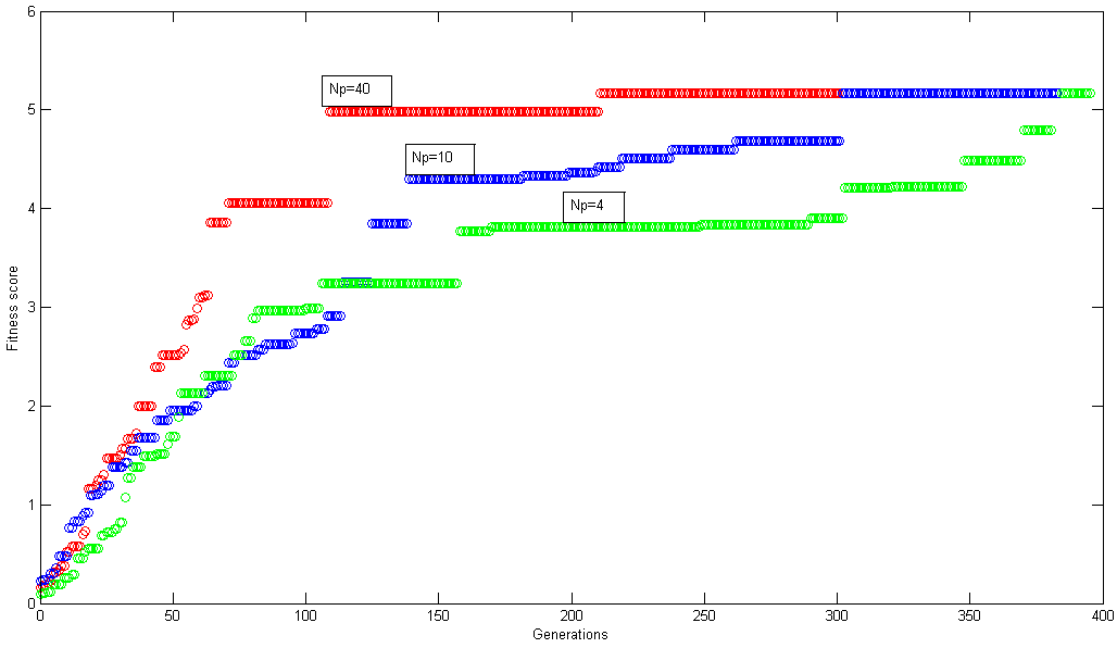

Figure 9 - EPA-stage with different candidate solutions number

In our case, designing a filter with a length $N = 40$, we chose the number of candidate solution $N_p = 40$ and we set $\sigma = 0.0005$.

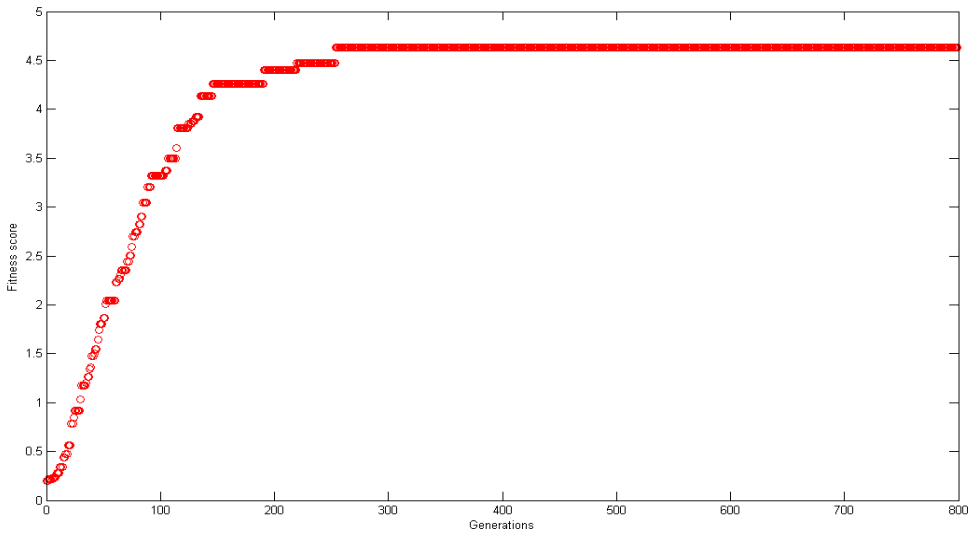

Figure 10 - EPA maximizing the fitness score

To obtain a high-quality solution with a good fitness score, it is necessary to perform a sufficient number of evolutionary programming algorithm iterations, so that the fitness score starts to converge to the best candidate solution. For this reason we chose to perform 800 iterations as shown in Figure 10. As we can see in the plot, the trend of the fitness score starts to converge to the maximum value after almost 250 generations, reaching a fitness score of 4.6341, as shown in the following zoomed plot.

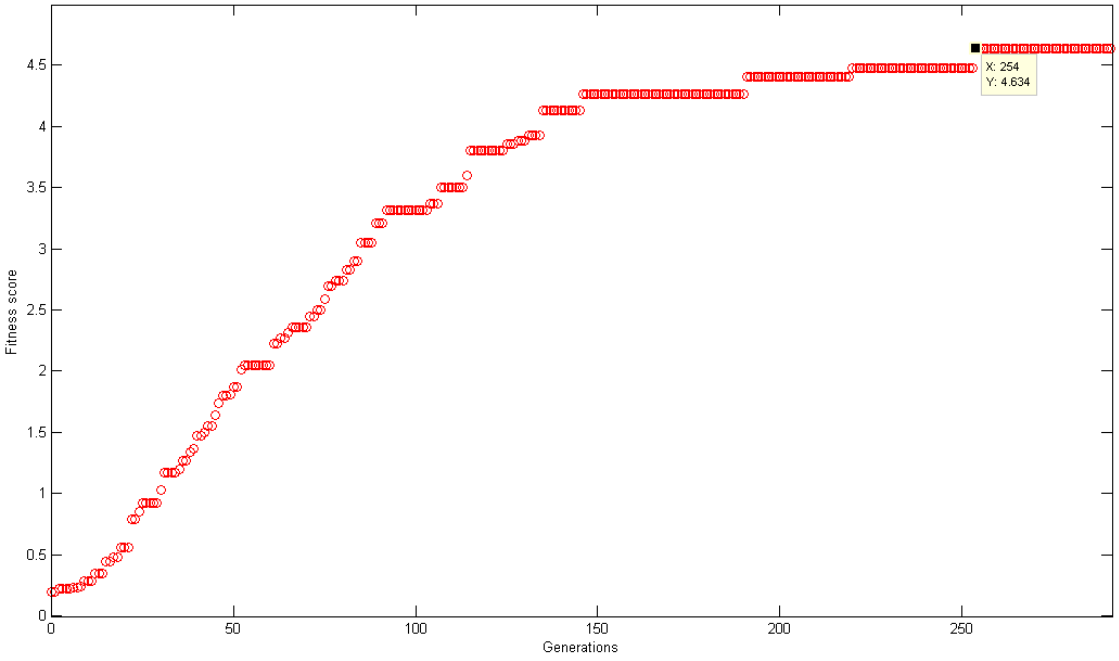

Figure 11 - EPA reaching the maximum fitness score

6.2. Performance verification

At the end of the optimizing stage we obtain the best solution for our filter; in other words we obtain a solution composed by the 40 pairs of coefficients $h_A(k)$ and $h_B(k)$ used to calculate the parameters g_1 and g_2 which are necessary to the filter to build the output signal by filtering the harmonic part that overlaps to the fundamental frequency.

At this point we can test the filter algorithm utilizing the artificial current signals 49/50/51 Hz corrupted by strong third- to thirteenth-order odd harmonics as represented in Figure 12.

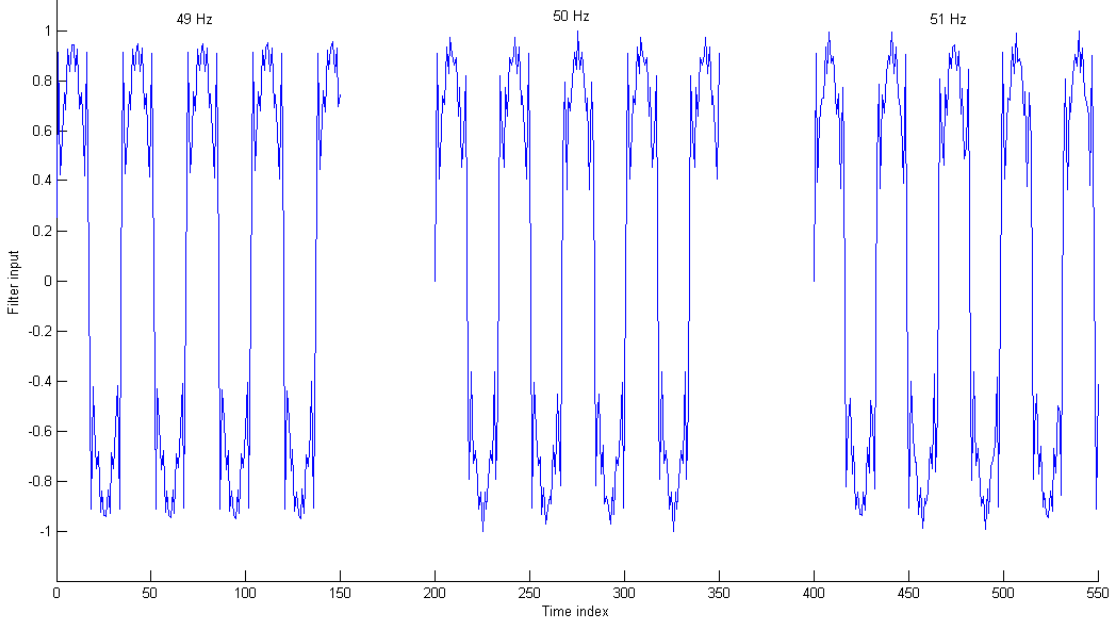

Figure 12 - Artificial current signals corrupted by harmonics

These signals are meant for comprehension purposes only and they are not attributable to the current waveforms of any particular electrical or electronic device. The amplitude of harmonic frequencies and of the fundamental are set in a way to make it easier to understand the attenuation capabilities of the filter. The total harmonic distortion of these test signals is 36.7%, calculable with the formula (2.8) given in the second chapter.

When the test signal is used to feed the optimized MGP-FIR with $N = 40$, the multiplicative general parameters g_1 and g_2 have an adaptive process as shown in the following picture.

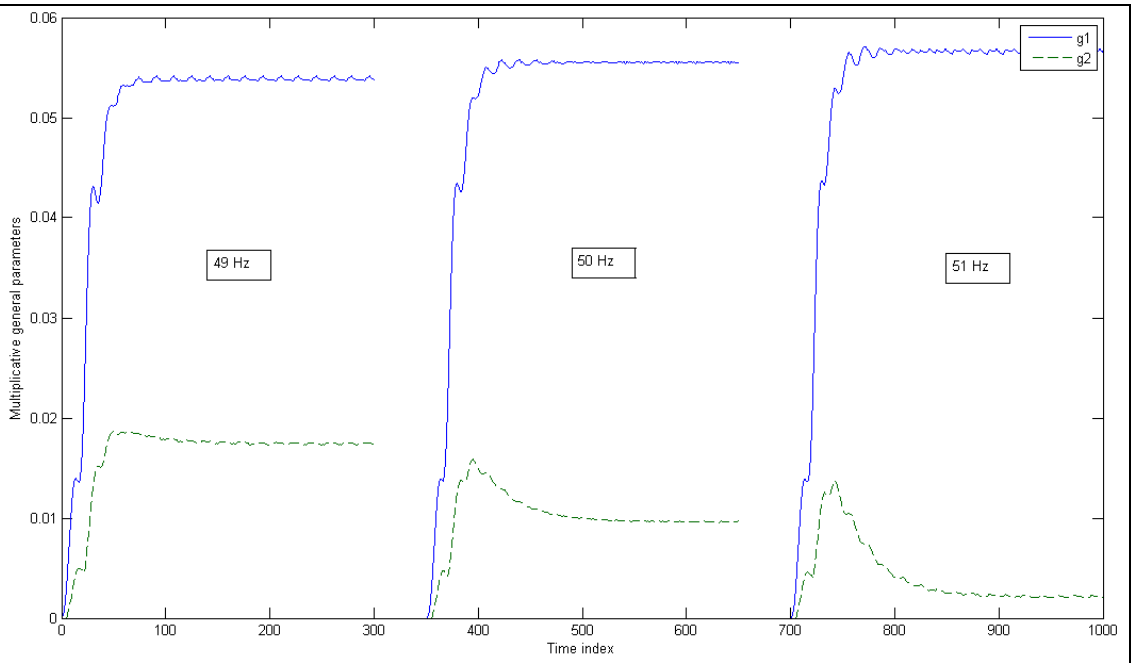

Figure 13 - Adaptation of multiplicative general parameters

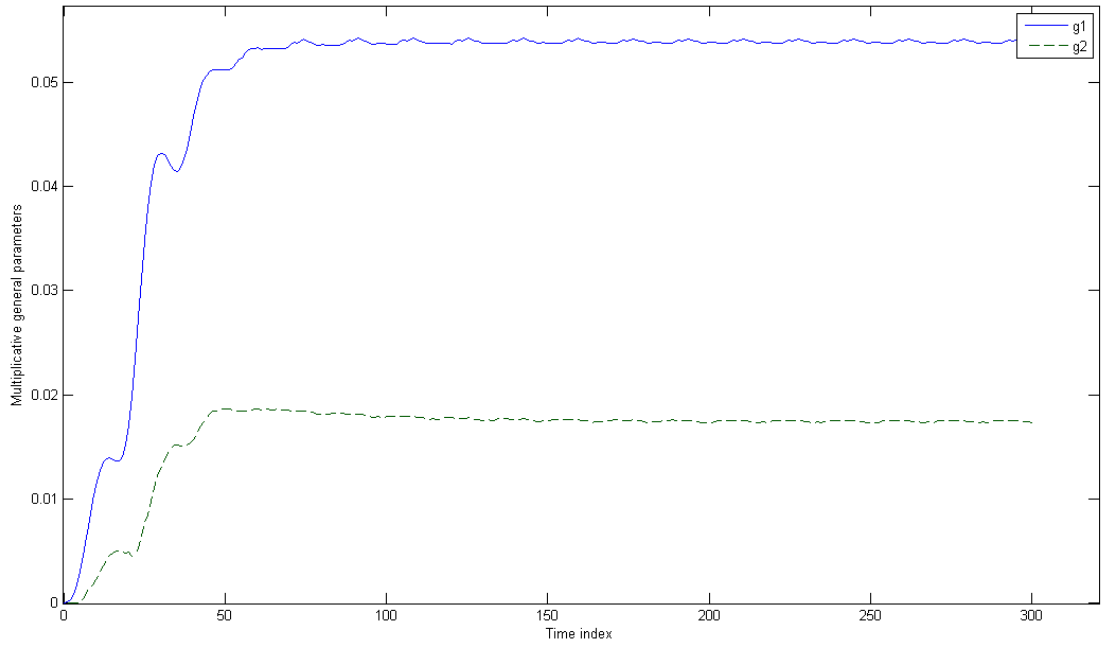

Figure 14 - Oscillations during adaptation of multiplicative general parameters (49 Hz)

As we can see, more or less for all three different frequencies, the adaptation processes converge around 100 samples, and after that the parameters have small periodical oscillation, more visible in the zoomed Figure 14 that refers to the parameters of the signal with fundamental frequency of 49 Hz.

These oscillations are typical for reduced-rank adaptive systems, because the filter cannot track all the correlating signal components [17]. More details about this phenomenon will be given in the following chapters discussing about the filter

generation of new harmonics. At this point, to have a practical proof of the correct operation of the filter, it is useful to make a comparison between the waveform of the input signal and the filter output, cleaned from the harmonics.

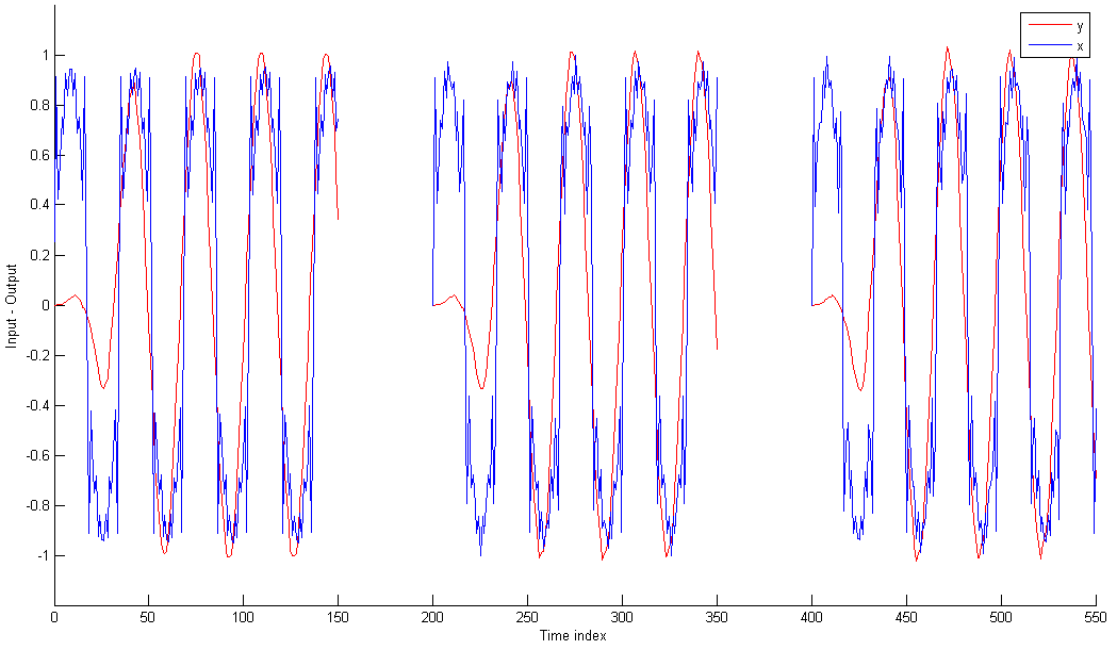

Figure 15 - Comparison input-output of the filter for the three test signals

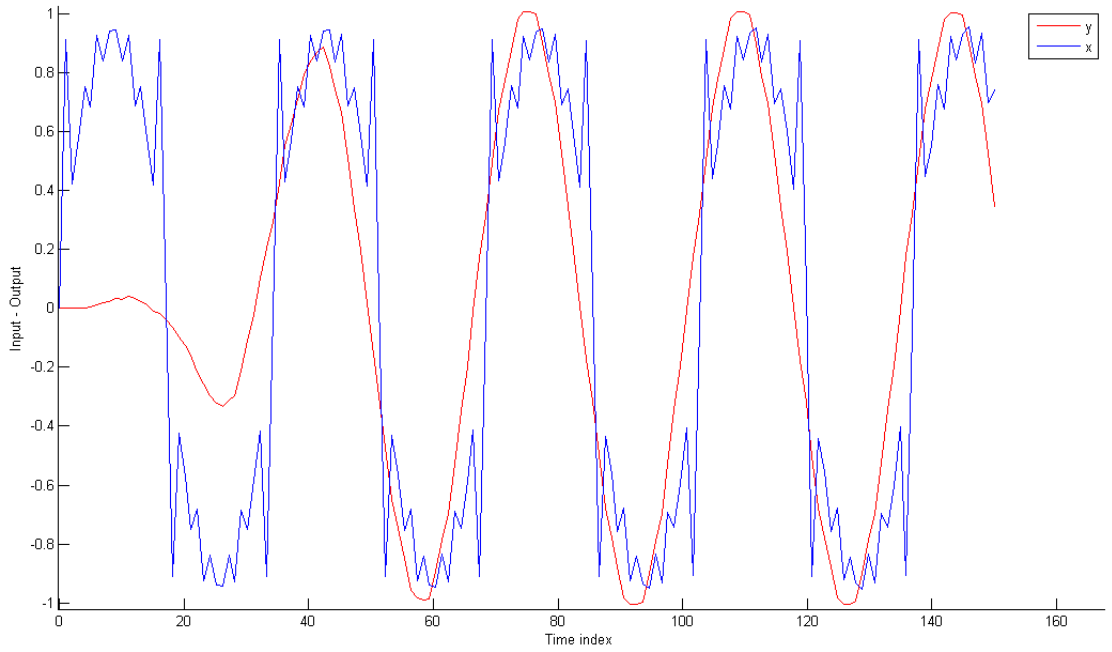

Figure 16 - Comparison input-output of the filter for test signal of 49 Hz

The waveforms of the output, represented with the red line in the pictures, seem good sinusoids and are almost perfectly cleaned from the harmonics. This means that the filter does a great job and the harmonics are almost completely attenuated. Further

evidence can be provided by looking at the error between the outputs and the ideal sine waves with appropriate frequencies (49/50/51 Hz).

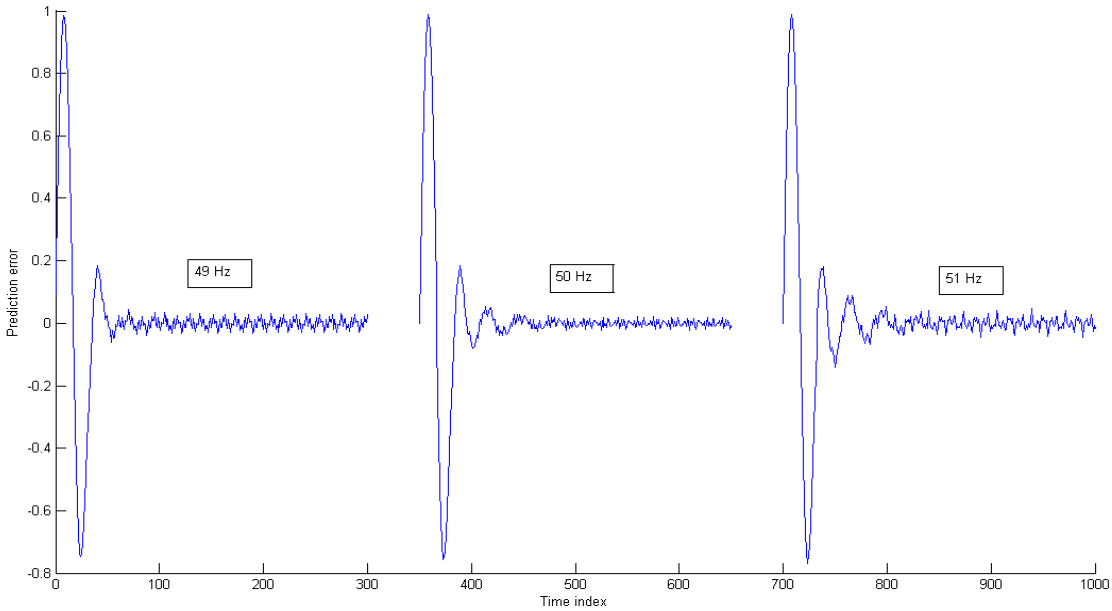

Figure 17 - Prediction error

The image shows how, for all three test signals, the prediction error oscillates around zero immediately after the adaptation step of the multiplicative parameters.

Turning to the frequency domain, we can make a qualitative study of the efficiency of the filter. In fact, going to analyze, by means of the Fourier transform, the spectra of the filter input and output, we can have a better feedback, in terms of quality and numbers, about the attenuation carried out by the filter. Omitting the fundamental frequency, in the following images we can observe at first all odd order harmonics from the third to the thirteenth present in the input signal, and subsequently the spectrum of the output signal that reveals an excellent attenuation, more or less homogeneous, of all harmonics.

Figure 18 refers to the input test signal with fundamental frequency of 49 Hz. It is possible to observe as almost all harmonics are practically cancelled, except the third, the seventh and the eleventh, which are respectively attenuated by 92.6%, 95.8% and 88.3%.

Figure 19 refers, instead, to the input test signal with the fundamental frequency equal to 50 Hz and also in this case it is possible to observe an excellent attenuation of all the odd harmonics. The worst case that can be considered is that of the eleventh harmonic in which there is the worst attenuation, equal to 93.4%.

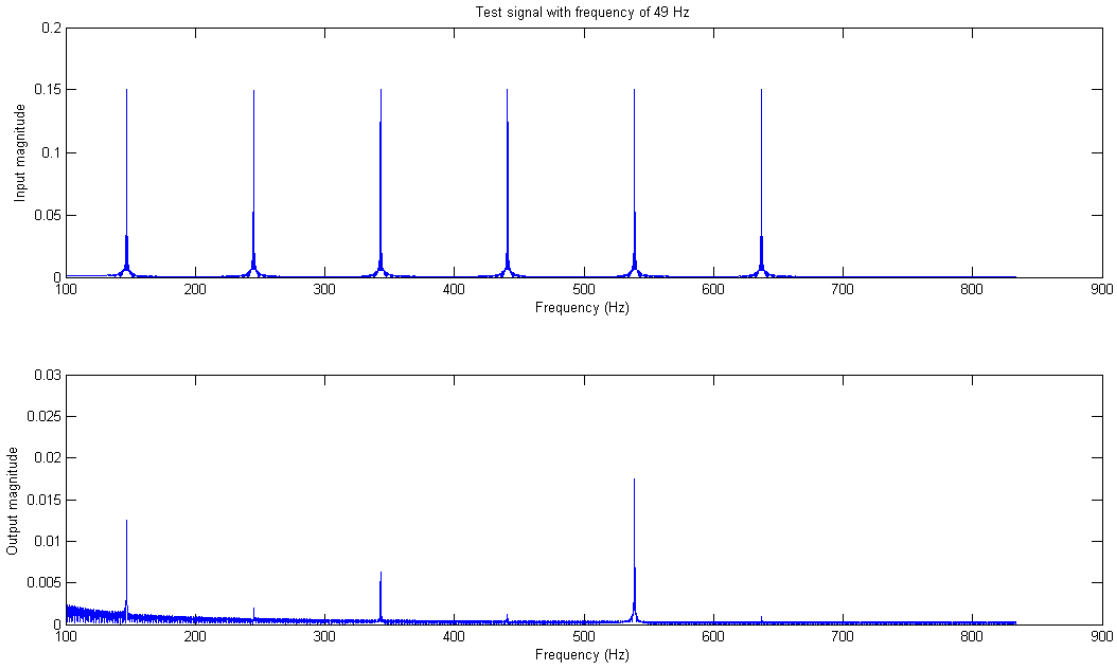

Figure 18 - Input and output spectra with test signal of 49 Hz

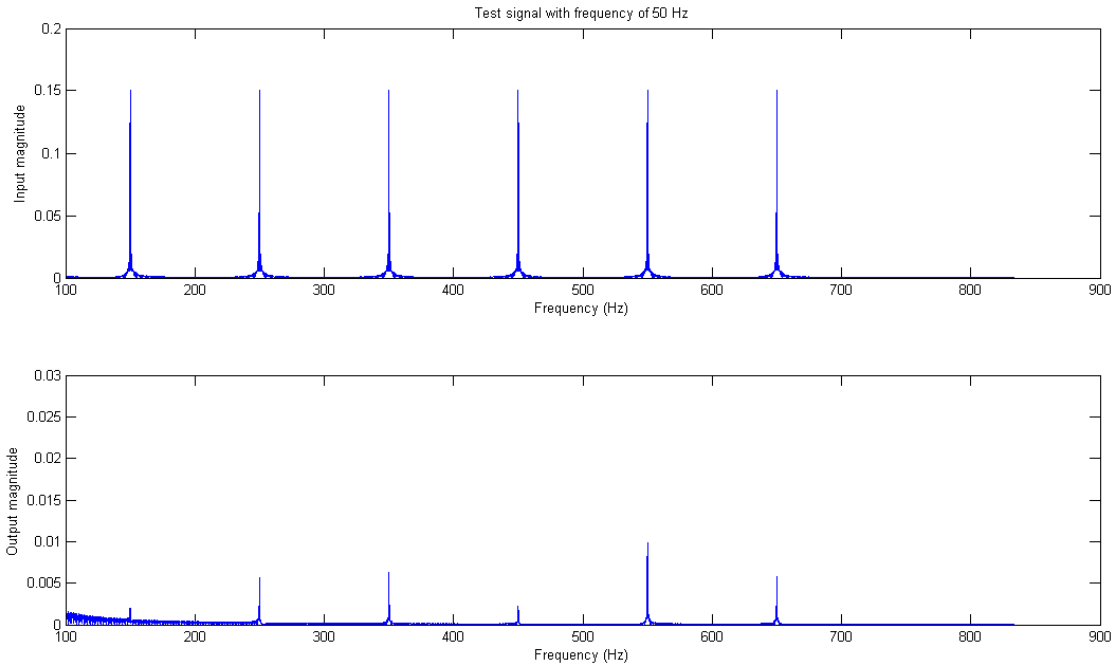

Figure 19 - Input and output spectra with test signal of 50 Hz

For the last case, with the input test signal with fundamental frequency of 51 Hz (Figure 20) we have “the worst general attenuation”: the best attenuated harmonic is the ninth with an abatement of 97%, the worst one is the seventh with an attenuation of 91.5%.

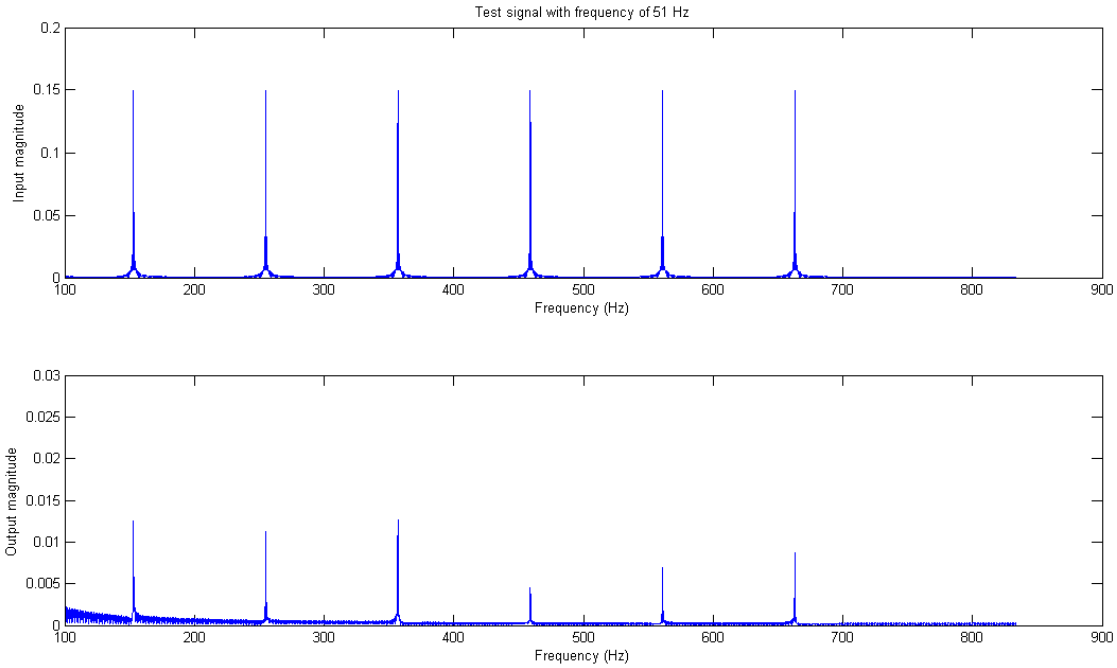

Figure 20 - Input and output spectra with test signal of 51 Hz

The table below shows the amplitudes of the odd harmonics at the filter output. As we can see, the amplitudes of the harmonics in the input signals are all the same. There are different behaviors by analyzing the amplitudes of the harmonics present in the output and from these we can calculate the THD. It can be observed how we can reach a great reduction of the THD in the case, for example, of the signal with a frequency of 50Hz, while the worst result occurs with the input signal of frequency 51 Hz.

Table 2 - Comparison of harmonic contents in filters' input and output

Harmonic Number	Input 49/50/51 Hz	Output 49 Hz	Output 50 Hz	Output 51 Hz
1st	1	1	1	1
3rd	0.15	0.0125	0.0020	0.0125
5th	0.15	0.0020	0.0056	0.0112
7th	0.15	0.0063	0.0063	0.0127
9th	0.15	0.0012	0.0022	0.0045
11th	0.15	0.0175	0.0098	0.0069
13th	0.15	0.0010	0.0058	0.0087
THD %	36.7	2.25	1.45	2.42

A final analysis can be undertaken evaluating the instantaneous magnitude response of the filter, with the three different test signals in the input with frequency 49/50/51 Hz.

As we can see in Figure 21, Figure 22 and Figure 23, this filtering approach offers good characteristics of selective bandpass response and effective attenuation of specific harmonic components, those one with odd order. We do not care about the peaks present at the other frequencies because they are related to frequencies which are not present in the input signals and to which we are not interested; therefore they do not represent a problem in our application.

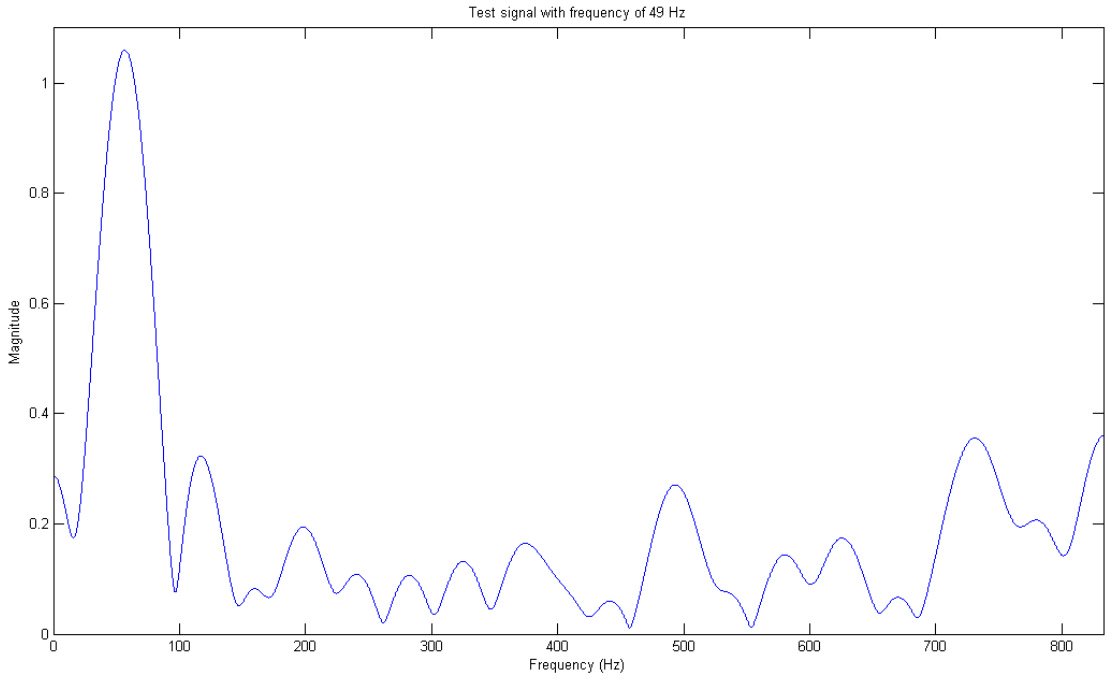

Figure 21 - Instantaneous magnitude response of the filter with test signal of 49 Hz

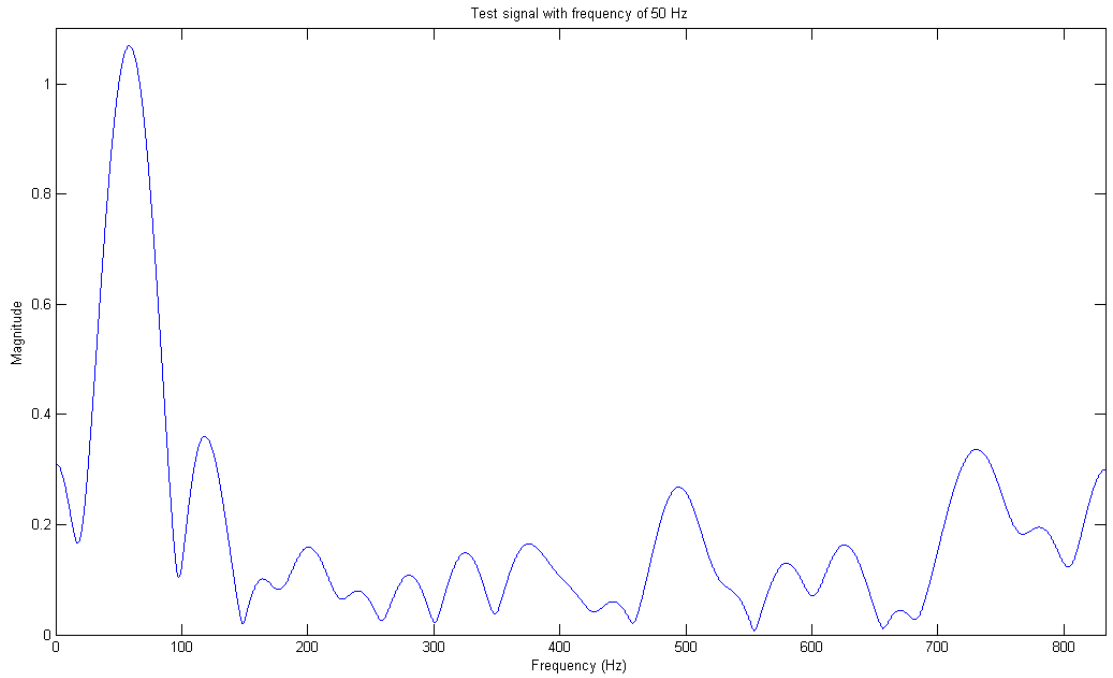

Figure 22 - Instantaneous magnitude response of the filter with test signal of 50 Hz

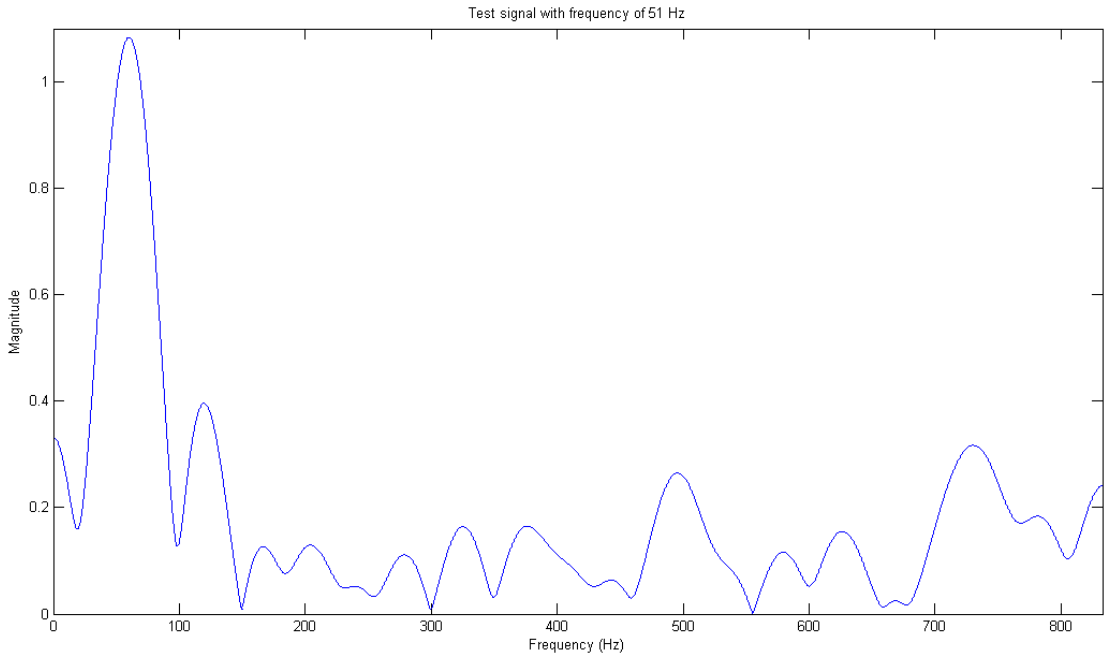

Figure 23 - Instantaneous magnitude response of the filter with test signal of 51 Hz

7. New harmonics generation

As mentioned in the previous chapter, observing the process of adaptation of the two multiplicative parameters g_1 and g_2 it is obvious to conclude that there is the presence of a fluctuating trend. These periodical oscillations of the two parameters used for the calculation of the output of the filter lead us to conclude that new harmonics, different than those in the input, may be present in the output signal and they are automatically generated by the adaptive process.

7.1. Detection of the new harmonics

We start to address this problem with a new research of the global optimum solution composed by two multiplicative parameters, and the study of their waveforms:

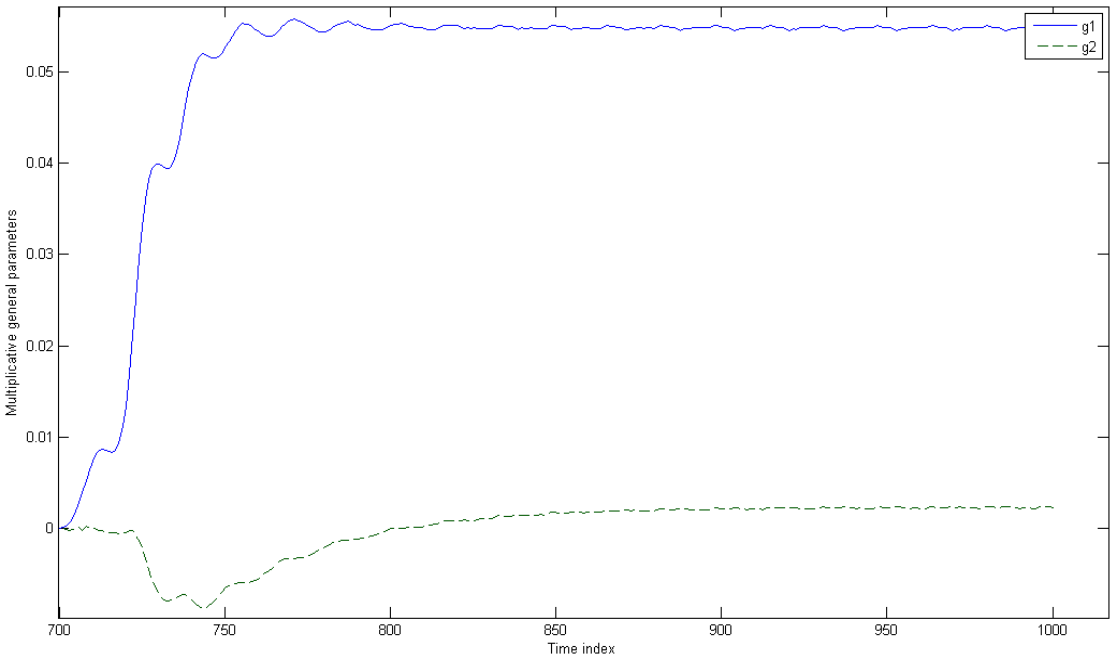

Figure 24 - Oscillations during adaptation of multiplicative general parameters (51 Hz)

The picture above shows the periodically oscillating trends during the adaptive process of g_1 and g_2. More details are observable in Figure 25 and Figure 26 where the oscillations are more visible.

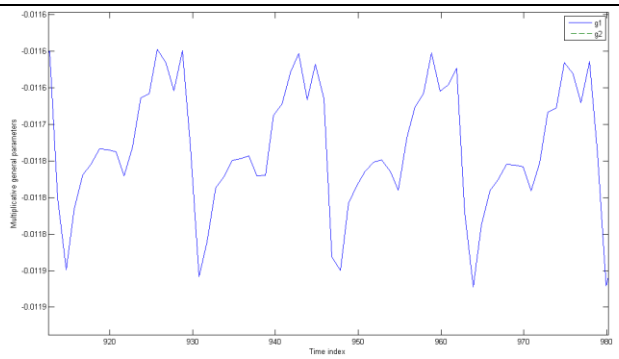

Figure 25 - Periodical oscillation during the adaptation process of g_1

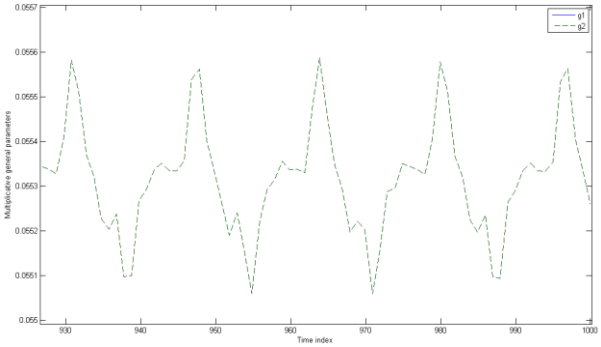

Figure 26 - Periodical oscillation during the adaptation process of g_2

To study better this problem, it is good to limit our analysis using an input test signal with the presence of only one odd order harmonic at time.

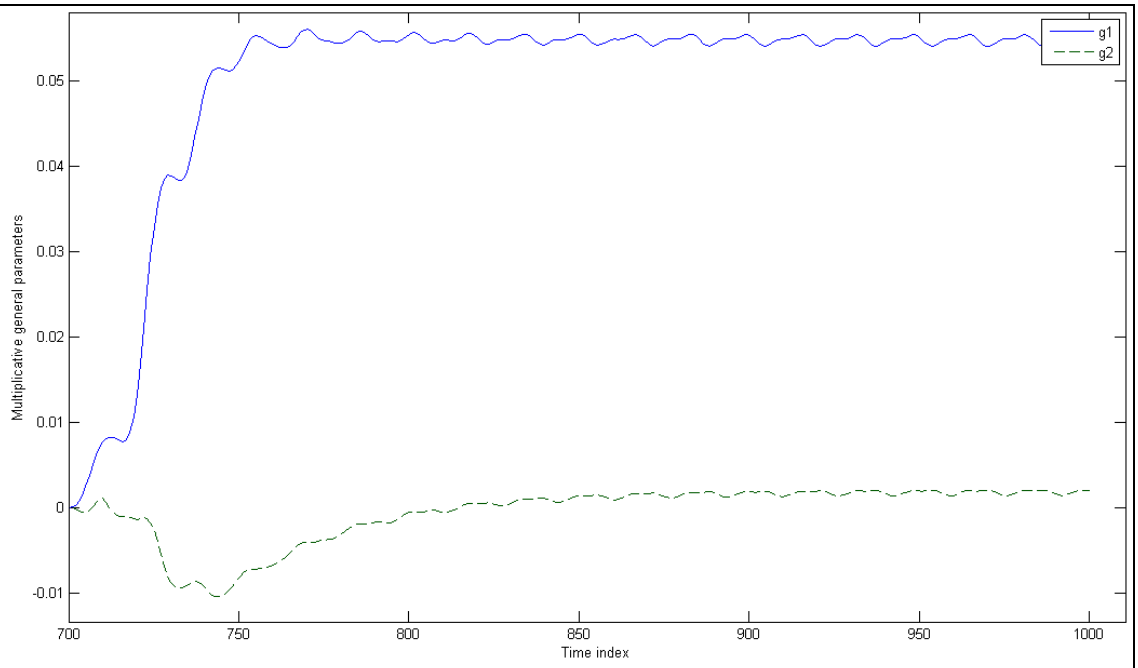

Figure 27 - Multiplicative general parameters adaptation with only the 3rd harmonic in the input signal (51 Hz)

We can consider for example the only presence of the third order odd harmonic, with slightly amplified amplitude so we can better detect the presence of any new harmonics. In the Figure 27 we can observe that the oscillating behavior of the multiplicative parameters is still present during the adaptive stage and it appears more amplified compared with the general case in which the input test signal is corrupted by all harmonics from 3rd to 13th order.

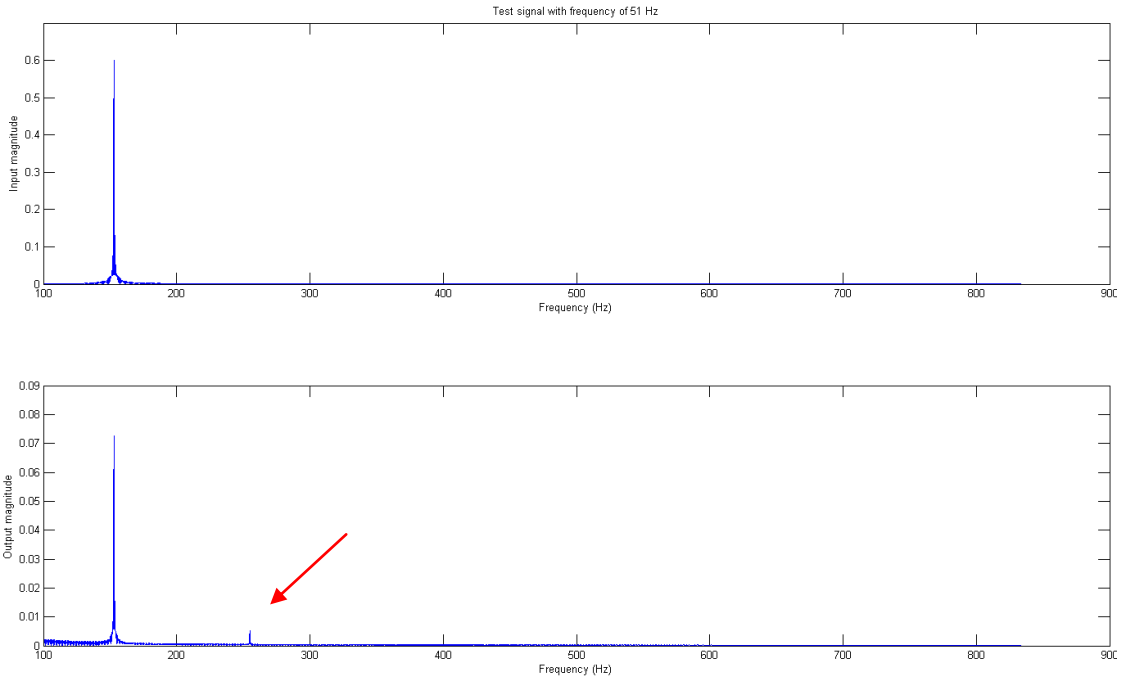

Figure 28 - Presence of a new harmonic in the output

At this point, if we analyze the spectrum of the output (Figure 28), we can observe that the third harmonic is well attenuated, in fact it appears to have amplitude in the input signal of 0.6 while in the output the amplitude is only about 0.07 but there is present also another harmonic, the one of the fifth order. This one was not part of the input signal so we can deduce that has been generated within our filtering algorithm. The fifth harmonic is clearly visible but we cannot be sure that it is the only one because also other harmonics could be present but with lower amplitudes.

7.2. Analytical motivation of the problem

The generation of new harmonics has to have an analytical motivation. They are generated within our filtering algorithm, so in this section we will try to find the reason analyzing better the mathematical equations on which the filter is based.

Reviewing the equations for the calculation of the two multiplicative parameters that we saw in the fifth chapter:

$$g_1(n+1)=g_1(n)+\mu[x_F(n)-y(n-p)]\sum_{k=0}^{N-1} h_A(k)x(n-k) \quad (7.1)$$

$$g_2(n+1)=g_2(n)+\mu[x_F(n)-y(n-p)]\sum_{k=0}^{N-1} h_B(k)x(n-k) \quad (7.2)$$

and the equations of the input and that one to calculate the output:

$$y(n)=g_1(n)\sum_{k=0}^{N-1} h_A(k)x(n-k) + g_2(n)\sum_{k=0}^{N-1} h_B(k)x(n-k) \quad (7.3)$$

$$x(n) = sin(\omega T_S n) + \sum_{m\in\{3,5,7,9,11,13\}} 0.15 \cdot sin(\omega m T_S n) \quad (7.4)$$

We can modify the equation of the input to consider a simple example with the presence of only the 3rd harmonic with amplitude slightly increased:

$$x(n) = sin(\omega T_S n) + 0.6 \cdot sin(3\omega T_S n) \quad (7.5)$$

To further simplify the research of new harmonics, we can totally omit the numerical coefficients representing the amplitude of sines and concentrate only on the order of frequencies that will meet during this analysis.

Observing the equations (7.1) and (7.2) it can be deduced that they are composed of two main terms:

- Prediction error $[x_F(n)-y(n-p)]$
- Filtering part $\sum_{k=0}^{N-1} h(k)x(n-k)$

If we assume that the error between the ideal signal and the actual minimum is approximated to a simple error of amplitude of the fundamental sine wave, whereas we not analyze the amplitudes, we can write:

$$[x_F(n)-y(n-p)] = \sin(\omega T_S n) \quad (7.6)$$

For the filtering part we cannot consider an ideal case in which the third harmonic is completely filtered and canceled, but we can assume that our filter performs a good job letting unchanged the fundamental frequency and attenuating the amplitude of the third harmonic. Without considering the multiplicative coefficients, we can write:

$$\sum_{k=0}^{N-1} h(k)x(n-k) = \sin(\omega T_S n) + \sin(3\omega T_S n) \quad (7.7)$$

With the above assumptions and the known trigonometric equation:

$$\sin(\alpha)\sin(\beta) = \frac{1}{2}[\cos(\alpha-\beta) - \cos(\alpha+\beta)]$$

and hypothesizing to be in the first step, we rewrite the equation (7.1) considering that also μ is a simple numerical coefficient (for the multiplicative parameter g_2 is the same):

$$\begin{aligned} g_1(1) &= \sin(\omega T_S)\,[\sin(\omega T_S n) + \sin(3\omega T_S)] \\ &= \frac{1}{2}[1 + \cos(2\omega T_S)] + \frac{1}{2}[\cos(2\omega T_S) + \cos(4\omega T_S)] \\ &= \frac{1}{2} + \cos(2\omega T_S) + \frac{1}{2}\cos(4\omega T_S) \end{aligned}$$

With the same assumptions and using the trigonometric equation:

$$\sin(\alpha)\cos(\beta) = \frac{1}{2}[\sin(\alpha+\beta) + \sin(\alpha-\beta)]$$

we can calculate the output, observing that the terms which compose it are the coefficients g_1 and g_2 just calculated and the filtering part:

$$\begin{aligned} y(1) &= g_1(1)\sum_{k=0}^{N-1} h_A(k)\,x(1-k) + \cdots \\ &= \left[\frac{1}{2} + \cos(2\omega T_S) + \frac{1}{2}\cos(4\omega T_S)\right][\sin(\omega T_S) + \sin(3\omega T_S)] + \cdots \\ &= \frac{1}{2}[\sin(\omega T_S) + \sin(3\omega T_S)] + \\ &\quad + \frac{1}{2}[\sin(3\omega T_S) - \sin(\omega T_S)] + \frac{1}{2}[\sin(5\omega T_S) + \sin(\omega T_S)] + \\ &\quad + \frac{1}{2}[\sin(5\omega T_S) - \sin(3\omega T_S)] + \frac{1}{2}[\sin(7\omega T_S) - \sin(\omega T_S)] + \cdots \end{aligned}$$

Leaving aside the signs and considering that in an ideal case we do not have the zeroing for mathematical annulment of the sines, we can conclude that given an input signal consisting of a fundamental sine wave plus the harmonic of third order, using our algorithm, in output we will find the filtered input signal with the addition of two new odd harmonics: the fifth and the seventh.

$$y(1) = \sin(\omega T_S) + \sin(3\omega T_S) + \sin(5\omega T_S) + \sin(7\omega T_S)$$

This signal is then used to calculate the prediction error then, the new harmonics will also be present in the two multiplicative parameters g_1 and g_2.

7.3. Analysis with one harmonic in the input signal

Now that we know the reason for the generation of new harmonics, we can make an analysis feeding our filter with the fundamental frequency plus one odd harmonic at time and see what we find in the adaptive process of the two multiplicative coefficients and in the output. In the following pictures are presented the spectral analysis results of the adaption process of multiplicative parameters g_1 and g_2 and of the filter output for the test signal at the frequency of 50 Hz and with an odd harmonic from the 3rd to the 13th at time.

As we can see in all the graphs relating to the two multiplicative parameters, in the Figure 29 and in the Figure 30, the spectrum of g_1 and g_2 always presents the odd harmonic injected with the input signal plus the first harmonic of one higher order. In some cases are quite clearly visible even other higher order harmonics, but the first one with odd-order higher than the injected harmonic, has always very strong amplitude.

In all cases, it is the single injection of the harmonic of the third order which causes the generation of a new more evident harmonic (the fifth).

With regard to the spectrum of the output, by analyzing the graphs in the Figure 31, we can conclude that it is never too evident the presence of harmonics of higher or lower order than that one of the harmonic injected in input, but by the action of the filter it has a magnitude highly attenuated.

Finally, the Table 3 shows the amplitudes of the main harmonics present in the spectra of the two multiplicative parameters and of the output. To have a qualitative limit beyond which the amplitude of a harmonic can be considered relevant, I decided to consider only the harmonics with amplitude greater than 0.05, which are the harmonics with an amplitude higher than about 8% of that one injected with the test signal in input (with amplitude of 0.6). In the rows of the table there are one by one the harmonics injected individually with the test signal, while in the columns we can observe the new generated harmonics.

The Matlab code relative to this research part is consultable in the Appendix B and in the Appendix C are presented the figures relative to the analysis with the test signals at the frequencies of 49 and 51 Hz.

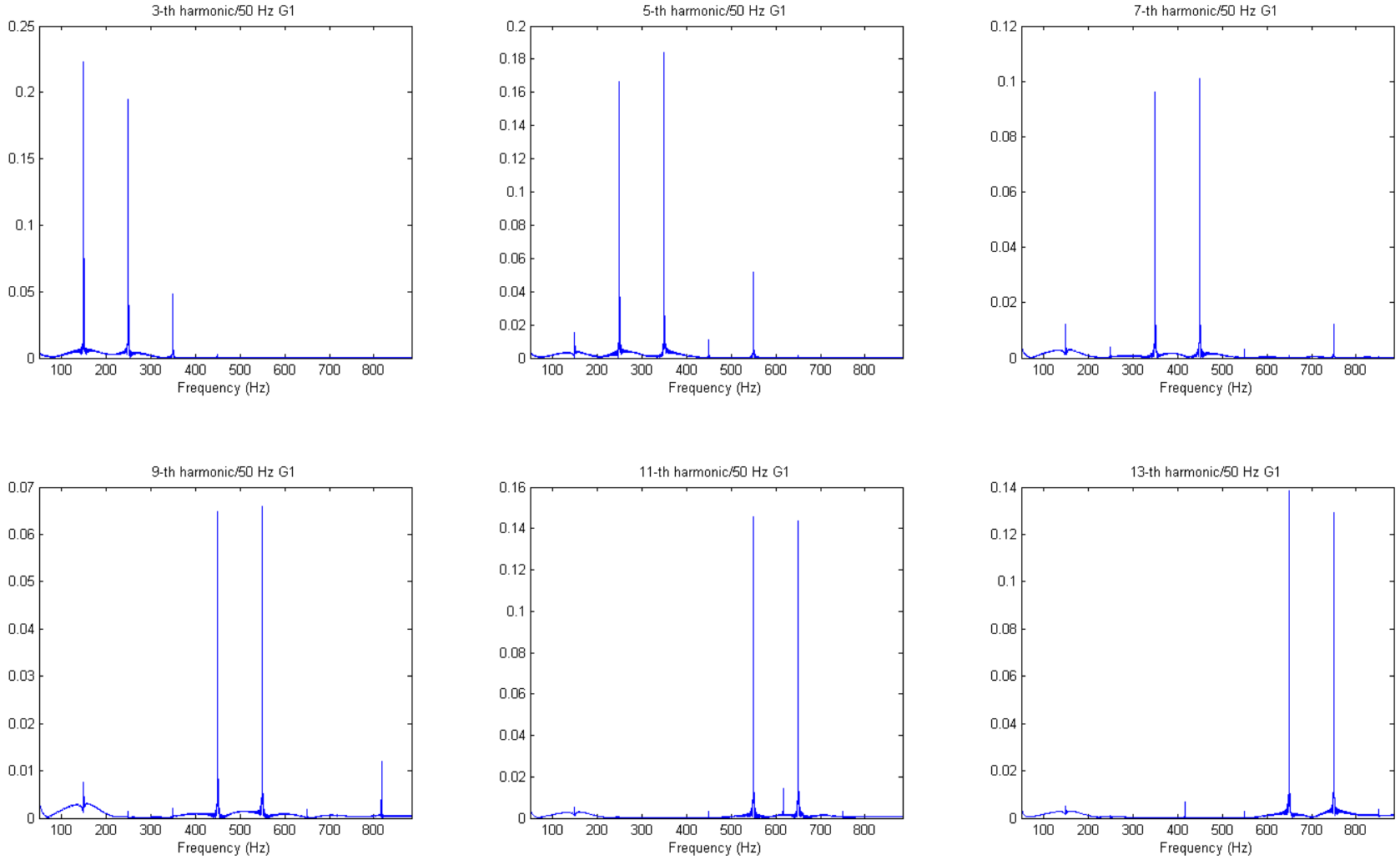

Figure 29 - Analysis of g_1 (50Hz) with one harmonic in the input signal

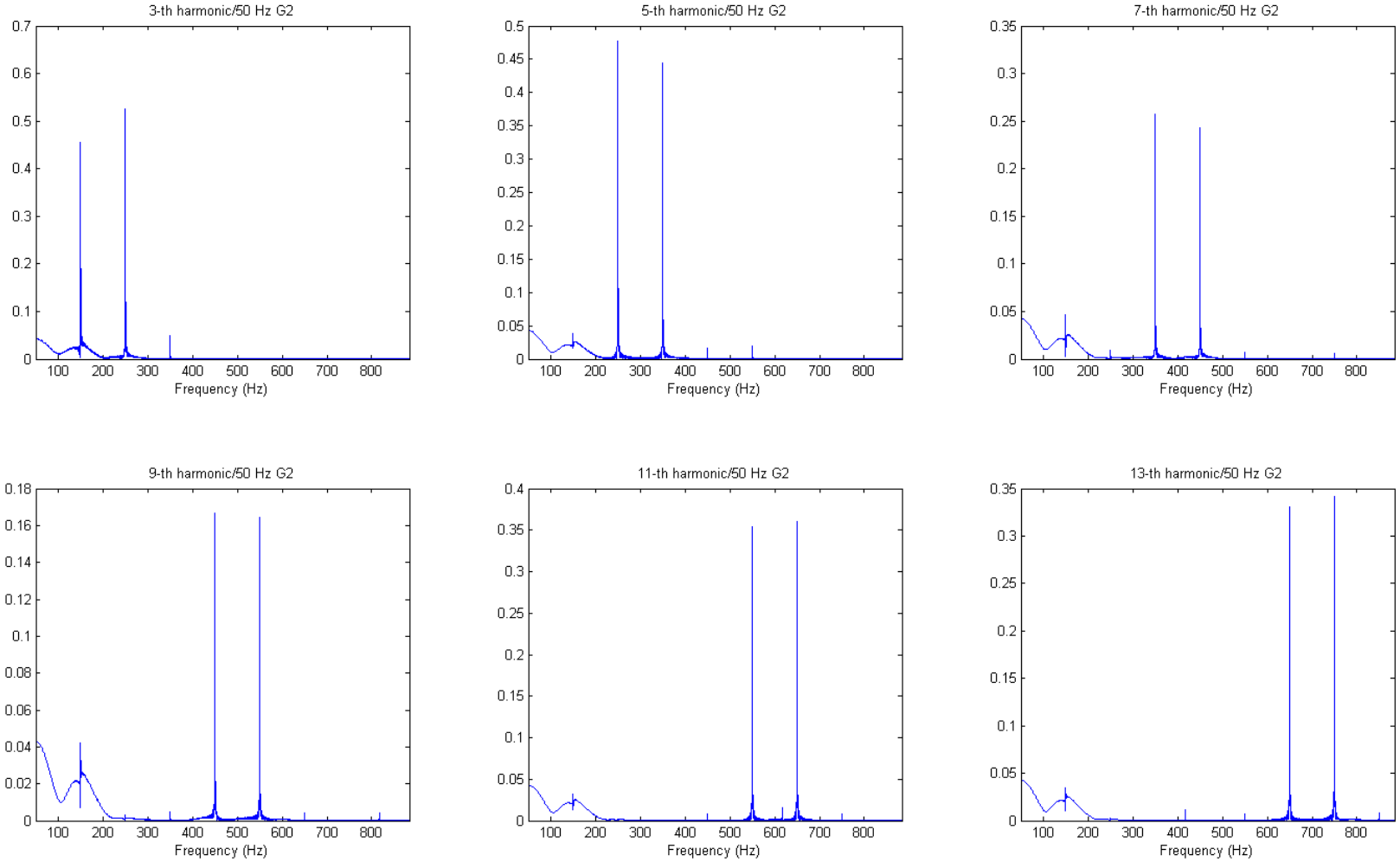

Figure 30 - Analysis of g_2 (50Hz) with one harmonic in the input signal

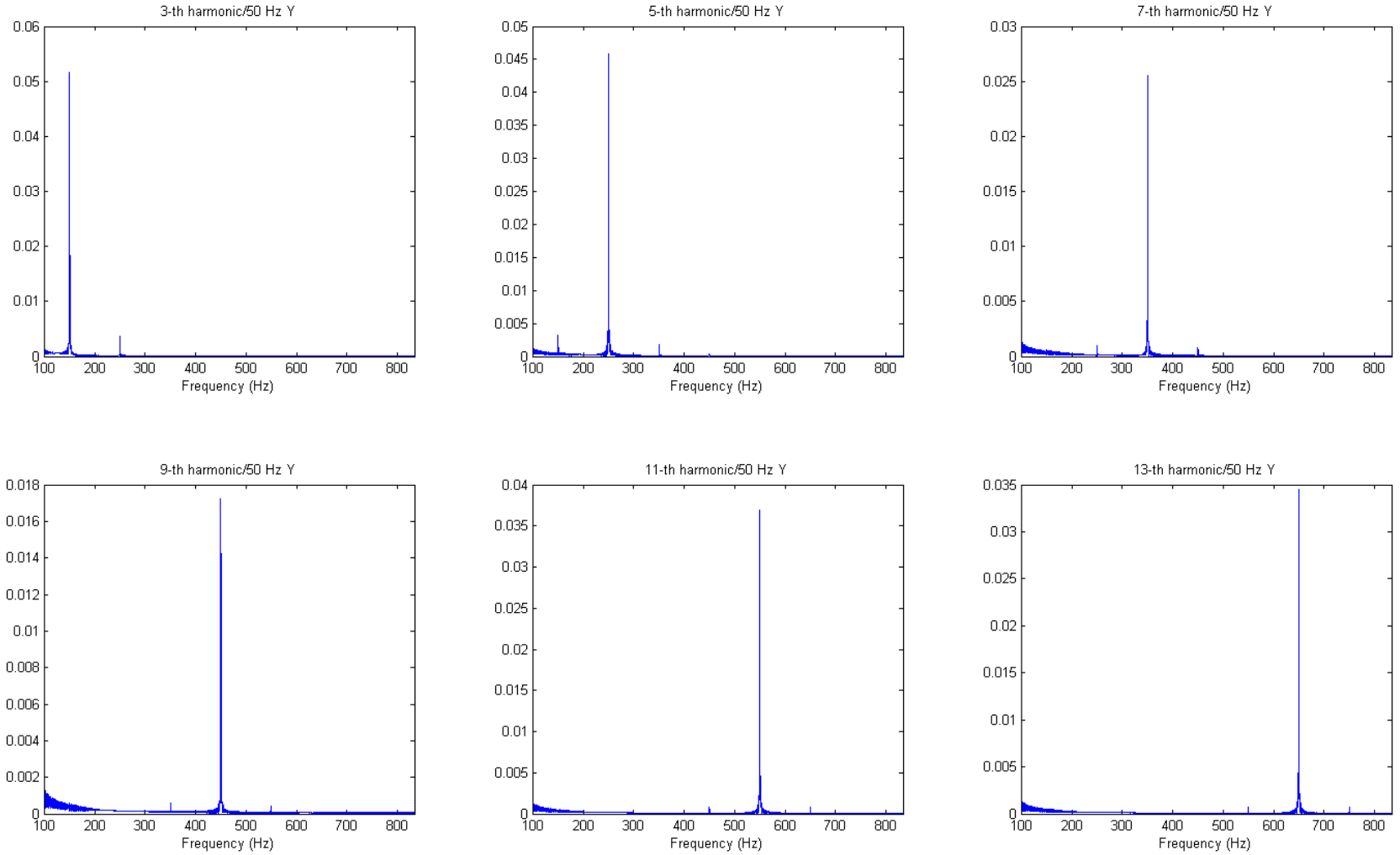

Figure 31 - Analysis of the output (50Hz) with one harmonic in the input signal

Table 3 - Amplitudes of the main new generated harmonics in the spectra of g_1, g_2 and output with one harmonic in the input signal at 49/50/51 Hz

49 Hz - G1_FFT analysis

	3-th	5-th	7-th	9-th	11-th	13-th	15-th
3-th	0.2994	0.2636	0.0530	0	0	0	0
5-th	0	0.1925	0.2106	0	0.0567	0	0
7-th	0	0	0	0	0	0	0
9-th	0	0	0	0.1503	0.1532	0	0
11-th	0	0	0	0	0.0982	0.0940	0
13-th	0	0	0	0	0	0.1567	0.1445

49 Hz - G2_FFT analysis

	3-th	5-th	7-th	9-th	11-th	13-th	15-th
3-th	0.6151	0.7160	0.0873	0	0	0	0
5-th	0	0.5500	0.5134	0	0	0	0
7-th	0	0	0.1269	0.1213	0	0	0
9-th	0.0618	0	0	0.3864	0.3801	0	0
11-th	0	0	0	0	0.2378	0.2401	0
13-th	0.0691	0	0	0	0	0.3806	0.3903

49 Hz - Y_FFT analysis

	3-th	5-th	7-th	9-th	11-th	13-th	15-th
3-th	0.0707	0	0	0	0	0	0
5-th	0	0.0542	0	0	0	0	0
7-th	0	0	0	0	0	0	0
9-th	0	0	0	0	0	0	0
11-th	0	0	0	0	0	0	0
13-th	0	0	0	0	0	0	0

50 Hz - G1_FFT analysis

	3-th	5-th	7-th	9-th	11-th	13-th	15-th
3-th	0.2229	0.1949	0	0	0	0	0
5-th	0	0.1664	0.1838	0	0.0514	0	0
7-th	0	0	0.0963	0.1009	0	0	0
9-th	0	0	0	0.0649	0.0658	0	0
11-th	0	0	0	0	0.1457	0.1438	0
13-th	0	0	0	0	0	0.1384	0.1291

50 Hz - G2_FFT analysis

	3-th	5-th	7-th	9-th	11-th	13-th	15-th
3-th	0.4547	0.5253	0	0	0	0	0
5-th	0	0.4767	0.4440	0	0	0	0
7-th	0	0	0.2576	0.2433	0	0	0
9-th	0	0	0	0.1668	0.1643	0	0
11-th	0	0	0	0	0.3538	0.3601	0
13-th	0	0	0	0	0	0.3309	0.3415

50 Hz - Y_FFT analysis

	3-th	5-th	7-th	9-th	11-th	13-th	15-th
3-th	0.0517	0	0	0	0	0	0
5-th	0	0	0	0	0	0	0
7-th	0	0	0	0	0	0	0
9-th	0	0	0	0	0	0	0
11-th	0	0	0	0	0	0	0
13-th	0	0	0	0	0	0	0

51 Hz - G1_FFT analysis

	3-th	5-th	7-th	9-th	11-th	13-th	15-th
3-th	0.2916	0.2727	0.0832	0	0	0	0
5-th	0	0.1270	0.1426	0	0	0	0
7-th	0	0	0.2375	0.2518	0	0	0
9-th	0	0	0	0.1092	0.1094	0	0
11-th	0	0	0	0	0.2062	0.2036	0
13-th	0	0	0	0	0	0.1158	0.1102

51 Hz - G2_FFT analysis

	3-th	5-th	7-th	9-th	11-th	13-th	15-th
3-th	0.6673	0.7361	0.0509	0	0	0	0
5-th	0	0.3663	0.3405	0	0	0	0
7-th	0.1129	0	0.6394	0.6054	0	0	0
9-th	0	0	0	0.2671	0.2637	0	0
11-th	0	0	0	0	0.4967	0.5039	0
13-th	0	0	0	0	0	0.2777	0.2875

51 Hz - Y_FFT analysis

	3-th	5-th	7-th	9-th	11-th	13-th	15-th
3-th	0.0713	0	0	0	0	0	0
5-th	0	0	0	0	0	0	0
7-th	0	0	0.0634	0	0	0	0
9-th	0	0	0	0	0	0	0
11-th	0	0	0	0	0.0512	0	0
13-th	0	0	0	0	0	0	0

7.4. Analysis with two harmonics in the input signal

In a similar way, we can make an analysis feeding the filter with the fundamental frequency plus two odd harmonics at time and see what are the new harmonics generated during the adaptive process of the two multiplicative coefficients and in the output. In the following pages the pictures show the spectral analysis results of the adaption process of multiplicative parameters g_1 and g_2 and of the filter output for the test signal at the frequency of 50 Hz with all the possible pairs of odd harmonics from the 3rd to the 13th.

Unlike the previous analysis, observing the Figure 32 and Figure 33 relating to the two multiplicative parameters, we can observe the generation of even harmonics. They are well visible in the spectrum of both g_1 and g_2 and are included in the range between the 4th and the 17th. In both figures it is possible to observe as in the spectra the density of new harmonics generated is increased only for some pairs of harmonics in the input signal, such as the fifth and the ninth, the fifth and the thirteenth or the ninth and thirteenth. Moreover, unlike the spectrum of g_2 where almost all the harmonics have an amplitude smaller than that one of the two harmonics in input (0.6 also in this analysis), in the spectrum of g_1 is possible to observe that in some cases certain harmonics are strongly amplified during the adaptive process reaching amplitudes higher than 1. This fact is quite unique and distinctive and is always present even if we try to process the search for a new optimal solution of the filter coefficients, passing perhaps to have larger amplitudes in the multiplicative parameter g_2. It is assumed that the motivation is connected to the zeros present between the coefficients of h_A, used to calculate g_1, or between the coefficients of h_B, used to calculate g_2.

Analyzing the spectrum of the output in the Figure 34, we have never the presence of the 7th to 17th order harmonics but, in some cases, it is possible to observe a new harmonic, that one of 2nd order. In all cases the harmonics present in input are well attenuated by the action of the filter, as evidenced by the fact that no harmonic has an amplitude greater than 0.15.

Finally, the Table 4 shows the amplitudes of the main harmonics present in the spectra of the two multiplicative parameters and of the output. Also in this analysis, to have a qualitative limit beyond which the amplitude of a harmonic can be considered relevant, I decided to consider only the harmonics with amplitude greater than 0.05. In the rows of the table there are one by one the pairs of the harmonics injected with the test signal, while in the columns we can observe the new generated harmonics.

In the Appendix D is consultable the Matlab code relative to this research part.

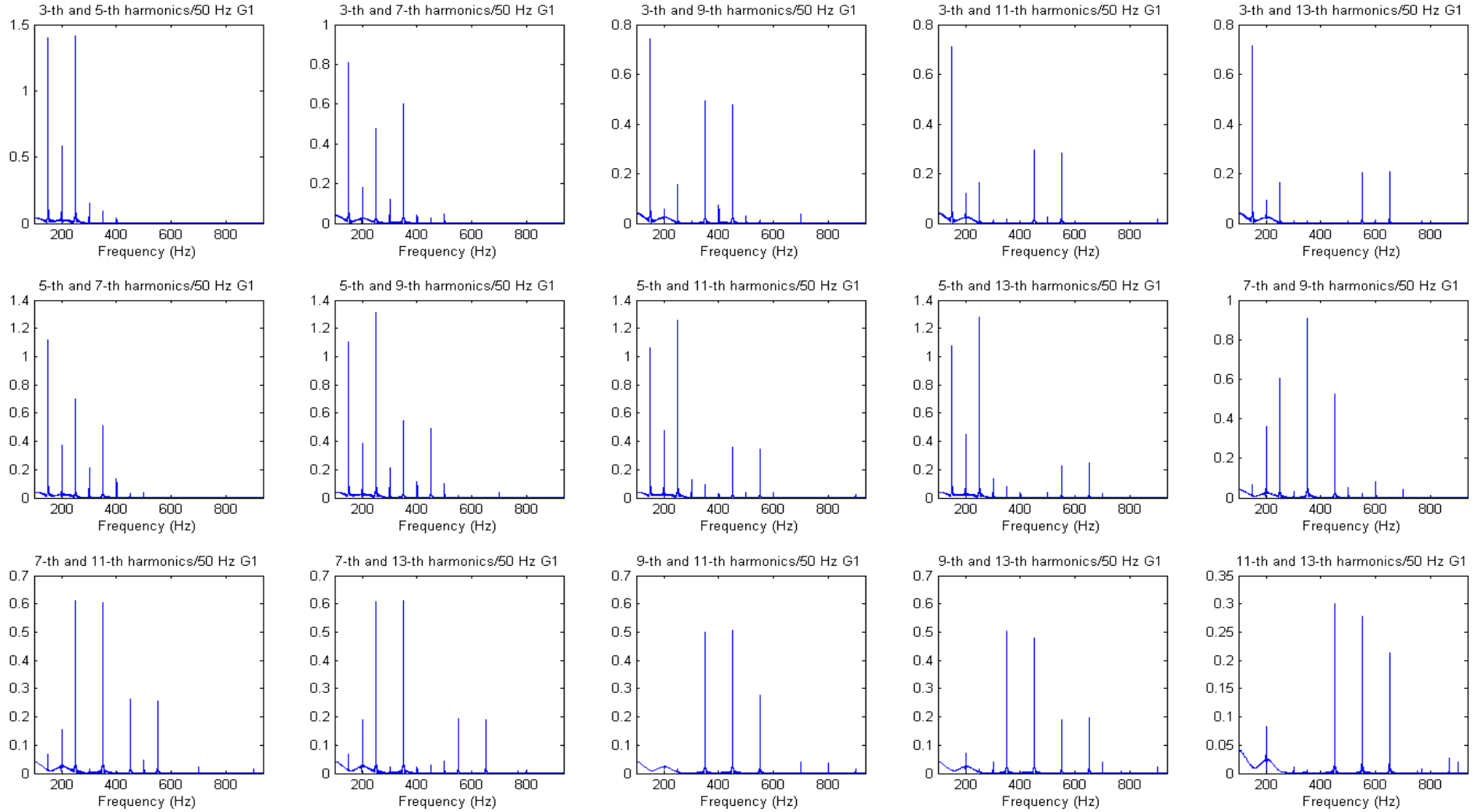

Figure 32 - Analysis of g_1 (50Hz) with two harmonics in the input signal

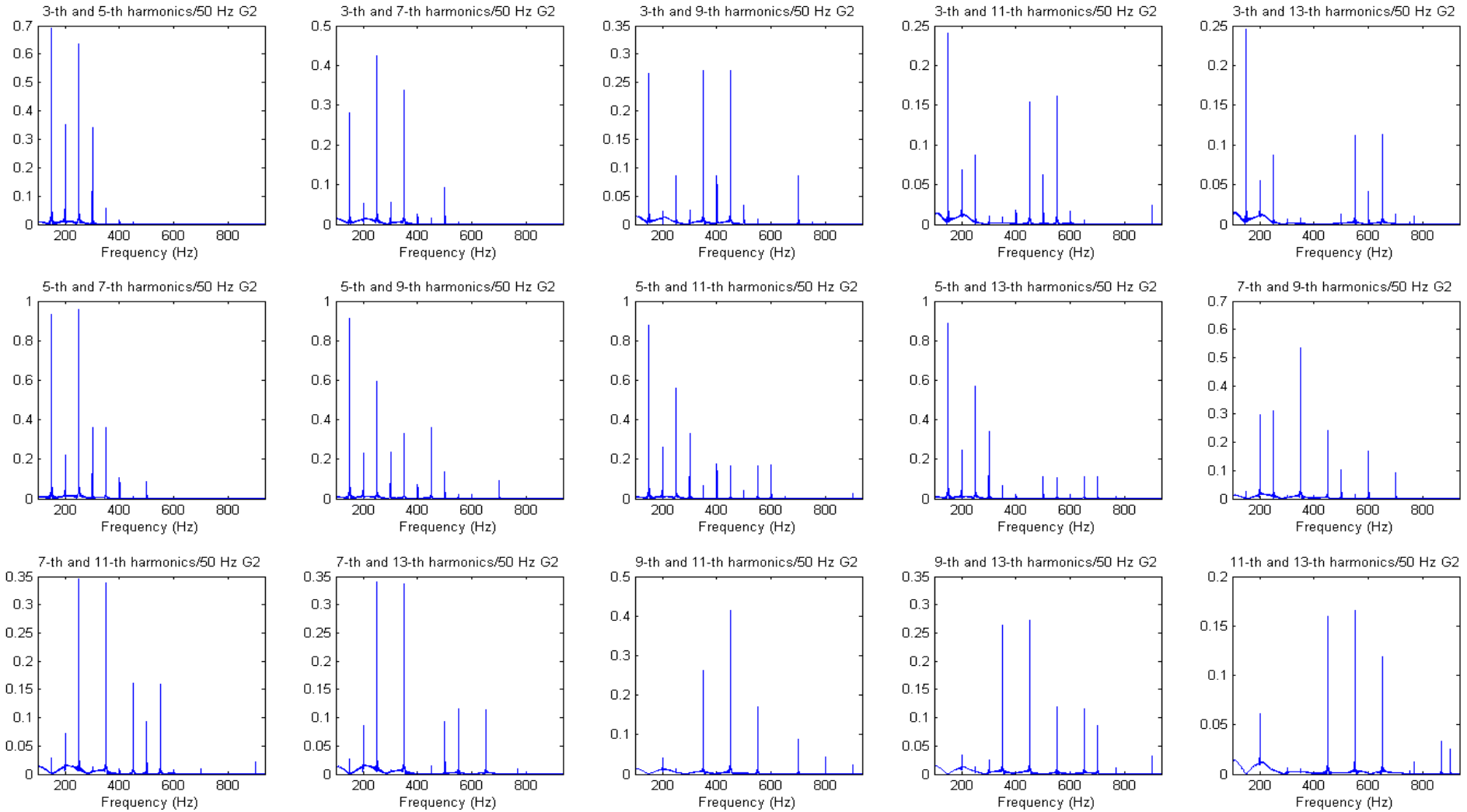

Figure 33 - Analysis of g_2 (50Hz) with two harmonics in the input signal

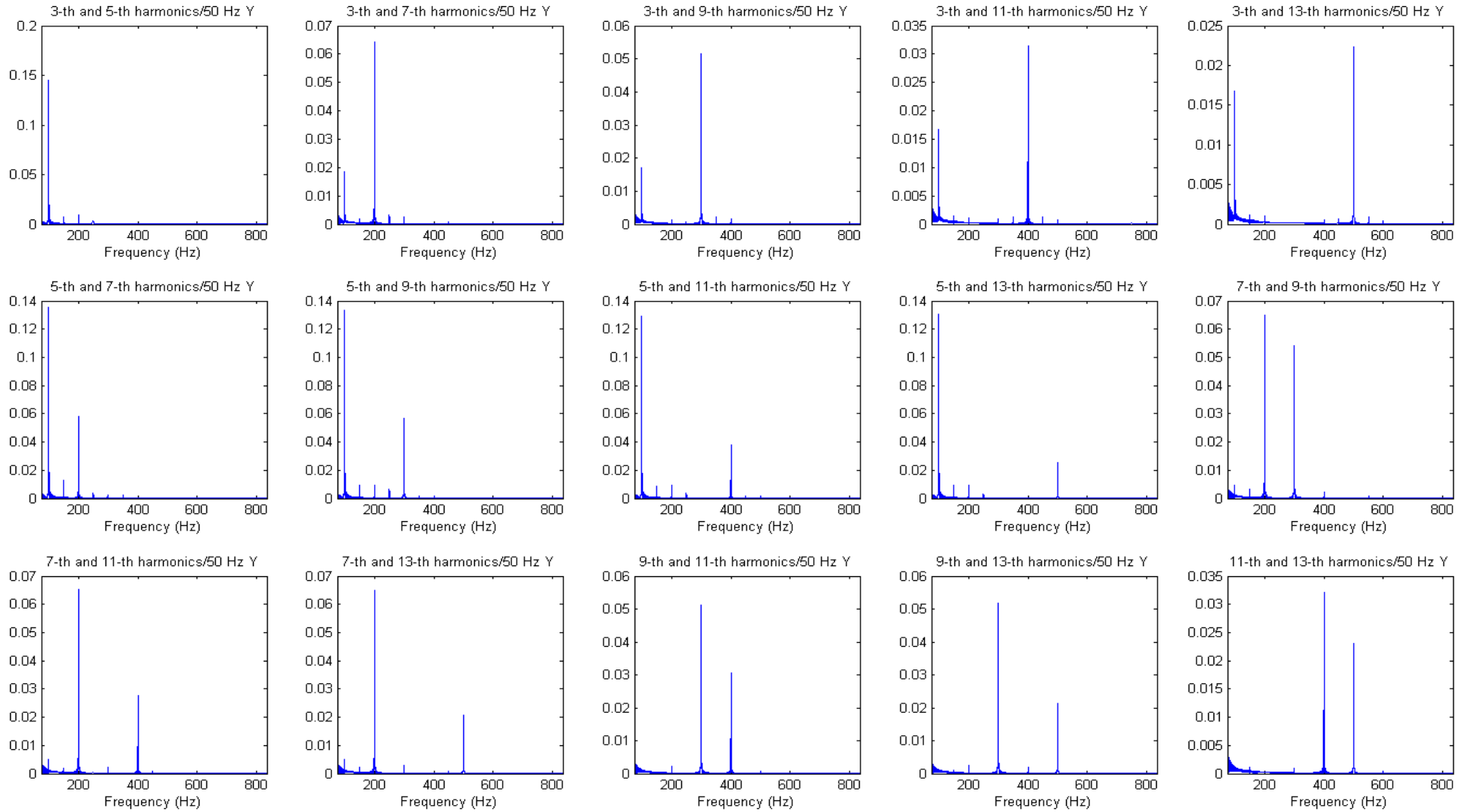

Figure 34 - Analysis of the output (50Hz) with two harmonics in the input signal

Table 4 - Amplitudes of the main new generated harmonics in the spectra of g_1, g_2 and output with two harmonics in the input signal at 50 Hz

50 Hz - G1_FFT analysis

	3-th	4-th	5-th	6-th	7-th	8-th	9-th	10-th	11-th	12-th	13-th	14-th	15-th	16-th	17-th
3-th + 5-th	1.4030	0.5856	1.4160	0.1548	0.0901	0	0	0	0	0	0	0	0	0	0
3-th + 7-th	0.8103	0.1784	0.4788	0.1207	0.5990	0	0	0	0	0	0	0	0	0	0
3-th + 9-th	0.7443	0.0557	0.1553	0	0.4913	0.0748	0.4773	0	0	0	0	0	0	0	0
3-th + 11-th	0.7122	0.1222	0.1633	0	0	0	0.2951	0	0.2850	0	0	0	0	0	0
3-th + 13-th	0.7166	0.0919	0.1630	0	0	0	0	0	0.2050	0	0.2071	0	0	0	0
5-th + 7-th	1.1214	0.3693	0.7008	0.2133	0.5132	0.1360	0	0	0	0	0	0	0	0	0
5-th + 9-th	1.1007	0.3899	1.3159	0.2154	0.5453	0.1169	0.4919	0.0998	0	0	0	0	0	0	0
5-th + 11-th	1.0595	0.4782	1.2588	0.1301	0.0920	0	0.3591	0	0.3451	0	0	0	0	0	0
5-th + 13-th	1.0743	0.4490	1.2759	0.1380	0.0823	0	0	0	0.2275	0	0.2439	0	0	0	0
7-th + 9-th	0.0667	0.3588	0.6050	0	0.9086	0	0.5245	0.0505	0	0.0833	0	0	0	0	0
7-th + 11-th	0.0677	0.1559	0.6118	0	0.6050	0	0.2633	0	0.2547	0	0	0	0	0	0
7-th + 13-th	0.0680	0.1892	0.6094	0	0.6096	0	0	0	0.1931	0	0.1911	0	0	0	0
9-th + 11-th	0	0	0	0	0.4998	0	0.5074	0	0.2778	0	0	0	0	0	0
9-th + 13-th	0	0.0727	0	0	0.5023	0	0.4804	0	0.1883	0	0.1975	0	0	0	0
11-th + 13-th	0	0.0834	0	0	0	0	0.3010	0	0.2786	0	0.2134	0	0	0	0

50 Hz - G2_FFT analysis

	3-th	4-th	5-th	6-th	7-th	8-th	9-th	10-th	11-th	12-th	13-th	14-th	15-th	16-th	17-th
3-th + 5-th	0.6909	0.3519	0.6351	0.3402	0.0555	0	0	0	0	0	0	0	0	0	0
3-th + 7-th	0.2810	0.0528	0.4253	0.0550	0.3385	0	0	0.0929	0	0	0	0	0	0	0
3-th + 9-th	0.2660	0	0.0863	0	0.2703	0.0858	0.2714	0	0	0	0	0.0851	0	0	0
3-th + 11-th	0.2405	0.0683	0.0875	0	0	0	0.1541	0.0623	0.1613	0	0	0	0	0	0
3-th + 13-th	0.2460	0.0551	0.0873	0	0	0	0	0	0.1118	0	0.1131	0	0	0	0
5-th + 7-th	0.9343	0.2239	0.9595	0.3602	0.3631	0.1053	0	0.0868	0	0	0	0	0	0	0
5-th + 9-th	0.9133	0.2325	0.5923	0.2387	0.3305	0.0711	0.3619	0.1358	0	0	0	0.0934	0	0	0
5-th + 11-th	0.8780	0.2615	0.5579	0.3286	0.0693	0.1790	0.1679	0	0.1676	0.1703	0	0	0	0	0
5-th + 13-th	0.8886	0.2460	0.5718	0.3396	0.0692	0	0	0.1136	0.1084	0	0.1116	0.1141	0	0	0
7-th + 9-th	0	0.2992	0.3129	0	0.5334	0	0.2420	0.1028	0	0.1675	0	0.0922	0	0	0
7-th + 11-th	0	0.0728	0.3451	0	0.3390	0	0.1617	0.0939	0.1600	0	0	0	0	0	0
7-th + 13-th	0	0.0860	0.3412	0	0.3365	0	0	0.0939	0.1157	0	0.1145	0	0	0	0
9-th + 11-th	0	0	0	0	0.2624	0	0.4138	0	0.1695	0	0	0.0873	0	0	0
9-th + 13-th	0	0	0	0	0.2645	0	0.2730	0	0.1187	0	0.1159	0.0861	0	0	0
11-th + 13-th	0	0.0616	0	0	0	0	0.1602	0	0.1662	0	0.1185	0	0	0	0

50 Hz - Y_FFT analysis

	2-th	3-th	4-th	5-th	6-th	7-th	8-th	9-th	10-th	11-th	12-th	13-th	14-th	15-th	16-th	17-th
3-th + 5-th	0.1447	0	0	0	0	0	0	0	0	0	0	0	0	0	0	0
3-th + 7-th	0	0	0.0643	0	0	0	0	0	0	0	0	0	0	0	0	0
3-th + 9-th	0	0	0	0	0.0516	0	0	0	0	0	0	0	0	0	0	0
3-th + 11-th	0	0	0	0	0	0	0	0	0	0	0	0	0	0	0	0
3-th + 13-th	0	0	0	0	0	0	0	0	0	0	0	0	0	0	0	0
5-th + 7-th	0.1357	0	0.0580	0	0	0	0	0	0	0	0	0	0	0	0	0
5-th + 9-th	0.1336	0	0	0	0.0571	0	0	0	0	0	0	0	0	0	0	0
5-th + 11-th	0.1289	0	0	0	0	0	0	0	0	0	0	0	0	0	0	0
5-th + 13-th	0.1304	0	0	0	0	0	0	0	0	0	0	0	0	0	0	0
7-th + 9-th	0	0	0.0650	0	0.0542	0	0	0	0	0	0	0	0	0	0	0
7-th + 11-th	0	0	0.0652	0	0	0	0	0	0	0	0	0	0	0	0	0
7-th + 13-th	0	0	0.0651	0	0	0	0	0	0	0	0	0	0	0	0	0
9-th + 11-th	0	0	0	0	0.0513	0	0	0	0	0	0	0	0	0	0	0
9-th + 13-th	0	0	0	0	0.0518	0	0	0	0	0	0	0	0	0	0	0
11-th + 13-th	0	0	0	0	0	0	0	0	0	0	0	0	0	0	0	0

8. Consideration of the signs

The FPGAs are digital integrated circuits whose implemented functionality is not set by the manufacturer so that he can produce it on a large scale at low cost. As devices that do not have a great computational power, it is important to find a compromise between the processing time required and the operations that the integrated circuit has to perform. To open the doors to the cost-effective implementation of our filter on one of these devices, it is important to try to simplify the computations that our filtering algorithm has to perform during its operational process. During this stage, we test our filter returning to use the test signal composed by all the odd order harmonics, from the third to the thirteenth, with amplitude equal to 0.15. The idea is to simplify the arithmetic calculations starting from the first operation that the algorithm performs, that is the calculation of the coefficients g_1 and g_2. Recall the two equations for their calculation:

$$g_1(n+1)=g_1(n)+\mu[x_F(n)-y(n-p)]\sum_{k=0}^{N-1}h_A(k)x(n-k) \quad (8.1)$$

$$g_2(n+1)=g_2(n)+\mu[x_F(n)-y(n-p)]\sum_{k=0}^{N-1}h_B(k)x(n-k) \quad (8.2)$$

The simplest idea for the simplification of the calculations is to take account only the sign (±1) of the two terms which compose the equations and are already discussed in the previous chapter: prediction error and filtering part.

Going in order, we will try to analyze the behavior of the filter, taking into account only the sign of the prediction error, observing the output signal and calculating the THD, and then performing the same analysis for the filtering part. If the results will be positive, we will try to analyze a simultaneous consideration of both the signs of the two terms, reaching the maximum level of simplification.

Obviously, the first consideration to make is that we have to change the value of μ because with these updates we will have a change in the timing of convergence of the two multiplicative parameters.

8.1. Sign of the prediction error

As we know, the prediction error is the error between the output of our filter and the ideal output. Considering that the maximum amplitude of the sine wave is equal to 1, until now, the calculated prediction error was a number with an absolute value

always less than 1 and with positive or negative sign. With this change, evaluating the sign of the prediction error, we always have a value greater than before, and because we keep unchanged the value of the filtering part, we will go to reduce our constant μ to reach a satisfactory convergence of the multiplicative parameters.

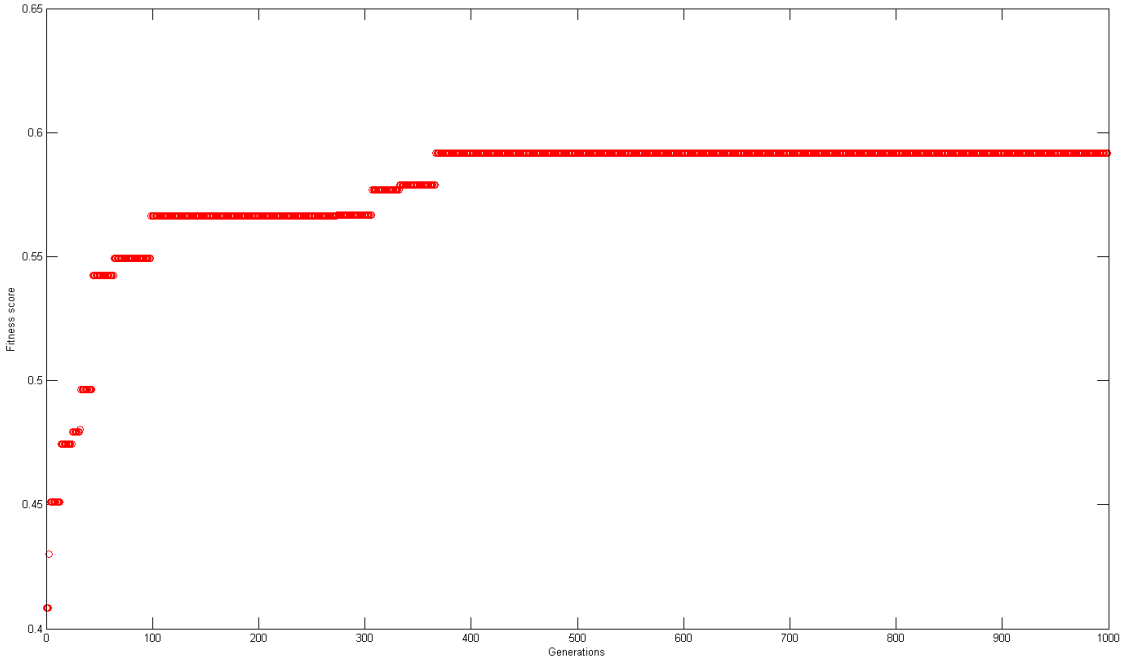

Figure 35 - EPA stage considering the sign of the prediction error

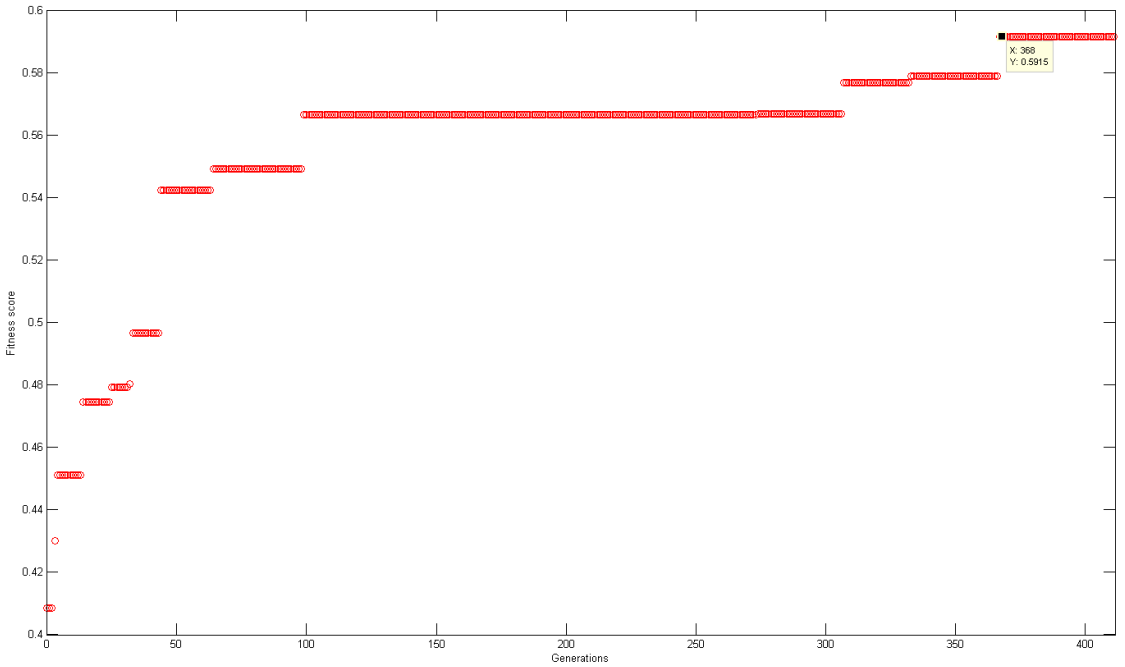

Figure 36 - Maximum fitness score considering the sign of the prediction error

In the other hand, reducing the value of μ we need to increase the number of calculated samples in order to give time to the two multiplicative parameters to achieve a state of convergence.

After several tests of simple search of the optimal value, it emerged that the best value of the constant μ, which represents a good compromise between convergence times not too long and THD satisfactory, is 0.000055 if we increase the number of samples to 800.

As we can see in the Figure 35 and Figure 36, the fitness function takes much longer time to reach the optimal value, even after 300 generations still occur increases to the value of convergence. In addition, it does not reach values similar to the fitness function of the normal filter. This is because, if we analyze the equations for its calculation, recall below, we immediately realize that the value of $ITAE$ is definitely higher than that one of the previous tests because we consider a higher number of samples.

$$F = \frac{a}{ITAE \cdot max\{NG_{49\,Hz}, NG_{50\,Hz}, NG_{51\,Hz}\}} \quad (8.3)$$

$$ITAE = \sum_{n=1}^{800} n|e(n)| + \sum_{n=801}^{1600} (n-300)|e(n)| + \sum_{n=1601}^{2400} (n-600)|e(n)| \quad (8.4)$$

$$NG(n) = \sum_{k=0}^{N-1} [g_1(n_L)h_A(k)]^2 + \sum_{k=0}^{N-1} [g_2(n_L)h_B(k)]^2 \quad (8.5)$$

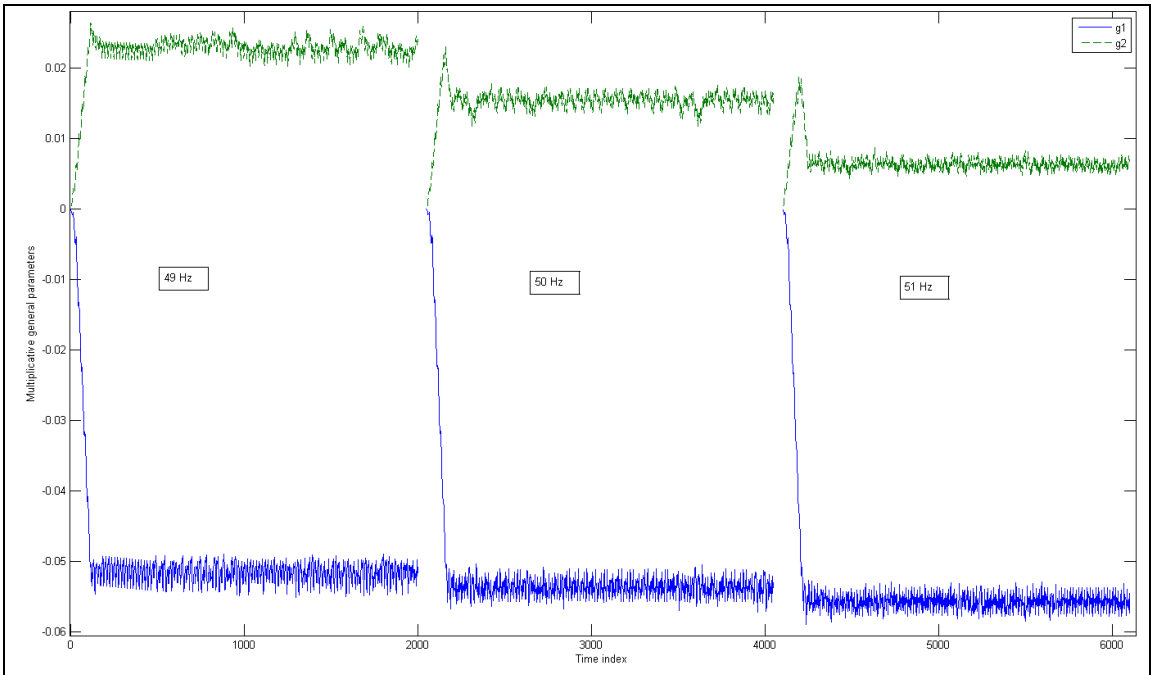

Figure 37 - Adaptation of multiplicative general parameters considering the sign of the prediction error

With reference to the two multiplicative parameters, we can see in the plot above that they have a more fluctuating trend with respect to the convergence value that is reached after about 250 samples calculated. Despite the negative sign of g_2, the values of the two parameters are very similar to those of the normalized filter.

Also in this case, a practical proof of the correct operation of the filter is given by the comparison between the waveform of the output of the filter and the input signal, with the respective frequencies of 49/50/51 Hz.

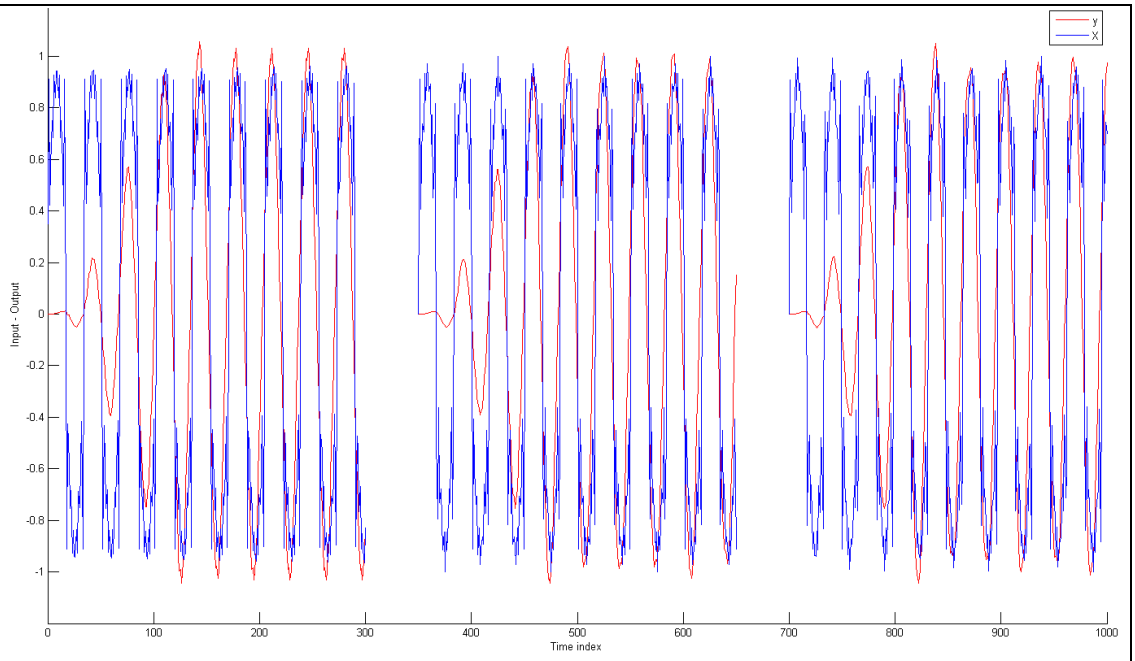

Figure 38 - Comparison input-output of the filter that considers the sign of the prediction error

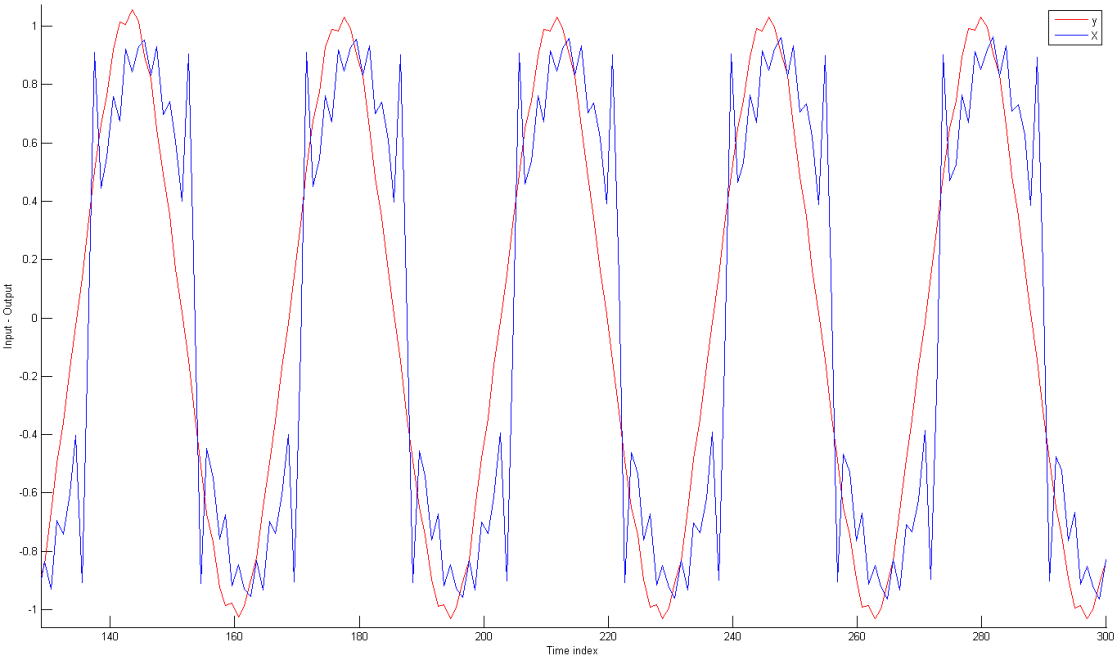

Figure 39 - Comparison input-output of the filter that considers the sign of the prediction error, for test signal of 49 Hz

As we can observe, the output signal of the filter takes more time, almost 125 samples instead of the 50s in the normalized filter, to reach the stage of adaptation in which it follows properly the input, cleaning it by the harmonics. This is also

demonstrated by analyzing the error between the outputs and the ideal sine waves with appropriate frequencies (49/50/51 Hz).

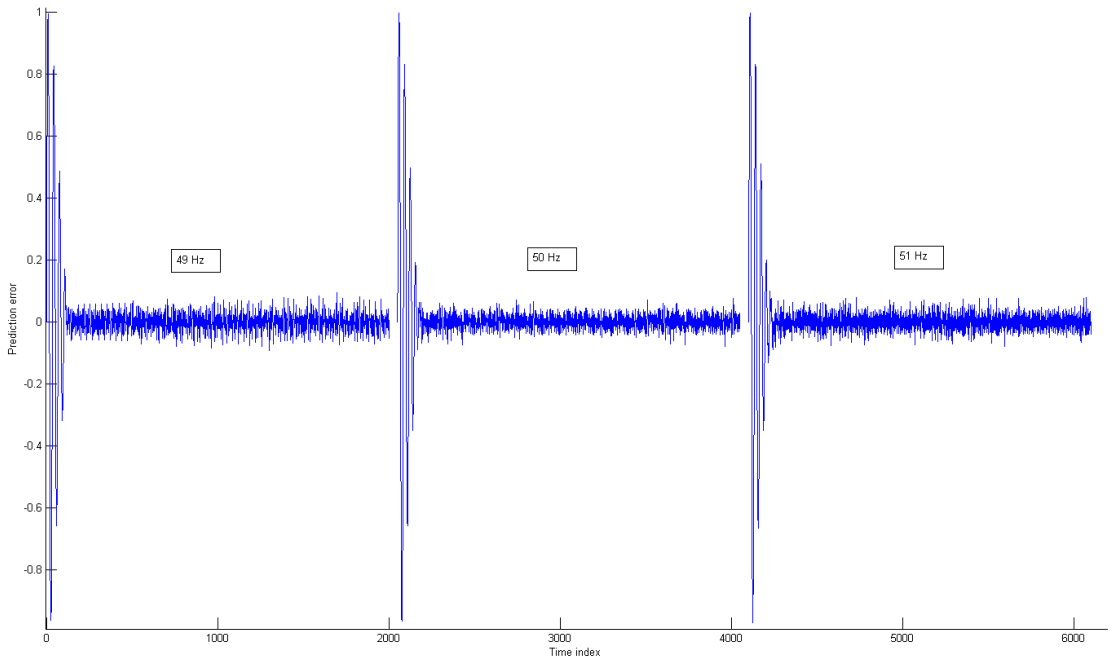

Figure 40 - Error outputs-ideal sine waves of the filter that considers the sign of the prediction error

The efficiency of the filter is further emphasized turning to the frequency domain and making a qualitative study of the spectra of the filter input and output. The good attenuation carried out by the filter is witnessed by the small amplitudes of all the odd harmonics that are presented in the input signal and are well attenuated in the output of the filter.

Figure 41 refers to the test signal with fundamental frequency of 49 Hz. We can observe that all the harmonics present in the input signal result, in output, well attenuated and all with amplitude lower than 0.03. The frequencies with considerable amplitudes are the third, the fifth, the eleventh and the thirteenth, which are respectively attenuated by 83.3%, 89.9%, 91.8% and 90.2%. All the other harmonics have a higher attenuation.

Considering the test signal with the frequency of 50 Hz (Figure 42) we can conclude that the situation is even better. The only peaks that can be observed in the spectrum of the output signal are related to the 5^{th} and the 13^{th} harmonic, respectively with amplitudes of 0.0178 and 0.0115. For these two frequencies the filter operates an attenuation of 88.1% and 92.3%.

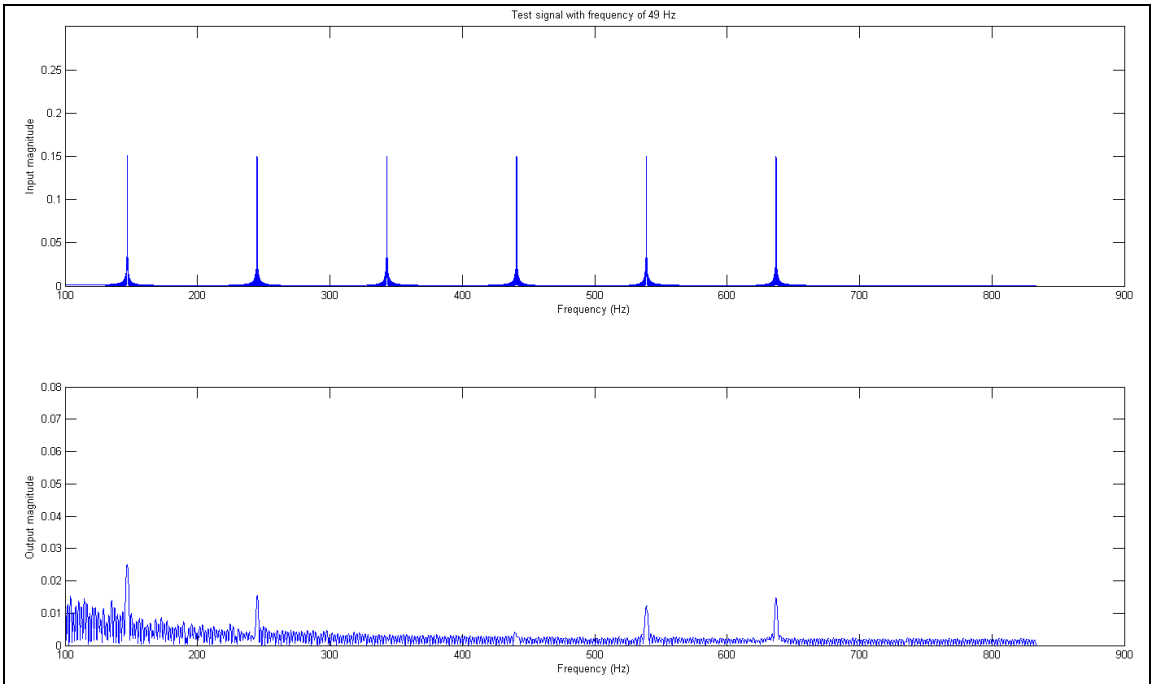

Figure 41 - Input-output spectra considering the sign of the prediction error (49 Hz)

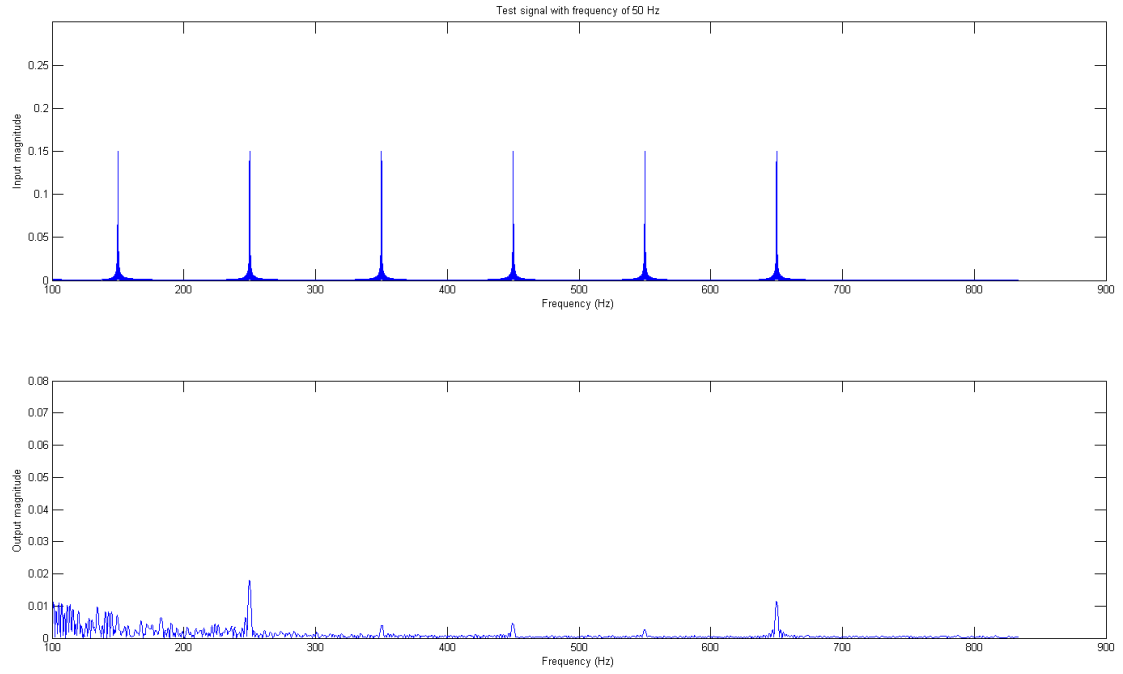

Figure 42 - Input-output spectra considering the sign of the prediction error (50 Hz)

Finally, for the last case, the one with the test signal with a frequency of 51 Hz, we can observe that the spectrum of the output is very similar to the previous case. All harmonics have negligible amplitudes, except the fifth and the thirteenth which present an abatement of 81.5% and 92.8%.

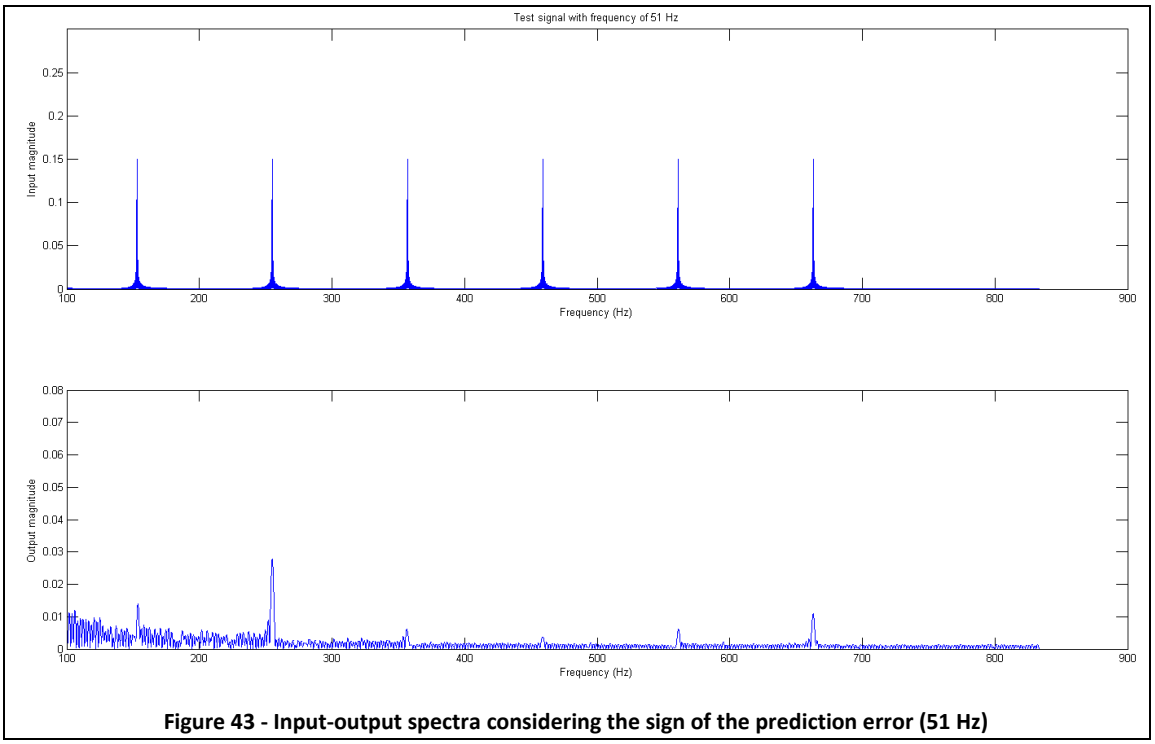

Figure 43 - Input-output spectra considering the sign of the prediction error (51 Hz)

Table 5 - Comparison of harmonic contents in filters' input and output with the prediction errors' sign consideration

Harmonic Number	Input 49/50/51 Hz	Output 49 Hz	Output 50 Hz	Output 51 Hz
1st	1	1	1	1
3rd	0.15	0.0251	0.0060	0.0107
5th	0.15	0.0151	0.0178	0.0278
7th	0.15	0.0023	0.0039	0.0054
9th	0.15	0.0028	0.0047	0.0037
11th	0.15	0.0123	0.0027	0.0058
13th	0.15	0.0147	0.0115	0.0108
THD %	36.7	3.52	2.30	3.29

In the Table 5 are shown the amplitudes of the odd harmonics present in the output of the filter. As discussed above, we have a general good attenuation for every harmonic in every test signal considered, but the most important information that we can obtain from this table is the value of the THDs calculated. If we compare these

values with the THDs obtained from the normalized filter and showed in the Table 2, to the previous chapter 6, we can observe that the THDs related to the filter that considers only the sign of the prediction error in the calculation of the multiplicative parameters, are at most 1.27 percentage units higher than those of the normal filter. For the test signals with the frequency of 50 and 51 Hz, the percentage difference is reduced to 0.85 and 0.87 units. This means that the change made to the filter can actually be considered an improvement. It is true that we have a worsening of the attenuation of the harmonics, but it is a small price to pay so that if it can be considered negligible with respect to the implementation of the filter on a low cost electronic device, it is reasonable to implement the change. Having one multiplication less in the computation of the multiplicative parameters, their number is reduced from 5 to 4 and, and considering that μ is a power of 2 lower than 1, g_1 and g_2 can be calculated with a simple shift to the right of the digits that rap represent the filtering part.

8.2. Sign of the filtering part

Unlike the previous case, the filtering part, being the sum of the products between the fixed-basis filter coefficients and the samples of the test signal input, until now was a number with an absolute value always bigger than 1 and with positive or negative sign.

If we consider the sign of the filtering part, we have a value smaller than before and, considering that the maximum value that the prediction error can give us is 1, if we do not raise enough our constant μ we risk to have a too slow convergence of the output signal cleaned by harmonics compared with the input, or worse, an output signal which will never reach the amplitude of the ideal sine wave and therefore will be strongly attenuated.

After several tests it was concluded that the value of the constant that best meets the objectives is 0.0028 and the number of samples that we need to reach a convergence of the multiplicative parameters is 9000. With this values, in reality, we do not get results that can be considered satisfactory and which demonstrate a real applicability of this change introduced. In fact, if we consider the following figures, we can observe how the output signals align well in frequency with the input signal, after an initial transient which is the time needed to the parameters to achieve the convergence. However, what happens is that the output signals do not reach the maximum amplitude of input and, resulting similar to square wave, it is obvious that a spectrum analysis could detect a high harmonic content. Even after several tests and

changes the value of the constant μ and the number of samples, it was not possible to obtain a better result. This aspect certainly has an analytical motivation that might be interesting study in a future in-depth analysis.

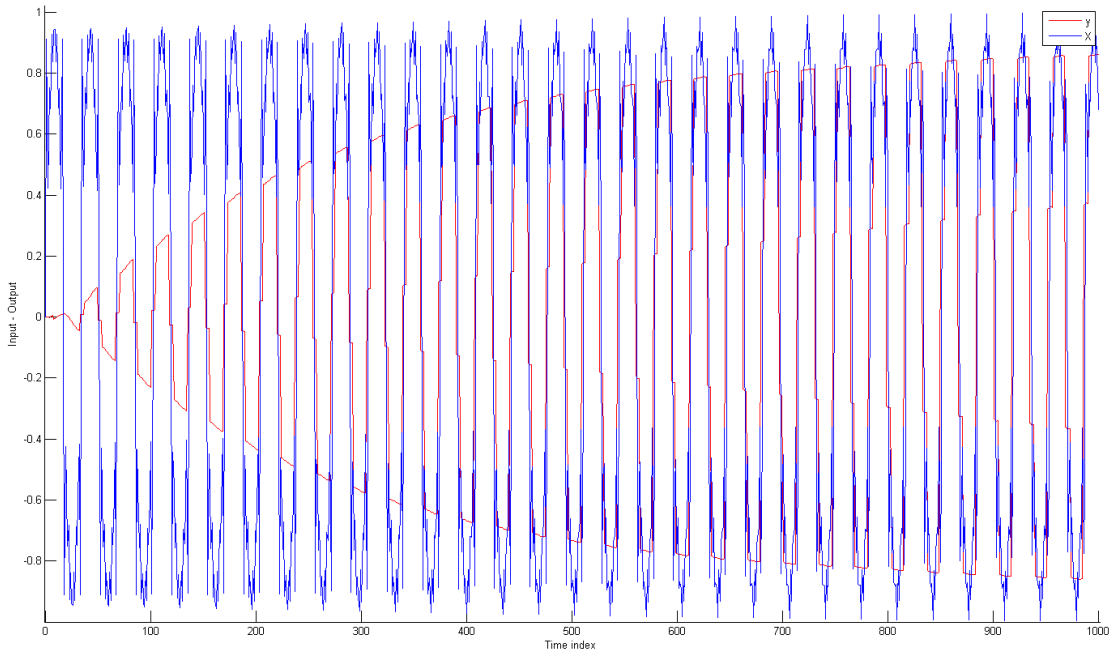

Figure 44 - Comparison input-output of the filter that considers the sign of the filtering part (49 Hz)

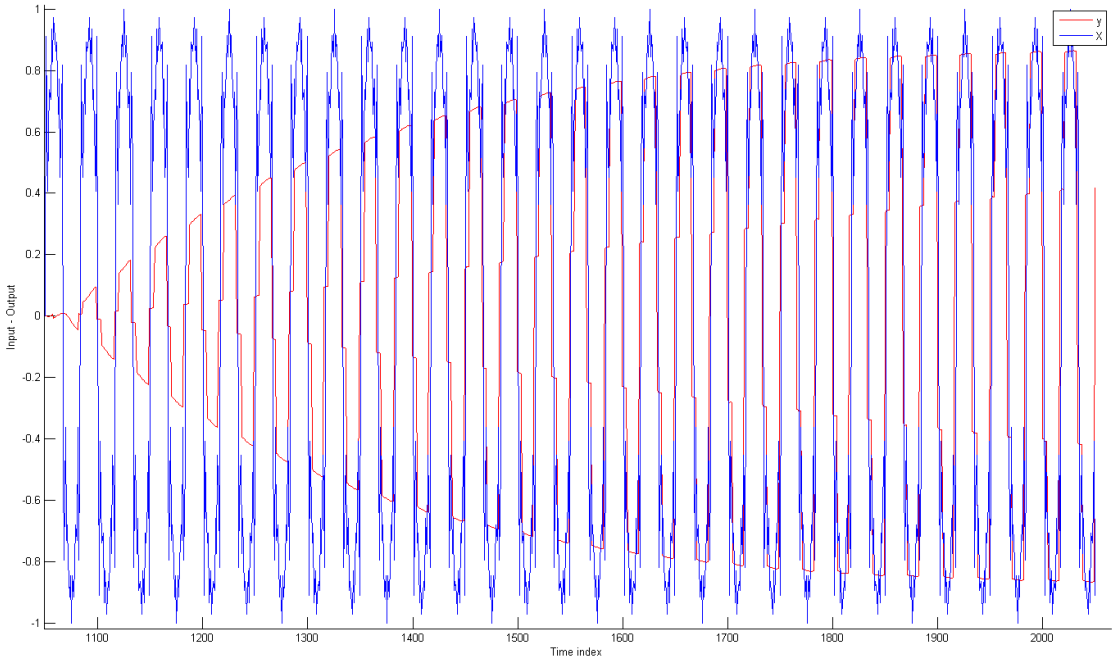

Figure 45 - Comparison input-output of the filter that considers the sign of the filtering part (50 Hz)

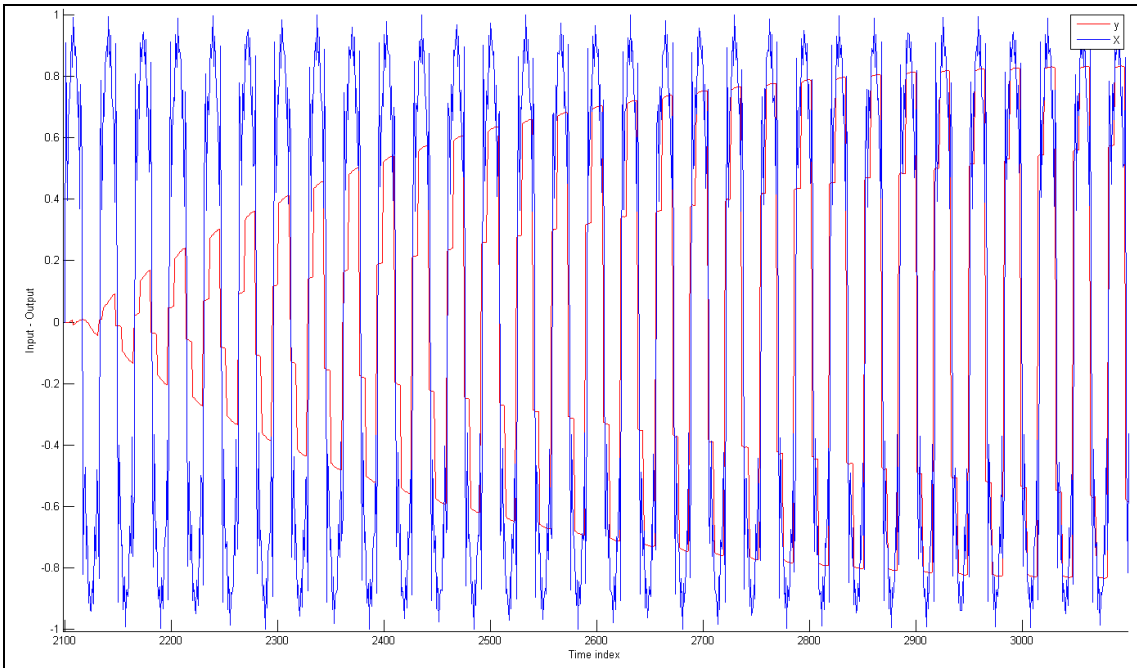

Figure 46 - Comparison input-output of the filter that considers the sign of the filtering part (51 Hz)

As we can observe, the output signal of the filter needs a lot of time, almost 800 samples, to reach its maximum value. In each case the wave obtained is not sinusoidal and cannot be considered perfectly clean by the harmonics present in the input. Also, if we look carefully, it presents some steps in the transition from positive to negative half-wave and vice versa. This fact represents a phase shift between the two signals, better seen if we consider the prediction error.

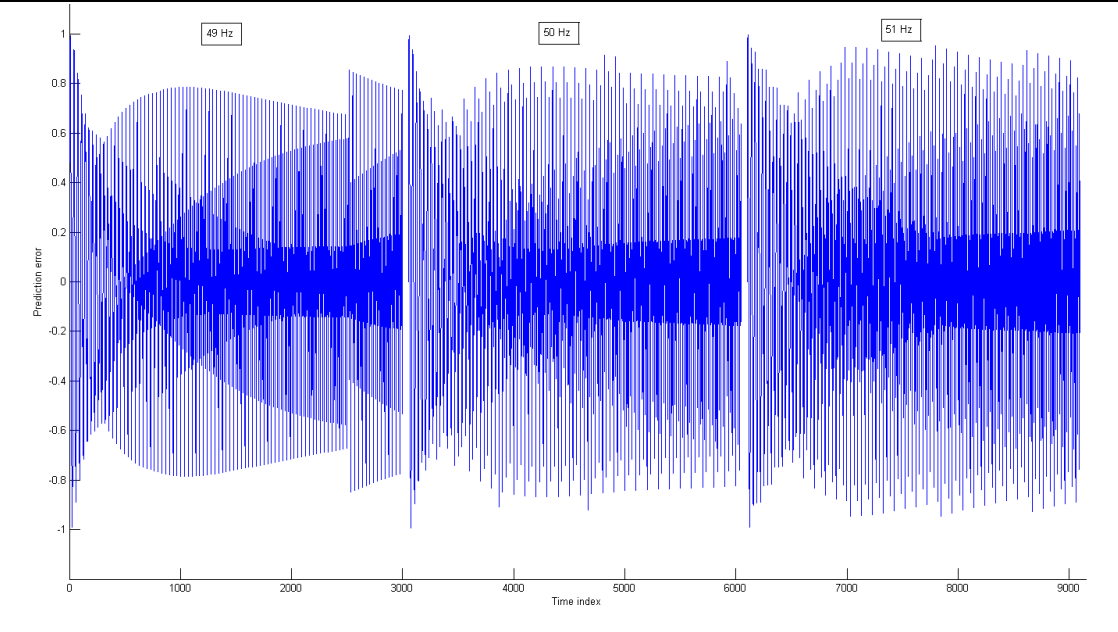

Figure 47 - Error outputs-ideal sin waves of the filter that considers the sign of the filtering part

Whereas therefore the previous figures, it is obvious that the prediction error for all three frequencies will maintain the rather high values. The problem of the phase

shift mentioned above is clearly visible in the figure below if we consider the peaks, of 0.8/0.9, that the prediction error shows for all three test signals. Furthermore, the error is most dense in the range -0.2/0.2, which is exactly the difference between the maximum value of the ideal signal and the amplitude of the square wave obtained by us.

Despite the fitness function reaches a convergence value quickly enough, after approximately 150 generations, its maximum value is still rather small due to the fact that, also this time, we use a high number of samples which increase strongly the value *ITAE*, reducing the value of the fitness function.

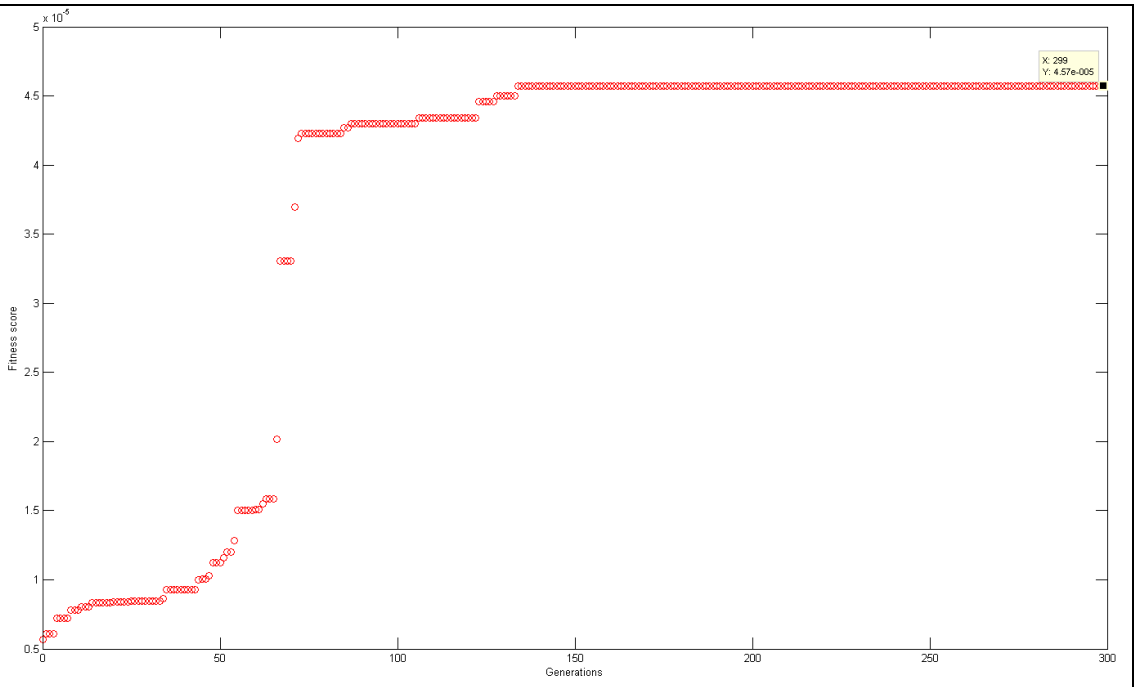

Figure 48 - EPA stage considering the sign of the filtering part

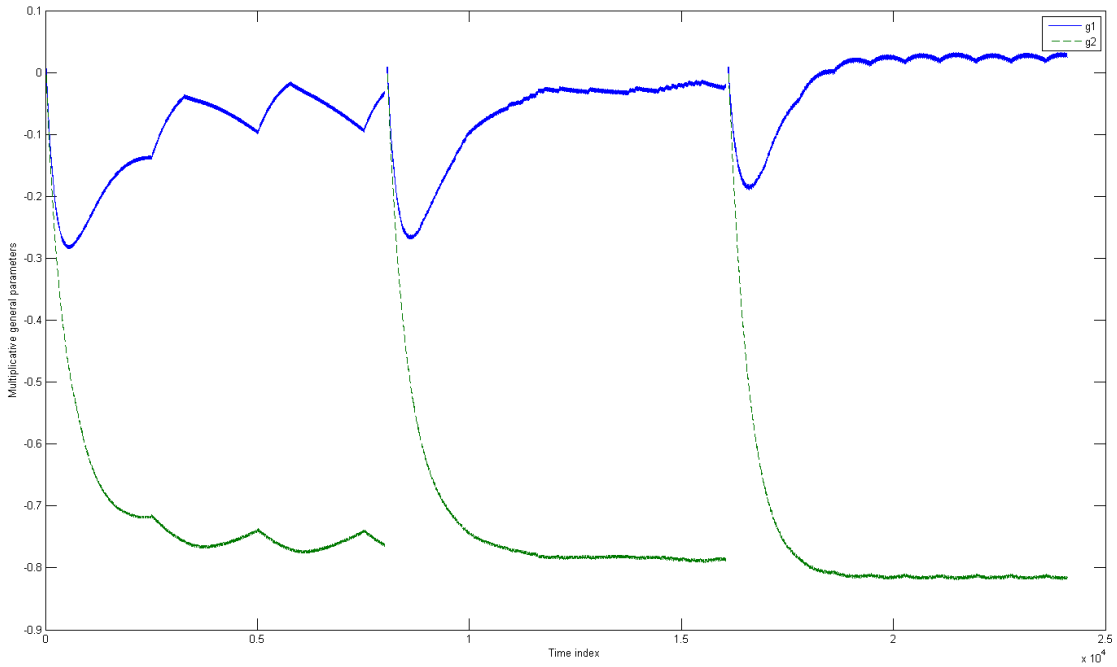

Figure 49 - Adaptation of multiplicative general parameters considering the sign of the filtering part

With reference to the two multiplicative parameters, we can see in the picture above that is not possible to say that they reach a convergence to a value for all the cases. Considering the test signal with the frequencies of 49 Hz, there is a high oscillation of g_1 and g_2 around a single value, while in the second and in the third cases the oscillations are reduced.

Obtaining these results, it makes no sense to proceed with a qualitative analysis of the spectrum of the output signals because, as already said, getting square waves, their spectrum will be rich of odd harmonics of each order. Least of all an analysis of the value of THD would prove that this introduced change could be exploited for the use of our filtering algorithm on low cost electronic devices.

9. Conclusions

In the previous chapters of this thesis the problem of the harmonic distortion, its sources and the possible effects were presented in detail. We observed the possible solutions adoptable to reduce the problems, distinguishing the filtering systems that base on the frequency domain and those one that base on time domain. Subsequently we have focused our attention on a particular type of filter, the adaptive filter, which is part of the second group and that allows having a good attenuation of harmonics making use of digital signal processing to manipulate the signal corrupted by harmonics.

The next step was to present the specific multiplicative general parameter filter that was the central point of this thesis. We studied how the algorithm on which the filter is based works and the main equations used to obtain the output signal.

Furthermore, we have understood how the optimization procedure based on evolutionary programming works and how the algorithm uses it to get the two parameters which best meet the requirements of attenuation.

At this point we tested the performances of the filter feeding the algorithm with three test sinusoids at the frequencies of 49, 50 and 51 Hz corrupted by odd harmonics.

In the chapter 7 we have dealt with the detection of the generation of new harmonics observable in the convergence of the multiplicative parameters, trying to find an analytical motivation of the problem. Testing the filter with the input signals corrupted by a single odd harmonic at a time, we analyzed which are the new harmonics presented in the multiplicative parameters and if they were present also in the output signal. The same analysis has been conducted with the input signals with two odd harmonics at time. Studying the spectra of g_1, g_2 and output, we have obtained, through an appropriate Matlab code, useful tables with analytical values of the harmonics. Thanks to this work was effectively verified a disadvantage of this filtering algorithm that, on the one hand processes well the work for cleaning the input signals, on the other, basing its operation on a feedback, self-generates new odd harmonics, albeit with amplitudes definitely negligible.

Finally, the last chapter presents two attempts to simplify the computational demand of the filtering algorithm in order to enhance its applicability on low-cost devices like FPGAs.

In the first case were tested the performance of the filter that, in the calculation of the multiplicative parameters, considers the sign of the prediction error and not the

entire analytical value. After several tests and the choice of the most suitable constant μ, tests have shown that the filter output is a sinusoid perfectly cleaned of harmonics, with good amplitude of the fundamental frequency and no phase shift with the corrupted input signal. The total harmonic distortion values of all the test signals (49/59/51 Hz) demonstrate how the filter should fulfill his work of harmonic suppression on the input signal, allowing to conclude that the introduced change can have an real applicability.

In the second case the goal was to test the performance of the filter that, in the calculation of the multiplicative parameters, considers the sign of the filtering part. In this case, the search of the values of constant μ and number of samples most suitable has proved more complicated than we expected. Even after more than 200 hours of Matlab simulations with various modifications of the two above mentioned values, has not been possible to find a solution that best approached the requirements. At the end, the performance shown are relative to the best case obtained, but which cannot be considered applicable in the reality because, the square wave behavior of the output led inherently a high content of harmonics and a phase shift compared with the input.

Appendix A

```
%% Initializations
N=40;
Np=40;
g1=0;
g2=0;
y_1=0;
y_2=0;
mu=0.0005;
d_line=zeros(1,N);
NG=0;
NG_max=0;
ITAE=0;
Fitness=0;
step=0;

%% Create initial random population
for r=1:Np
    for c=1:N
        h1_old(r,c)=randi([-1 1],1,1);%Generate integer values drawn
        if h1_old(r,c)==0;             uniformly from -1:1
            h2_old(r,c)=randsample([-1 1],1);
        else
            h2_old(r,c)=0;
        end
    end
    not_zero=nnz(h1_old(r,:))+nnz(h2_old(r,:));%Evaluation of the
end                                              number of nonzero
                                                 coefficients
h1_new=h1_old;
h2_new=h2_old;

%% Loop of the evolutionary programming algorithm
while step<250
    %% Single element mutations
    for r=1:Np
        k=randi([1 N],1,1);  %Random choice of the element to mutate
        if h1_old(r,k)==0;
            h1_new(r,k)=randsample([-1 1],1);
            h2_new(r,k)=0;
        elseif h1_old(r,k)==1;
            h1_new(r,k)=randsample([-1 0],1);
            if h1_new(r,k)==-1;
                h2_new(r,k)=0;
            else h2_new(r,k)=randsample([-1 1],1);
            end
        else
            h1_new(r,k)=randsample([0 1],1);
            if h1_new(r,k)==1;
                h2_new(r,k)=0;
            else h2_new(r,k)=randsample([-1 1],1);
            end
        end
    end

    h1=[h1_old;h1_new];
    h2=[h2_old;h2_new];
```

```
%% Fitness evaluation
for r=1:(2*Np)
    for f=0:2
        freq=49+f;                  %freq=49/50/51Hz Ts=0.6ms
        HC=pi*freq*1.2*10^-3;       %=2*0.6*10^-3=1.2*10^-3

        X=zeros(1,303);
        XF=zeros(1,303);

        %Creation of the distorted evaluation signal
        for n=1:302
            hv=HC*n;
            X(n+1)=sin(hv);
            XF(n+1)=X(n+1);                    %sin 49/50/51Hz
            for m=3:2:13
                X(n+1)=X(n+1)+0.15*sin(m*hv); %sin 49/50/51Hz
            End                                 distorted
        end

        g1=0;
        g2=0;
        y_1=0;
        y_2=0;
        d_line=zeros(1,N);

        %Creation of the output and error
        for k=1:300
            for i=N:-1:2
                d_line(i)=d_line(i-1);         %Update delay line
            end
            d_line(1)=X(k);                    %New input sample
            g1_in=sum(h1(r,:).*d_line);        %Input for g1
            g2_in=sum(h2(r,:).*d_line);        %Input for g2
            y=g1*g1_in+g2*g2_in;               %MGP-FIR output
            p_error=XF(k)-y_2;                 %Prediction error
            y_2=y_1;                           %Update delayed y
            y_1=y;                              samples
            g1_latest=g1;                      %Save g1 and g2
            g2_latest=g2;
            g1=g1+mu*p_error*g1_in;            %g1 adaption
            g2=g2+mu*p_error*g2_in;            %g2 adaption
            p_error_history(k)=p_error;        %Save prediction
            y_fin(k)=y;                         error
        end

        %NG computation
        NG=sum((g1_latest*h1(r,:)).*(g1_latest*h1(r,:)))
        +sum((g2_latest*h2(r,:)).*(g2_latest*h2(r,:)));
        if NG<0.0524    %Give penalty
             =10;
        end
        if NG>NG_max    %Search the maximum NG between 49/50/51 Hz
            NG_max=NG;
        end

        %ITAE computation
        for n=1:300
            ITAE=ITAE+n*abs(p_error_history(n));
```

```
            end
        end
        Fitness(r)=1000/(NG_max*ITAE);    %Fitness computation
                ITAE=0;
        NG_max=0;

    end

    [bests,index]=sort(Fitness,'descend');%Sort the population
    for r=1:Np                          %Select the Np fittest slutions
        h1_old(r,:)=h1(index(r),:);
        h2_old(r,:)=h2(index(r),:);
    end
    h1_new=h1_old;
    h2_new=h2_old;
end
```

Appendix B

```
function [f_axis]=new_harm_one(mu,N,h1,h2);
points=10000;
f_axis=(1/(0.6*10^-3))/2*linspace(0,1,points/2+1);
cnames = {'3-th','5-th','7-th','9-th','11-th','13-th','15-th'};
rnames = {'3-th','5-th','7-th','9-th','11-th','13-th'};

%% New Harmonics
for f=0:2
    for r=0:2:10
        freq=49+f;                          %freq=49/50/51Hz Ts=0.6ms
        HC=pi*freq*1.2*10^-3;               %=2*0.6*10^-3=1.2*10^-3

        %Creation of the distorted evaluation signal
        for n=1:4802
            hv=HC*n;
            X(n+1)=sin(hv);
            XF(n+1)=X(n+1);                     %sin 50Hz
            for m=3+r:2:3+r                     %3->13th harmonics
                X(n+1)=X(n+1)+0.6*sin(m*hv);    %sin 50Hz distorted
            end
        end

        g1=0;
        g2=0;
        y_1=0;
        y_2=0;
        d_line=zeros(1,N);

        %Creation of the output and error
        for k=1:4800
            for i=N:-1:2
                d_line(i)=d_line(i-1);      %Update delay line
            end
            d_line(1)=X(k);                 %New input sample
            g1_in=sum(h1(1,:).*d_line);     %Input for g1
            g2_in=sum(h2(1,:).*d_line);     %Input for g2
            y=g1*g1_in+g2*g2_in;            %MGP-FIR output
            p_error=XF(k)-y_2;              %Prediction error
            y_2=y_1;                        %Update delayed y samples
            y_1=y;
            g1=g1+mu*p_error*g1_in;         %g1 adaption
            g2=g2+mu*p_error*g2_in;         %g2 adaption
            p_error_history(k)=p_error;     %Save prediction error
            y_fin(k)=y;
            trend_g1(k)=g1_in*p_error;
            trend_g2(k)=g2_in*p_error;
        end

        %Spectrum of g1
        G1_FFT=fft(trend_g1,points)/4800;
        figure(11+f)
        hold on
        subplot(2,3,1+(r/2))
        plot(f_axis+49+f,2*abs(G1_FFT(1:points/2+1)))
        xlim([49+f 884])
        xlabel('Frequency (Hz)')
```

```
str = sprintf('%d-th harmonic/%d Hz G1',3+r,49+f);
title(str)
hold off

%Spectrum of g2
G2_FFT=fft(trend_g2,points)/4800;
figure(14+f)
hold on
subplot(2,3,1+(r/2))
plot(f_axis+49+f,2*abs(G2_FFT(1:points/2+1)))
xlim([49+f 884])
xlabel('Frequency (Hz)')
str = sprintf('%d-th harmonic/%d Hz G2',3+r,49+f);
title(str)
hold off

%Spectrum of the output
Y_FFT=fft(y_fin,points)/4800;
figure(17+f)
hold on
subplot(2,3,1+(r/2))
plot(f_axis(600:end),2*abs(Y_FFT((round((points/2+1)*(100/833
)))):points/2+1)))
xlim([98+f 834])
xlabel('Frequency (Hz)')
str = sprintf('%d-th harmonic/%d Hz Y',3+r,49+f);
title(str)
hold off

%Search the harmonics
for n=1:7
    if
2*abs(max(G1_FFT(round(((points/2+1)*(n*100/(833+49+f))):roun
d((points/2+1)*((n*100+100)/(833+49+f)))))))  > 0.05
dat_g1(r/2+1,n)=2*abs(max(G1_FFT(round(((points/2+1)*(n*100/(
833+49+f))):round((points/2+1)*((n*100+100)/(833+49+f)))))));
    else dat_g1(r/2+1,n)=0;
    end

    if
2*abs(max(G2_FFT(round(((points/2+1)*(n*100/(833+49+f))):roun
d((points/2+1)*((n*100+100)/(833+49+f)))))))  > 0.05
dat_g2(r/2+1,n)=2*abs(max(G2_FFT(round(((points/2+1)*(n*100/(
833+49+f))):round((points/2+1)*((n*100+100)/(833+49+f)))))));
    else dat_g2(r/2+1,n)=0;
    end

    if
2*abs(max(Y_FFT(round(((points/2+1)*(n*100/(833))):round((poi
nts/2+1)*((n*100+100)/(833)))))))  > 0.05
dat_y(r/2+1,n)=2*abs(max(Y_FFT(round(((points/2+1)*(n*100/(83
3+49+f))):round((points/2+1)*((n*100+100)/(833+49+f)))))));
    else dat_y(r/2+1,n)=0;
    end
end

%Create table
fig = figure(20);
```

```
        table_g1 = uitable('Position',[20 (250*(3-f)) 418
        130],'Parent',fig,'Data',dat_g1,'ColumnName',cnames,'RowName'
        ,rnames,'ColumnWidth',{50});
        table_g2 = uitable('Position',[450 (250*(3-f)) 418
        130],'Parent',fig,'Data',dat_g2,'ColumnName',cnames,'RowName'
        ,rnames,'ColumnWidth',{50});
        table_y = uitable('Position',[880 (250*(3-f)) 418
        130],'Parent',fig,'Data',dat_y,'ColumnName',cnames,'RowName',
        rnames,'ColumnWidth',{50});
        str_g1 = sprintf('%d Hz - G1_FFT analysis',49+f);
       str_g2 = sprintf('%d Hz - G2_FFT analysis',49+f);
       str_y = sprintf('%d Hz - Y_FFT analysis',49+f);
        uicontrol('Position',[20 (250*(3-f)+140) 220 20],'Parent',
        fig, 'Style', 'edit','String',str_g1);
        uicontrol('Position',[450 (250*(3-f)+140) 220 20],'Parent',
        fig, 'Style', 'edit','String',str_g2);
        uicontrol('Position',[880 (250*(3-f)+140) 220 20],'Parent',
        fig, 'Style', 'edit','String',str_y);
    end
    dat_g1=zeros(6,7);
    dat_g2=zeros(6,7);
    dat_y=zeros(6,7);
end
```

Appendix C

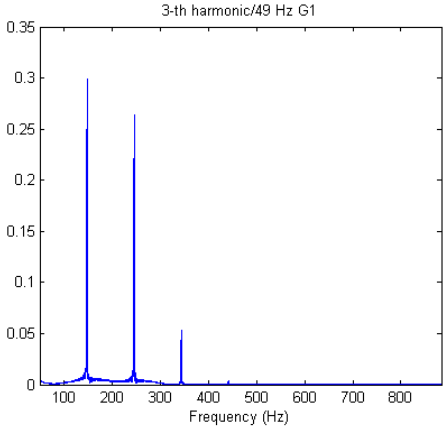
3-th harmonic/49 Hz G1
Frequency (Hz)

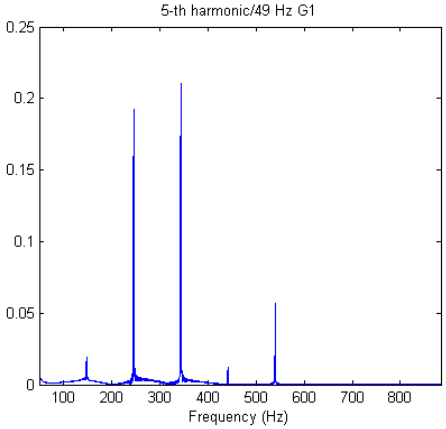
5-th harmonic/49 Hz G1
Frequency (Hz)

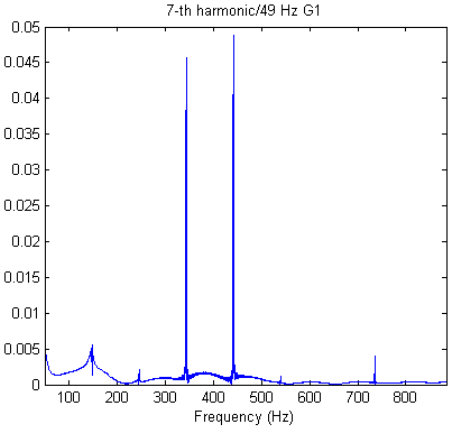
7-th harmonic/49 Hz G1
Frequency (Hz)

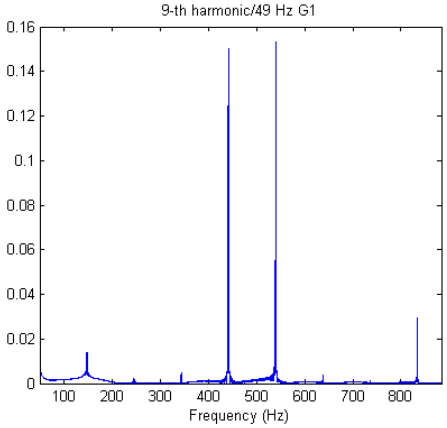
9-th harmonic/49 Hz G1
Frequency (Hz)

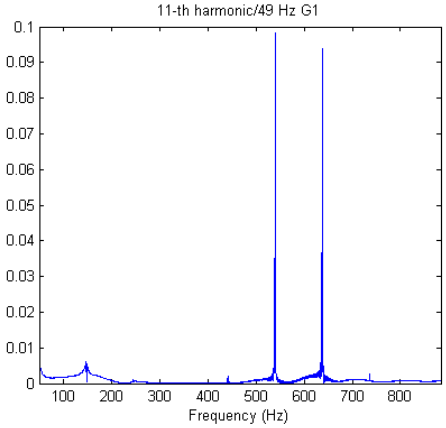
11-th harmonic/49 Hz G1
Frequency (Hz)

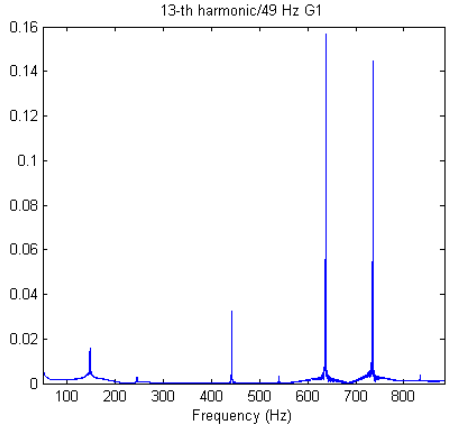
13-th harmonic/49 Hz G1
Frequency (Hz)

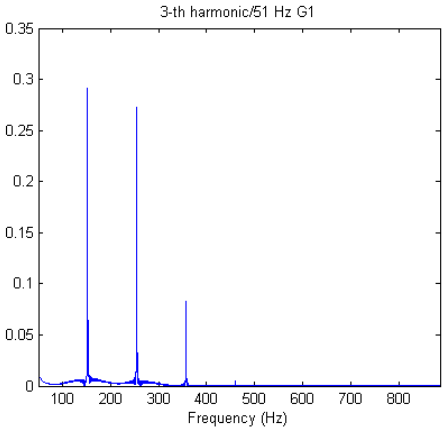
3-th harmonic/51 Hz G1
0.35
0.3
0.25
0.2
0.15
0.1
0.05
0
100 200 300 400 500 600 700 800
Frequency (Hz)

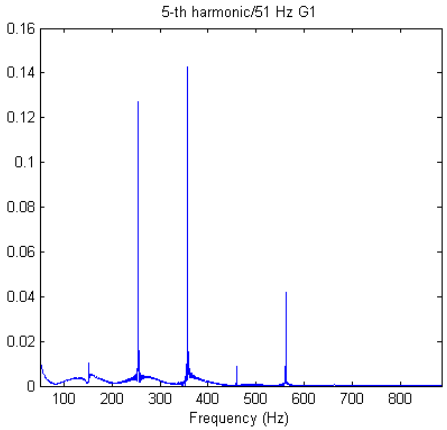
5-th harmonic/51 Hz G1
0.16
0.14
0.12
0.1
0.08
0.06
0.04
0.02
0
100 200 300 400 500 600 700 800
Frequency (Hz)

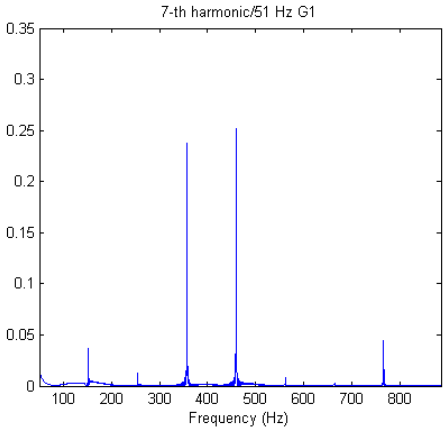
7-th harmonic/51 Hz G1
0.35
0.3
0.25
0.2
0.15
0.1
0.05
0
100 200 300 400 500 600 700 800
Frequency (Hz)

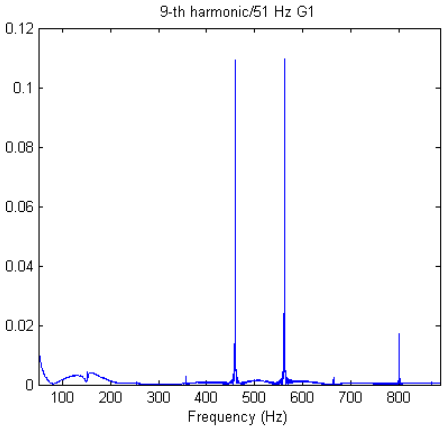
9-th harmonic/51 Hz G1
0.12
0.1
0.08
0.06
0.04
0.02
0
100 200 300 400 500 600 700 800
Frequency (Hz)

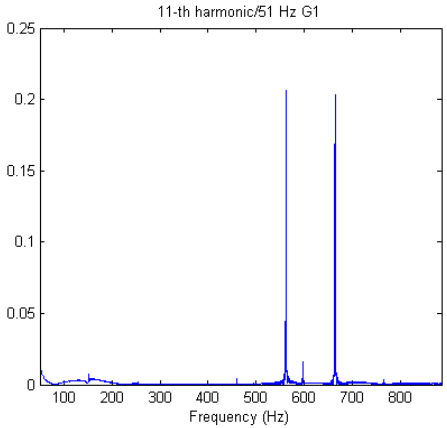
11-th harmonic/51 Hz G1
0.25
0.2
0.15
0.1
0.05
0
100 200 300 400 500 600 700 800
Frequency (Hz)

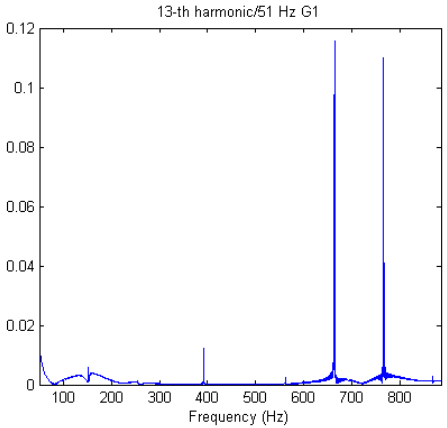
13-th harmonic/51 Hz G1
0.12
0.1
0.08
0.06
0.04
0.02
0
100 200 300 400 500 600 700 800
Frequency (Hz)

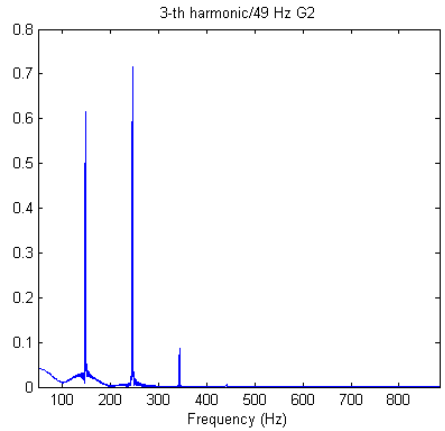
3-th harmonic/49 Hz G2
Frequency (Hz)

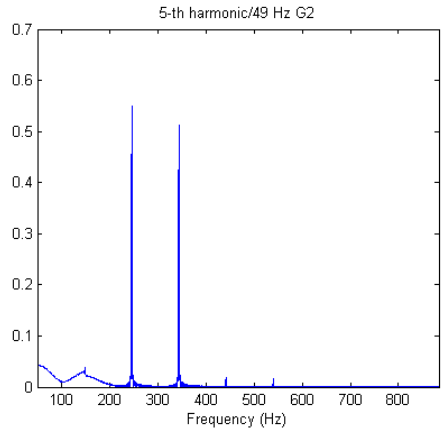
5-th harmonic/49 Hz G2
Frequency (Hz)

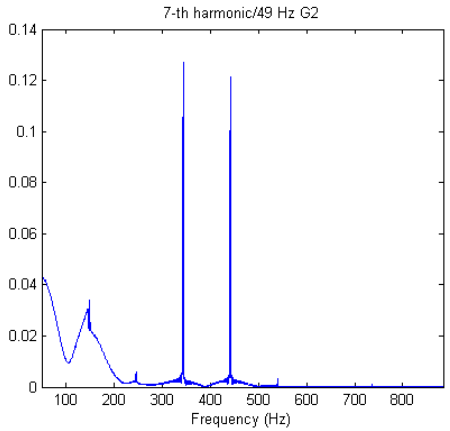
7-th harmonic/49 Hz G2
Frequency (Hz)

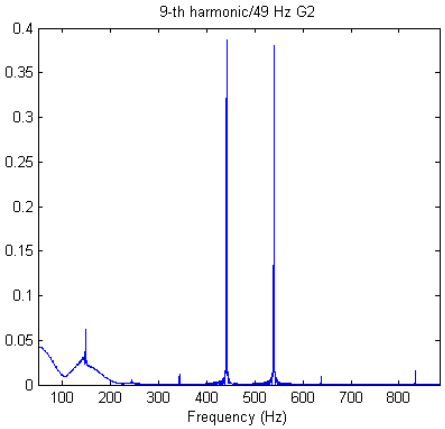
9-th harmonic/49 Hz G2
Frequency (Hz)

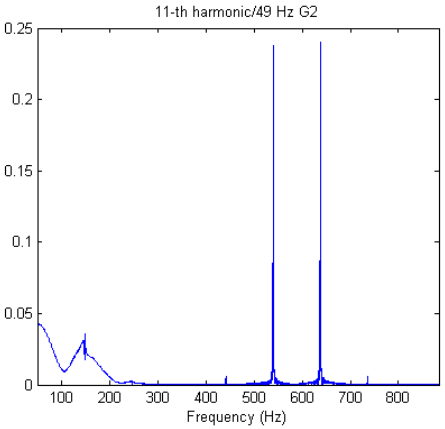
11-th harmonic/49 Hz G2
Frequency (Hz)

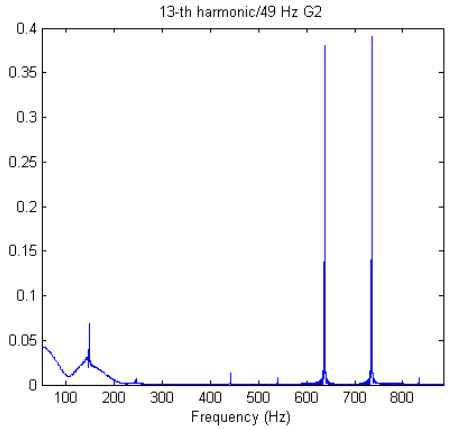
13-th harmonic/49 Hz G2
Frequency (Hz)

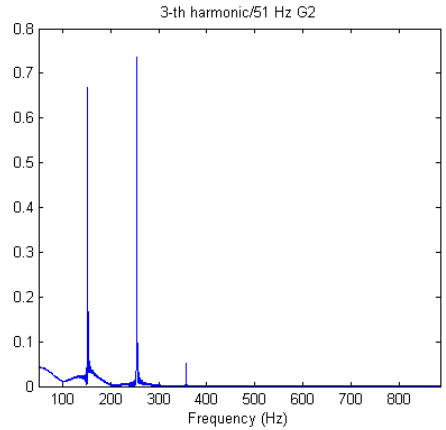
3-th harmonic/51 Hz G2
Frequency (Hz)

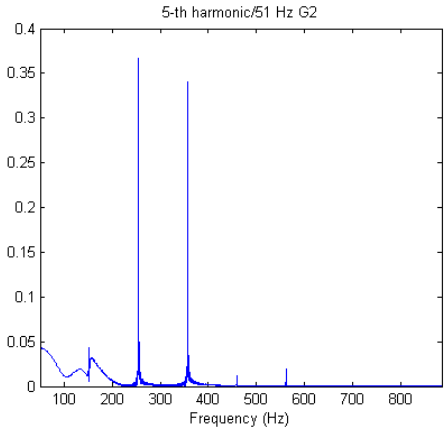
5-th harmonic/51 Hz G2
Frequency (Hz)

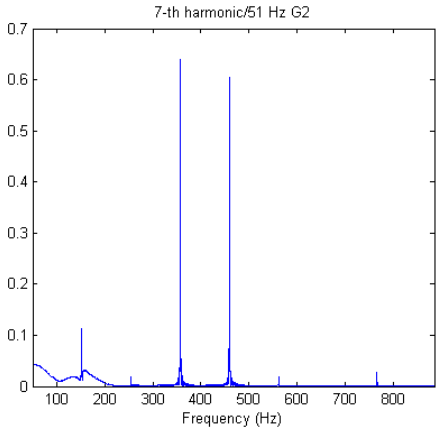
7-th harmonic/51 Hz G2
Frequency (Hz)

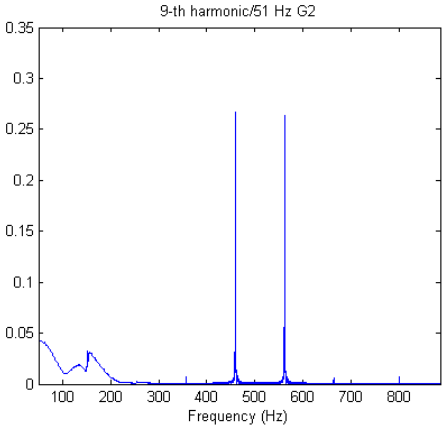
9-th harmonic/51 Hz G2
Frequency (Hz)

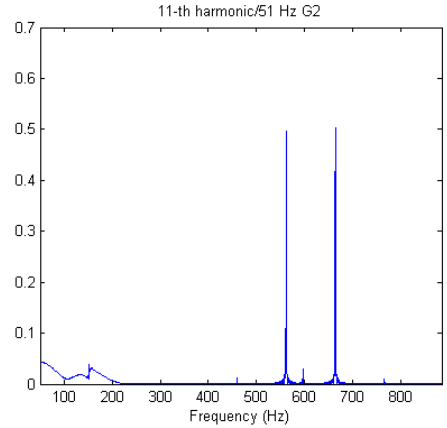
11-th harmonic/51 Hz G2
Frequency (Hz)

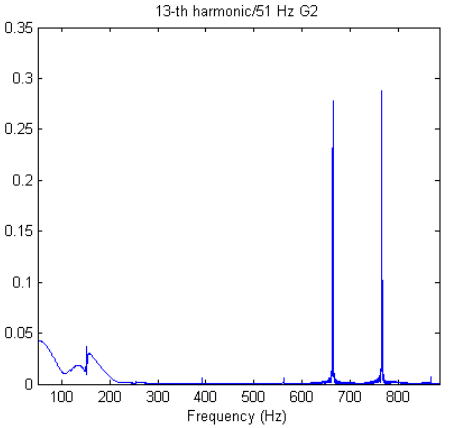
13-th harmonic/51 Hz G2
Frequency (Hz)

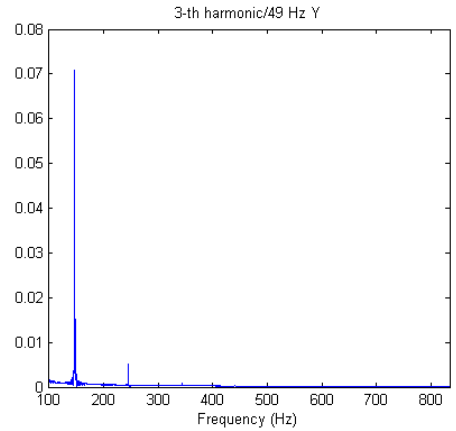
3-th harmonic/49 Hz Y
0.08
0.07
0.06
0.05
0.04
0.03
0.02
0.01
0
100 200 300 400 500 600 700 800
Frequency (Hz)

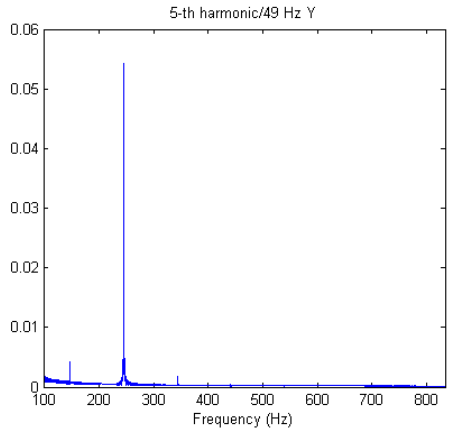
5-th harmonic/49 Hz Y
0.06
0.05
0.04
0.03
0.02
0.01
0
100 200 300 400 500 600 700 800
Frequency (Hz)

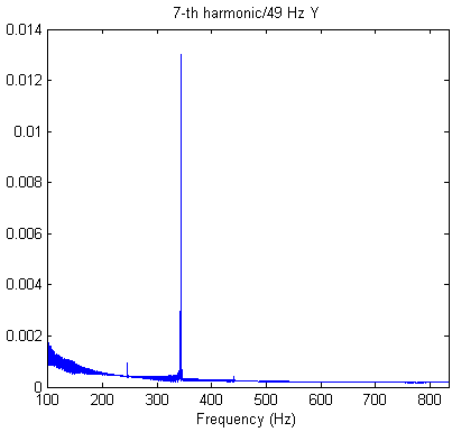
7-th harmonic/49 Hz Y
0.014
0.012
0.01
0.008
0.006
0.004
0.002
0
100 200 300 400 500 600 700 800
Frequency (Hz)

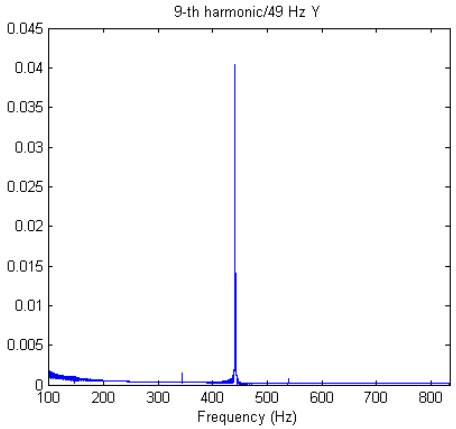
9-th harmonic/49 Hz Y
0.045
0.04
0.035
0.03
0.025
0.02
0.015
0.01
0.005
0
100 200 300 400 500 600 700 800
Frequency (Hz)

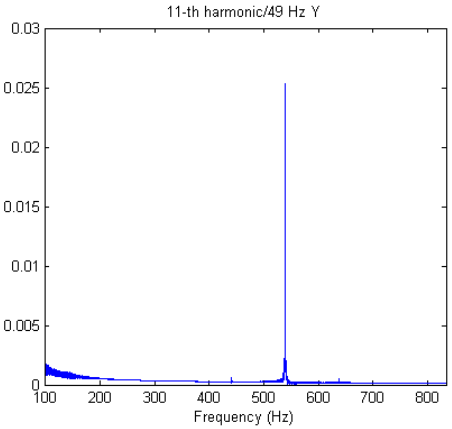
11-th harmonic/49 Hz Y
0.03
0.025
0.02
0.015
0.01
0.005
0
100 200 300 400 500 600 700 800
Frequency (Hz)

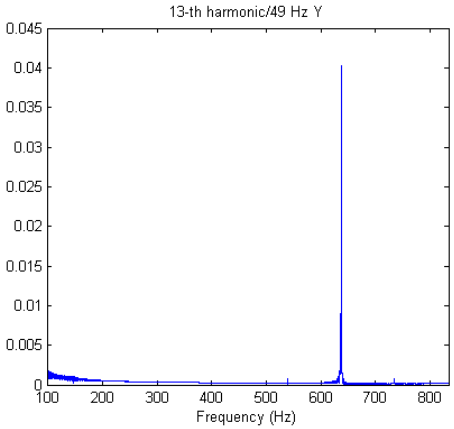
13-th harmonic/49 Hz Y
0.045
0.04
0.035
0.03
0.025
0.02
0.015
0.01
0.005
0
100 200 300 400 500 600 700 800
Frequency (Hz)

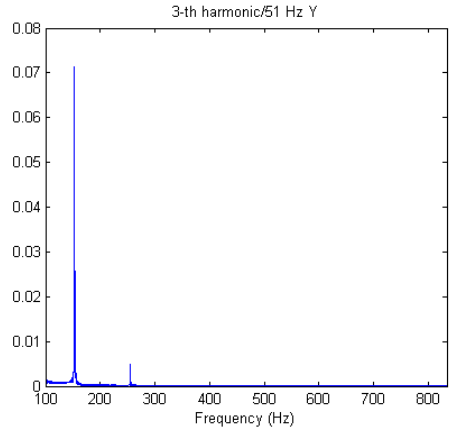
3-th harmonic/51 Hz Y
Frequency (Hz)

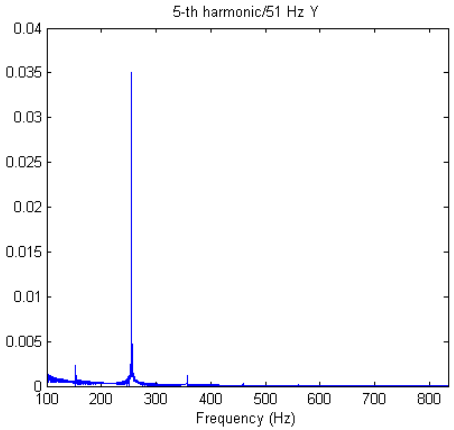
5-th harmonic/51 Hz Y
Frequency (Hz)

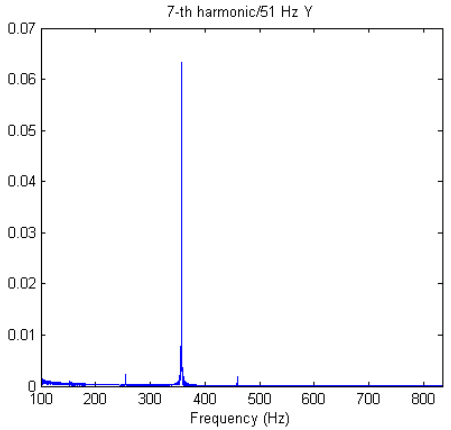
7-th harmonic/51 Hz Y
Frequency (Hz)

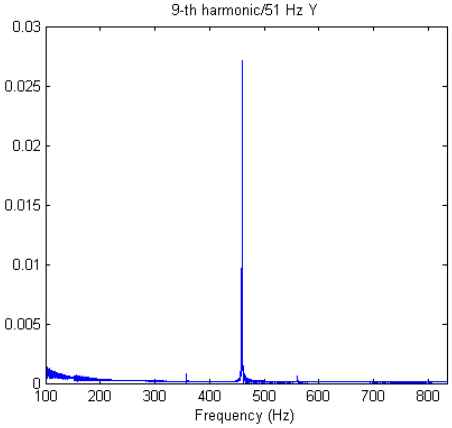
9-th harmonic/51 Hz Y
Frequency (Hz)

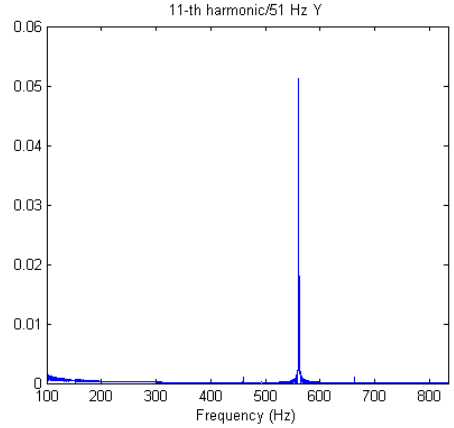
11-th harmonic/51 Hz Y
Frequency (Hz)

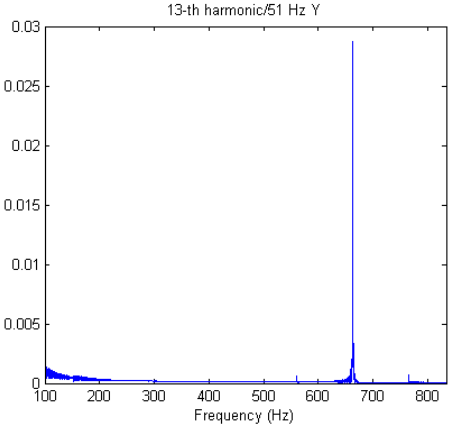
13-th harmonic/51 Hz Y
Frequency (Hz)

Appendix D

```
function [f_axis]=new_harm_two(mu,N,h1,h2);
points=10000;
f_axis=(1/(0.6*10^-3))/2*linspace(0,1,points/2+1);
cnames = {'3-th','4-th','5-th','6-th','7-th','8-th','9-th','10-
th','11-th','12-th','13-th','14-th','15-th','16-th','17-th','18-th'};
cnames_y = {'2-th','3-th','4-th','5-th','6-th','7-th','8-th','9-
th','10-th','11-th','12-th','13-th','14-th','15-th','16-th','17-th'};
rnames = {'3-th + 5-th','3-th + 7-th','3-th + 9-th','3-th + 11-
th','3-th + 13-th','5-th + 7-th','5-th + 9-th','5-th + 11-th','5-th +
13-th','7-th + 9-th','7-th + 11-th','7-th + 13-th','9-th + 11-th','9-
th + 13-th','11-th + 13-th'};

%% New Harmonics
for f=1:1
    ind=0;
    for r=0:2:8
        for d=r+2:2:10
            freq=49+f;                          %freq=49/50/51Hz Ts=0.6ms
            HC=pi*freq*1.2*10^-3;               %=2*0.6*10^-3=1.2*10^-3

            %Creation of the distorted evaluation signal
            for n=1:4802
                hv=HC*n;
                X(n+1)=sin(hv);
                XF(n+1)=X(n+1);
                for m=3+r:2:3+r
                    X(n+1)=X(n+1)+0.6*sin(3+r*hv)+0.6*sin(3+d*hv);
                end
            end

            g1=0;
            g2=0;
            y_1=0;
            y_2=0;
            d_line=zeros(1,N);

            %Creation of the output and error
            for k=1:4800
                for i=N:-1:2
                    d_line(i)=d_line(i-1);  %Update delay line
                end
                d_line(1)=X(k);             %New input sample
                g1_in=sum(h1(1,:).*d_line); %Input for g1
                g2_in=sum(h2(1,:).*d_line); %Input for g2
                y=g1*g1_in+g2*g2_in;        %MGP-FIR output
                p_error=XF(k)-y_2;          %Prediction error
                y_2=y_1;                    %Update delayed y samples
                y_1=y;
                g1=g1+mu*p_error*g1_in;     %g1 adaption
                g2=g2+mu*p_error*g2_in;     %g2 adaption
                p_error_history(k)=p_error; %Save prediction error
                y_fin(k)=y;
                trend_g1(k)=g1_in*p_error;
                trend_g2(k)=g2_in*p_error;
            end
```

```
ind=ind+1;

G1_FFT=fft(trend_g1,points)/4800;
figure(21+f)
hold on
subplot(3,5,ind)
plot(f_axis+98+f*2,2*abs(G1_FFT(1:points/2+1)))
xlim([98+f 933+f])
xlabel('Frequency (Hz)')
str = sprintf('%d-th and %d-th harmonics/%d Hz
G1',3+r,3+d,49+f);
title(str)
hold off

G2_FFT=fft(trend_g2,points)/4800;
figure(24+f)
hold on
subplot(3,5,ind)
plot(f_axis+98+f*2,2*abs(G2_FFT(1:points/2+1)))
xlim([98+f 933+f])
xlabel('Frequency (Hz)')
str = sprintf('%d-th and %d-th harmonics/%d Hz
G2',3+r,3+d,49+f);
title(str)
hold off

Y_FFT=fft(y_fin,points)/4800;
figure(27+f)
hold on
subplot(3,5,ind)
plot(f_axis,2*abs(Y_FFT(1:points/2+1)))
xlim([75 833+f])
xlabel('Frequency (Hz)')
str = sprintf('%d-th and %d-th harmonics/%d Hz
Y',3+r,3+d,49+f);
title(str)
hold off

%Search harmonics
for n=1:16
    if 2*abs(max(G1_FFT(round(((points/2+1)*((((n-
       1)*50)+25)/(833))):round((points/2+1)*((((n-
       1)*50)+75)/(833)))))))) > 0.05
       dat_g1(ind,n)=2*abs(max(G1_FFT(round(((points/2+1)
       *((((n-
       1)*50)+25)/(833))):round((points/2+1)*((((n-
       1)*50)+75)/(833)))))));
    else dat_g1(ind,n)=0;
    end
    if 2*abs(max(G2_FFT(round(((points/2+1)*((((n-
       1)*50)+25)/(833))):round((points/2+1)*((((n-
       1)*50)+75)/(833)))))))) > 0.05
       dat_g2(ind,n)=2*abs(max(G2_FFT(round(((points/2+1)
       *((((n-
       1)*50)+25)/(833))):round((points/2+1)*((((n-
       1)*50)+75)/(833)))))));
    else dat_g2(ind,n)=0;
    end
```

```
                if
                   2*abs(max(Y_FFT(round(((points/2+1)*((((n)*50)+25)
                   /(833))):round((points/2+1)*((((n)*50)+75)/(833)))
                   )))) > 0.05
                   dat_y(ind,n)=2*abs(max(Y_FFT(round(((points/2+1)*(
                   (((n)*50)+25)/(833))):round((points/2+1)*((((n)*50
                   )+75)/(833)))))));
                else dat_y(ind,n)=0;
                end
            end

            %Create table
            fig = figure(30+f);
            table_g1 = uitable('Position',[0 675 946
            292],'Parent',fig,'Data',dat_g1,'ColumnName',cnames,'RowN
            ame',rnames,'ColumnWidth',{50});
            table_g2 = uitable('Position',[0 340 946
            292],'Parent',fig,'Data',dat_g2,'ColumnName',cnames,'RowN
            ame',rnames,'ColumnWidth',{50});
            table_y = uitable('Position',[0 0 946
            292],'Parent',fig,'Data',dat_y,'ColumnName',cnames_y,'Row
            Name',rnames,'ColumnWidth',{50});
            str_g1 = sprintf('%d Hz - G1_FFT analysis',49+f);
            str_g2 = sprintf('%d Hz - G2_FFT analysis',49+f);
            str_y = sprintf('%d Hz - Y_FFT analysis',49+f);
            uicontrol('Position',[970 945 200 20],'Parent', fig,
            'Style', 'edit','String',str_g1);
            uicontrol('Position',[970 610 200 20],'Parent', fig,
            'Style', 'edit','String',str_g2);
            uicontrol('Position',[970 270 200 20],'Parent', fig,
            'Style', 'edit','String',str_y);
        end
    end
    dat_g1=zeros(15,16);
    dat_g2=zeros(15,16);
    dat_y=zeros(15,16);
end
```

References

[1] R. C. Dugan, M. F. McGranaghan and H. W. Beaty, *Electrical Power Systems Quality*, New York: McGraw-Hill, 1996.

[2] *Harmonic Distortion*, Pacific Corp, Pacific Power Utah Power, Salt Lake City, UT, 1998. Available from: http://www.pacificpower.net/content/dam/pacific_power/doc/Contractors_Suppliers/Power_Quality_Standards/1C_4_1.pdf [Accessed May 06, 2013]

[3] *Elimination of Harmonics in Installation*, American Power Conversion by Schneider Electric, West Kingston, RI, 2012. Available from: http://www.apcmedia.com/salestools/LARD-8YPBC8/LARD-8YPBC8_R0_EN.pdf [Accessed May 06, 2013]

[4] C. Sankaran, *Power Quality*, Boca Raton, FL: CRC Press, 2002.

[5] *Harmonic Disturbances in Networks and Their Treatment*, Schneider Electric, Rueil-Malmaison, France, 1999. Available from: http://triton.elk.itu.edu.tr/~ozdemir/EH-1.pdf [Accessed May 06, 2013]

[6] *Harmonics*, Controlled Power Company, Stephenson Highway Troy, MI, 1999. Available from: http://www.controlledpwr.com/whitepapers/ukharma2.pdf [Accessed May 06, 2013]

[7] *IEEE Recommended Practice and Requirements for Harmonic Control in Electrical Power Systems*, IEEE Standard 519, 1992.

[8] *Hazard of Harmonics and Neutral Overloads*, American Power Conversion by Schneider Electric, West Kingston, RI, 2003. Available from: http://www.apcdistributors.com/white-papers/Power/WP-

26%20Hazards%20of%20Harmonics%20and%20Neutral%20Overloads.pdf [Accessed May 06, 2013]

[9] *Power Factor Correction and Harmonics*, REO Inductive Components, Shropshire, United Kingdom, 2008. Available from: http://www.reo.co.uk/files/power_factor_correction_engl_02-08_1.pdf [Accessed May 06, 2013]

[10] H. Akagi, "Modern active filters and traditional passive filters", *Bulletin of the Polish Academy of Sciences*, Vol. 54, No. 3, pp. 255-269, 2006.

[11] A.M. Massoud, S.J. Finney and B.W. Williams, "Review of harmonic current extraction techniques for an active power filter", in Proceedings of the 11th International Conference on Harmonics and Quality of Power, Lake Placid, NY: IEEE Press, pp. 154-159, 2004.

[12] P.S.R. Diniz, *Adaptive Filtering: Algorithm and Practical Implementation*, Norwell, MA: Springer, 1997.

[13] T. Komrska, J. Žák, S.J. Ovaska and Z. Peroutka, "Current reference generator for 50-Hz and 16.7-Hz shunt active power filters", *International Journal of Electronics*, Vol. 97, No. 1, pp. 63-81, 2010.

[14] S.J. Ovaska, "Predictive filtering methods for power systems applications", in *Computationally Intelligent Hybrid Systems*: *The fusion of Soft Computing and Hard Computing*, Hoboken, NJ: John Wiley & Sons, 2005, ch. 7, pp. 203-240.

[15] O. Vainio and S.J. Ovaska, "Harmonics-resistant adaptive algorithm for line-frequency signal processing", *IEEE Transactions on Industrial Electronics*, Vol. 49, No.3, pp. 702-706, 2002.

[16] T. Bäck, *Evolutionary Algorithms in Theory and Practice*, New York, NY: Oxford University Press, 1996.

[17] S.J. Ovaska and O. Vainio, “Evolutionary-programming-based optimization of reduced-rank adaptive filters for reference generation in active power filters”, *IEEE Transactions on Industrial Electronics,* vol. 51, No. 4, pp. 910-916, 2004.